SOME CONTRIBUTIONS TO THE THEORY OF ELASTIC AND PLASTIC STABILITY

EINIGE BEITRÄGE ZUR THEORIE DER ELASTISCHEN UND PLASTISCHEN STABILITÄT

QUELQUES CONTRIBUTIONS A LA THÉORIE DE LA STABILITÉ ÉLASTIQUE ET PLASTIQUE

Prof. Ir. P. P. BIJLAARD,
Technische Hoogeschool Delft, Technical Adviser I. A. B. S. E.

1. General considerations on the plastic stability of thin plates and shells

1. 1. Tests by KOLLBRUNNER.

Our theory on the plastic stability of plates [1] [2] is based on the actual behaviour of structural steel with changing ratio of the deviator components which follows from the tests of HOHENEMSER and PRAGER [3] with tubes, so that we may assume that its results will be in good accordance with the actual behaviour of buckling plates. Nevertheless many designers will be more inclined to use it, if they possess a more direct demonstration of its applicability. This direct proof is given, anyhow for aluminium, by the extensive and careful tests on the buckling of plates, executed and published by KOLLBRUNNER [4].

The tests were effected with thin plates of avional, an aluminium alloy, whilst the stress strain graph of the material was determined by compression of short sheets. We will compare the tests as given by KOLLBRUNNER in his figures 33, 34 and 35 with the results of our theory. All these tests relate to plates, compressed in longitudinal direction and supported at the unloaded sides.

Fig. 33 refers to plates of which the unloaded sides are simply supported. According to our theory the buckling force per unit breadth of such plates is, if the entire plate deforms plastically [5]

$$h\,\sigma_P = (2\pi^2 EJ/b^2)(\sqrt{AD} + B + 2F) \qquad (1)$$

The modulus of elasticity E of avional is 715 000 kg/cm^2. The thickness h and the breadth b of the plates were 0.2 cm and 6.2 cm respectively, so that $\pi^2 EJ/b^2 = \pi^2 Eh^3/12\,b^2 = 122.8$ kg/cm. Furthermore, as in this case the

---

[1] BIJLAARD, Proc. Royal Neth. Acad. of Sciences, Amsterdam, nos. 5 and 7, 1938.
[2] BIJLAARD, Publ. Int. Ass. f. Bridge and Struct. Eng., Zurich, Vol. 6, p. 45—69.
[3] HOHENEMSER and PRAGER, Zeitschr. f. ang. Math. u. Mech., no. 1, 1932.
[4] KOLLBRUNNER, Mitt. a. d. Inst. f. Baustatik, Zurich, no. 17, 1946.
[5] BIJLAARD, lit. footnote 2, p. 55, eq. (38).

second principal stress is zero, so that $\beta = \varrho_2/\varrho_1 = 0$ and $\eta^2 = \beta^2 - \beta + 1 = 1$, values A, B, D and F in eq. (1) are given by [6])

$$\left.\begin{aligned} &A = \varphi_1/\varphi_4, \quad B = \varphi_2/\varphi_4, \quad D = \varphi_3/\varphi_4, \quad F = m/(2m + 2 + 3em), \\ \text{in which} \quad &\varphi_1 = m^2\{E + (4 + 3e)\tan\varphi\} \\ &\varphi_2 = 2m(mE + 2\tan\varphi) \\ &\varphi_3 = 4m^2(E + \tan\varphi) \\ &\varphi_4 = m(5m - 4 + 3em)E + \{4(m^2 - 1) + 3em^2\}\tan\varphi \end{aligned}\right\} \quad (2)$$

value m being $1/\nu = 10/3$, whilst ν is POISSON's ratio, $e = E\varepsilon_p/\sigma$ and $\tan\varphi = d\sigma/d\varepsilon_p$, the latter two values having to be measured from the stress-strain graph with pure compression at a stress σ equal to the buckling stress σ_p. Value ε_p is the plastic strain and $\tan\varphi$ is equal to [7]) $E E_t/(E - E_t)$, $E_t = d\sigma/d\varepsilon$ being the tangent modulus. With a stress $\sigma_p = 2200$ kg/cm^2 we find from the stress-strain graph of avional $E_t = 350\,000$ kg/cm$^2 = 0.49\ E$, $e = 0.065$, $\tan\varphi = 0.96\ E$, by which eqs. (2) yield $A = 0.655$, $B = 0.41$, $D = 1.02$, $F = 0.36$, so that it follows from eq. (1) that $\sigma_p = 3.886\ \pi^2 EJ/b^2h = 2385$ kg/cm^2, being more than the stress 2200 kg/cm^2 we started from. Assuming now a stress $\sigma_p = 2300$ kg/cm^2 we find in the same way $E_t = 300\,000$ kg/cm$^2 = 0.42\ E$, $e = 0.11$, $\tan\varphi = 0.725\ E$, $A = 0.59$, $B = 0.41$, $D = 0.985$, $F = 0.34$, $\sigma_p = 2276$ kg/cm^2. Interpolating linearly between assumed as well as between resulting values σ_p we finally find a buckling stress $\sigma_p = 2288$ kg/cm^2.

With these tests the eccentricity of the load was certainly such, that with buckling practically no discharge occurred, so that we shall have to assume that the plates showed no elastic region. Hence the buckling stress is indeed determined by eq. (1) only, in the same way as also in practice, in connection with small eccentricities, the critical stress for a plate, assumed to be plastic all over, is determinant for the strength of the plate, as we stated already previously [8]).

According to our theory [2]) the plate should buckle in waves with a half wave length $a/p = (A/D)^{1/4}\ b$. With a buckling stress 2288 kg/cm^2 we find $A = 0.60$ and $D = 0.99$, so that the half wave length $a/p = a_B = 0.88\ b$. This wave length will occur if the plate is free to select its most favourable wave length, i. e. if it is infinitely long. With the tests the loaded edges were not simply supported, but somewhat clamped, so that we have here about the same case as studied by SCHLEICHER [9]), where in the elastic region the transition from p to $p+1$ half waves occurs if $a = b\sqrt{p(p+2)}$. As in that case the most favourable half wave length is equal to the breadth b of the plate, we shall assume that with the tests this transition occurs when $a = a_B\sqrt{p(p+2)}$. In Table I we give successively the lengths a of the plates tested by KOLLBRUNNER, the limiting lengths $a_L = 0.88\ b\sqrt{(p-1)(p+1)}$ and $0.88\ b\sqrt{p(p+2)}$ on either side of these lengths a, the theoretical number of half waves $p_B = p$ between these limiting lengths according to our theory and the number of half waves p_T observed in the tests, the latter number followed by the number of tests in brackets.

---

[6]) BIJLAARD, lit. footnote 2, p. 50, eqs. (20)—(23).
[7]) BIJLAARD, lit. footnote 2, p. 53.
[8]) BIJLAARD, lit. footnote 2, p. 54, footnote 10.
[9]) SCHLEICHER, Mitt. Forsch. Gutehoffnungshütte Konzerns, vol. 1, 1931. Cf. TIMOSHENKO, Theory of Elastic Stability, p. 364.

Table I.

a	$3.2\,b$	$4.85\,b$	$6.45\,b$	$8.1\,b$
$a_L - a_L$	$2.49\,b - 3.40\,b$	$4.31\,b - 5.21\,b$	$6.10\,b - 6.98\,b$	$7.87\,b - 8.75\,b$
p_B	3	5	7	9
p_T	3 (3)	5 (3)	7 (3)	9 (3)

The conformity between theory and tests is complete.

The buckling stresses of the 12 testplates vary between 2040 and 2190 kg/cm², except one that yields the low value 1950 kg/cm². Hence, disregarding the latter value, the lowest buckling stress is only 11 % below our theoretical value 2288 kg/cm². As this discrepancy is not more than the percentage the experimental values in the elastic domain remain below the theoretical values, owing to unavoidable inaccuracies, and the theoretical values in the elastic domain being undoubtedly correct, we may conclude also that our buckling stresses for the plastic domain are accurate.

We now consider the buckling of plates of which the unloaded sides are fixed, the test results of which are given in KOLLBRUNNER's fig. 34. The plates have a thickness $h = 0.2$ cm and a breadth $b = 4.4$ cm. The buckling condition for these plates in the plastic domain is [10])

$$\alpha_1 \tanh(\alpha_1 b/2) + \alpha_2 \tan(\alpha_2 b/2) = 0 \tag{3}$$

in which

$$\left.\begin{aligned} \alpha_{1,2} &= \sqrt{\pm G\lambda^2 + \lambda\sqrt{H\lambda^2 + K\varphi^2}} \\ G &= \frac{B+2F}{D}, \quad H = \frac{(B+2F)^2 - AD}{D^2}, \quad K = 1/D \\ \varphi^2 &= \frac{h\,\sigma_p}{EJ}, \qquad \lambda = \pi p/a \end{aligned}\right\} \tag{4}$$

After assuming σ_P to be 3100 and 3150 kg/cm² it appears that its real value is about 3140 kg/cm². With $\sigma_P = 3150$ kg/cm² we found, in the same way as before, $E_t = 0.04\,E$, $e = 1.49$, $\tan\varphi = E/24$, $A = 0.157$, $B = 0.238$, $D = 0.485$, $F = 0.141$ and, according to eqs. (4) $G = 1.07$, $H = 0.825$, $K = 2.06$, $\varphi^2 = 1.32$. Assuming now $\lambda = 1.55$ we obtain $\alpha_1 = 2.435$ and $\alpha_2 = 0.89$, so that eq. (3) yields

$$\alpha_1 \tanh(\alpha_1 b/2) + \alpha_2 \tan(\alpha_2 b/2) = 0.27$$

instead of zero. Assuming now $\sigma_P = 3140$ kg/cm² we find $G = 1.072$, $H = 0.827$, $K = 2.01$, $\varphi^2 = 1.315$, yielding, with $\lambda = 1.55$, values $\alpha_1 = 2.431$ and $\alpha_2 = 0.872$, by which eq. (3) yields

$$\alpha_1 \tanh(\alpha_1 b/2) + \alpha_2 \tan(\alpha_2 b/2) = 0.02$$

so that σ_P is round *3140* kg/cm² with $\lambda = \pi p/a = 1.55$ and a half wave length $a_B = a/p = \pi/1.55 = 2.02$ cm $= 0.46\,b$.

Calculating in the same way the buckling stresses with other values λ it appeared that with $\lambda = 1.55$ the critical stress is about a minimum. In Table II we give the data for these tests, the limiting lengths a_L for p half waves being now assumed to equal $0.46\,b\sqrt{(p-1)(p+1)}$ and $0.46\,b\sqrt{p(p+2)}$.

[10]) BIJLAARD, lit. footnote 2, p. 57.

Table II.

a	4.55 b	6.80 b	9.10 b	11.35 b
$a_L - a_L$	4.11 b — 4.58 b	6.43 b — 6.88 b	8.73 b — 9.19 b	11.04 b — 11.50 b
p_B	9	14	19	24
p_T	9 (3)	13 (2), 14 (1)	18 (2), 19 (1)	24 (3)

Also here the conformity between theory and tests is very good.

One extraordinarily low value excepted, the buckling stresses for the other 11 tests are between 2830 and 3115 kg/cm^2, the lowest value being only 10 % below our theoretical value.

Finally considering fig. 35 [4]), referring to plates that are simply supported at one unloaded side and fixed at the other, with $h = 0.2$ cm and $b = 5.3$ cm, the buckling condition is given by [11])

$$\alpha_1 \coth \alpha_1 b - \alpha_2 \cot \alpha_2 b = 0 \qquad (5)$$

whilst α_1 and α_2 follow from eqs. (4). Here we find that the buckling stress σ_P acquires a minimum value with about $\lambda = 0.865$, hence with a half wave length $a/p = \pi/\lambda = 3.63$ cm $= 0.685\, b$, whilst $\sigma_P = 2882$ kg/cm^2. Making here the limiting lengths a_L for p half waves equal to $0.685\, b \sqrt{(p-1)(p+1)}$ and $0.685 \sqrt{p(p+2)}$, the data for this case are given in Table III.

Table III.

a	3.8 b	5.65 b	7.55 b	9.45 b
$a_L - a_L$	3.36 b — 4.05 b	5.44 b — 6.12 b	7.50 b — 8.20 b	8.88 b — 9.56 b
p_B	5	8	11	13
p_T	5 (1), 6 (3)	8 (3)	10 (1), 11 (2)	13 (1), 14 (2)

The conformity between our theory and the tests is here again better than could be demanded.

The buckling stresses of all thirteen tests vary from 2660 to 2850 kg/cm^2, the lowest value being only 8 % below our theoretical value.

Hence we may conclude, that KOLLBRUNNER's tests have proved the applicability of our theory to plates of aluminium, as the number of waves shows that the anisotropic behaviour of the material is exactly such as predicted by our theory, whilst the discrepancies of the buckling stresses are not more than in the elastic domain. As with nonchanging ratio of the deviator components the plastic behaviour of soft steel and aluminium is determined by the same laws, whilst our theory is based on the real behaviour of soft steel with changing ratio of the deviator components, it is not so great a jump to conclude also that our theory is applicable to plates of soft steel. Apart from that we showed already in our preceding paper [2]) that the results of the few tests with steel plates are not contradictory to our theory.

---

[11]) The condition is identical with that in the elastic domain, only α_1 and α_2 are now given by eqs. (4). In our paper, loc. cit. footnote 10, there is a misprint in this buckling condition; the latter function should be cot $\alpha_2 b$ instead of coth $\alpha_2 b$.

1. 2. On the plastic deformation of soft steel with changing ratio of the deviator components.

As it appears that the derivation of our fundamental formulae, given in our first paper [2]), is somewhat difficult to understand for readers who are not accustomed to work in problems of plasticity, we shall try to elucidate our line of thought a little more, whilst we shall also give a purely analytical derivation of our formulae that demands a less imaginative faculty.

The fundamental question is, that with the buckling of plates and shells another state of stress, with another ratio of the deviator components, is superposed on the initial state of stress and that with changing ratio of the deviator components the material no longer behaves quasi-isotropically, as with a constant ratio of these components, but behaves anisotropically. The components of the stress deviator being

$$\bar{\sigma}_x = \sigma_x - \sigma,\ \bar{\sigma}_y = \sigma_y - \sigma,\ \bar{\sigma}_z = \sigma_z - \sigma,\ \tau_{xy},\ \tau_{yz},\ \tau_{zx},\ \tau_{yx},\ \tau_{zy} \text{ and } \tau_{xz},$$

whilst $\sigma = (\sigma_x + \sigma_y + \sigma_z)/3$, the deviator components of the elastic deformation,

$$\bar{\varepsilon}_{xe} = \varepsilon_{xe} - \varepsilon = \bar{\sigma}_x/2G,\ \bar{\varepsilon}_{ye} = \varepsilon_{ye} - \varepsilon = \bar{\sigma}_y/2G,\ \bar{\varepsilon}_{ze} = \varepsilon_{ze} - \varepsilon = \bar{\sigma}_z/2G,$$
$$\gamma_{xye}/2 = \tau_{xy}/2G,\ \gamma_{yze}/2 = \tau_{yz}/2G, \text{ etc.}$$

in which $\varepsilon = (\varepsilon_{xe} + \varepsilon_{ye} + \varepsilon_{ze})/3$, are obviously always proportional to those of the stress deviator. However, the components ε_{xp}, ε_{yp}, ε_{zp}, $\gamma_{xyp}/2$, etc. of the plastic deformation tensor, which is identical with the plastic deformation deviator, as $\varepsilon_{xp} + \varepsilon_{yp} + \varepsilon_{zp} = 0$, are proportional to the components of the stress deviator only under special simplifying assumptions, whilst their increases are only proportional to the increases of the stress deviator components if the ratio of the stress deviator components remains constant. The elastic shearing energy that governs the plastic deformation may be expressed as follows

$$\begin{aligned} V_s &= \tfrac{1}{2}(\bar{\sigma}_x \bar{\varepsilon}_{xe} + \bar{\sigma}_y \bar{\varepsilon}_{ye} + \bar{\sigma}_z \bar{\varepsilon}_{ze} + \tau_{xy}\gamma_{xye} + \tau_{yz}\gamma_{yze} + \tau_{zx}\gamma_{zxe}) \\ &= (1/4G)\{\bar{\sigma}_x^2 + \bar{\sigma}_y^2 + \bar{\sigma}_z^2 + 2(\tau_{xy}^2 + \tau_{yz}^2 + \tau_{zx}^2)\} = S_1^2/4G \end{aligned} \tag{6}$$

Hence at the yield stress, where V_s is constant, also

$$S_1 = \sqrt{\bar{\sigma}_x^2 + \bar{\sigma}_y^2 + \bar{\sigma}_z^2 + 2(\tau_{xy}^2 + \tau_{yz}^2 + \tau_{zx}^2)} \tag{7}$$

is constant. HOHENEMSER and PRAGER [3]) executed tests at the yield stress with steel tubes that were alternately subjected to pure tension and to torsion, so that here too the ratio of the deviator components changed. They represented the stress deviator and the deformation deviator by representative vectors Γ_0 and T_0 in a nine-dimensional space, the components being equal to the nine components of the deviators. Hence, since at the yield stress S_1 is constant, according to eq. (7) the length of the stress vector Γ_0 and that of the vector T_{oe} of the elastic deformations will not change, whilst with constant ratio of the stress deviator components, the direction of all vectors does not change either. In that case the vectors of the plastic and elastic deformation, being for example $T_{op} = AB$ and $T_{oe} = BC$ respectively, will become after further deformation $T'_{op} = AB'$ and $T_{oe} = B'C' = BC$ respectively, whilst the representative vector Γ_0 of the stress deviator, being placed at the end of the total (i. e. elastic plus plastic) deformation course,

moves from C to C', its direction and length remaining constant (fig. 1). The excess plastic deformation BB' equals the excess total deformation CC'.

If, however, the direction of the total deformation course changes, as is the case with plastic buckling of plates, so that after having a direction AC, in which AB and BC represent the plastic and elastic deformation respectively, it proceeds in a direction CDE (fig. 2), several possibilities for the course of the excess plastic deformation exist. In our computations we assumed, that in the representative point E of the total deformation, the situation is the same as with a straight deformation course AE, so that, as the representative vector of the elastic deformation FE remains equal to BC, the excess plastic deformation is represented by BF, whilst the stress deviator is represented by Γ_{01} in E. So

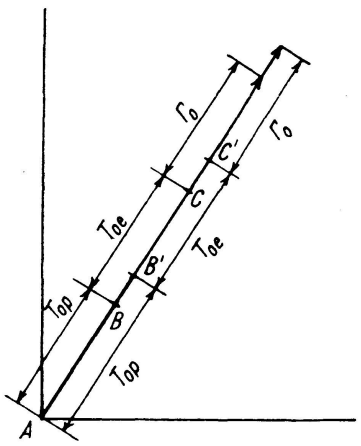

Fig. 1

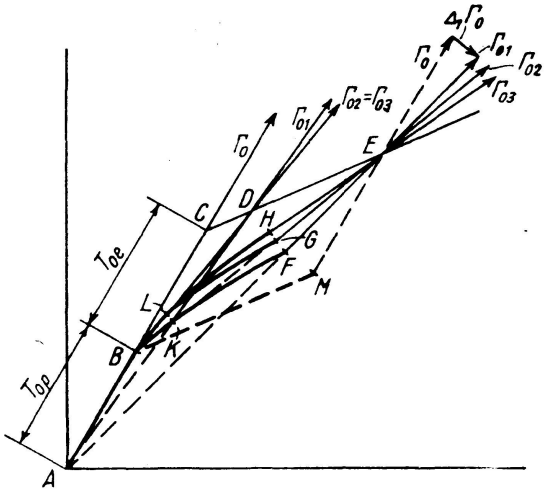

Fig. 2

we attributed a complete memory to the material. According to the tests of HOHENEMSER and PRAGER [3]), however, the memory of structural steel is not so complete. Free deformations, i. e. deformations during which the ratio of the deviator components does not change, are forgotten. Hence with an excess total deformation CE the free plastic deformation AB is forgotten, so that the continuation of the representative vector of the elastic deformation deviator, $GE = BC$, passes through B, the excess plastic deformation course being represented by BG and the stress deviator by Γ_{02}. Moreover superposed vibrations effected a total loss of remembrance, so that at any moment the excess plastic deformation components were proportional to the components of the stress deviator, by which the increase of the plastic deformation course has always the same direction as the representative vector of the stress deviator, so that the beginning H of the vector of the elastic deformation, $HE = BC$, is to be found on the trail curve BH belonging to the course of the total deformation CE, by which the excess plastic deformation course is given by BH and the vector of the stress deviator by Γ_{03}. In our former papers [1]) [2]) we called bodies with plastic deformation courses BF, BG and BH a HENCKY, HOHENEMSER-PRAGER and PRANDTL-REUSS body respectively.

With buckling the superposed excess deformations are infinitely small. With an infinitely small total deformation CD the excess plastic deformation for a material with a complete memory is given by BK, the continuation

of the elastic vector $KD = BC$ passing through A and the stress deviator being represented by Γ_{01} in D. With both partial (Γ_{02} in E) and complete (Γ_{03} in E) loss of remembrance the vectors of the elastic deformation will pass through B in this case, the excess plastic deformation being given by BL. As, however, deformations below the yield stress, where the tangent modulus $E_t = d\sigma/d\varepsilon$ has a positive value and with which we have to do with buckling, cannot be considered as free, as at the yield stress, if the ratio of the deviator components is constant, in our theory we took all preceding deformations into account and thus contributed a complete memory to the material. Hence we reckoned with the resulting stress vectors Γ_{01}. We did this especially, as in this way we were sure not to overestimate the buckling stresses of the plates. For in this case the excess stress deviator, which after an excess total deformation course CE is represented by $\Delta_1\Gamma_0$, is smaller than with partial or complete loss of remembrance, as may be seen directly in fig. 2. As with infinitely small excess deformation a partial or complete loss of remembrance amounts only to a neglect of the initial plastic deformation course AB, we may eventually take it into account in our formulae by equating value e to zero, as we did already in our first paper [2]), page 56, in order to compare our results with the tests of CHASE. The conformity of KOLLBRUNNER's tests with the results of our theory, obtained by taking value e into account, shows, however, that for aluminium it yields reliable results in that way, whilst with steel, where e is small, so that taking it into account or not makes little difference, we had better remain on the safe side.

It also follows from fig. 2 that the more the direction of the excess deformation course CD deviates from that of the initial deformation course AC, the more the direction of Γ_{01} will deviate from that of Γ_0, and the larger the excess stress deviator vector $\Delta_1\Gamma_0$ will be. Hence the excess stress and thus the resistance to buckling will be the higher, the more the ratio of the excess deformation deviator components differs from that of the original ones. We will demonstrate it under here too by comparing the plastic buckling stresses at the yield stress for several cases of buckling (Table IV).

If with buckling the material would deform quasi-isotropically, as was assumed by ROŠ-EICHINGER[16]) and CHWALLA, so that for example at the yield stress an excess deformation would not cause excess stresses and hence no excess elastic deformations, with which only plastic deformations would occur, an excess total deformation course CE would cause an equal excess plastic deformation course BM. The elastic deformation is then represented by ME, parallel to BC, whilst the resulting stress deviator is represented by Γ_0 in E, being parallel to Γ_0 in C, $\Delta\Gamma_0$ being zero. It is clear that such a behaviour is contrary to the actual mode of deformation of steel according to the experiments of HOHENEMSER and PRAGER.

1. 3. Purely analytical derivation of our fundamental formulae on the plastic stability of plates and shells.

From fig. 2 it follows that, with the mode of deformation as assumed by us, the total plastic deformation AK or AF and the state of stress, represented by Γ_{01} in D or E, determine each other reciprocally, the stresses with a total (elastic plus plastic) deformation AD or AE being the same as if this total deformation were built up along the straight line AD or AE.

Hence the excess stresses σ_x' and σ_y' with buckling can be determined by subtracting the initial stresses ϱ_1 and ϱ_2 before buckling from the total stresses σ_x and σ_y, belonging to the total strains ε_x and ε_y after buckling, — the way we followed in our first paper [2] [12]). We may, however, follow also a more direct way in order to find the relations between the excess stresses σ_x', σ_y' and τ_{xy}' and the excess strains ε_x', ε_y' and γ_{xy}' [13]), the primes indicating in point of fact differentials, so that for example σ_x' means $d\sigma_x$. For we may write

$$\left.\begin{aligned} d\varepsilon_x &= \frac{\partial \varepsilon_x}{\partial \sigma_x} d\sigma_x + \frac{\partial \varepsilon_x}{\partial \sigma_y} d\sigma_y + \frac{\partial \varepsilon_x}{\partial \tau_{xy}} d\tau_{xy} \\ d\varepsilon_y &= \frac{\partial \varepsilon_y}{\partial \sigma_x} d\sigma_x + \frac{\partial \varepsilon_y}{\partial \sigma_y} d\sigma_y + \frac{\partial \varepsilon_y}{\partial \tau_{xy}} d\tau_{xy} \\ d\gamma_{xy} &= \frac{\partial \gamma_{xy}}{\partial \sigma_x} d\sigma_x + \frac{\partial \gamma_{xy}}{\partial \sigma_y} d\sigma_y + \frac{\partial \gamma_{xy}}{\partial \tau_{xy}} d\tau_{xy} \end{aligned}\right\} \tag{8}$$

Furthermore the strains may be split into elastic and plastic strains, e. g.

$$\left.\begin{aligned} \varepsilon_x &= \varepsilon_{xe} + \varepsilon_{xp} \\ \frac{\partial \varepsilon_x}{\partial \sigma_x} &= \frac{\partial \varepsilon_{xe}}{\partial \sigma_x} + \frac{\partial \varepsilon_{xp}}{\partial \sigma_x} \end{aligned}\right\} \tag{9}$$

and

It needs no further explanation that

$$\left.\begin{aligned} \partial \varepsilon_{xe}/\partial \sigma_x &= \partial \varepsilon_{ye}/\partial \sigma_y = 1/E \\ \partial \varepsilon_{xe}/\partial \sigma_y &= \partial \varepsilon_{ye}/\partial \sigma_x = -1/mE \\ \partial \gamma_{xye}/\partial \tau_{xy} &= 1/G \end{aligned}\right\} \tag{10}$$

whilst all other partial derivatives of the elastic strains with respect to the stresses are zero.

In order to calculate the partial derivatives of the plastic strains we remark that, as the shearing energy governs the plastic deformation, a plane state of stress is equivalent to a linear stress

$$\sigma_q = \sqrt{\sigma_x^2 - \sigma_x \sigma_y + \sigma_y^2 + 3\tau_{xy}^2} \tag{11}$$

For a material with a complete memory the total plastic strains and the state of stress determine each other reciprocally, as explained above here [14]), so that we may write for the plastic strains, as the coefficient of lateral contraction m equals 2,

---

[12]) We may take this opportunity to indicate some disturbing misprints in our first paper [2]) of which, owing to the war, we could not read the proofs. Eqs. (11 a) and (11 b) read as follows

$$\varrho_1 = \frac{2}{3} E_p (2\varepsilon_{xp} + \varepsilon_{yp}) \quad (11\,a) \qquad \text{and} \qquad \varrho_2 = \frac{2}{3} E_p (2\varepsilon_{yp} + \varepsilon_{xp}) \quad (11\,b)$$

In eq. (37), p. 55, the first term in the large brackets should be Ap^2b^2/a^2 instead of Apb^2/a^2. In eq. (57), p. 60, all sine and cosine functions should be changed into sinh and cosh respectively. On p. 62 in eq. (61) sinh $\alpha_2 b$ should be sin $\alpha_2 b$ and in the formula for $\alpha'_{1,2}$ values h and N should be h' and N'. See also footnote 11.

[13]) Bijlaard, lit. footn. 1, eqs. (21)—(24), lit. footn. 2, eqs. (20)—(23).

[14]) For a material without remembrance, on the other hand, we have a relation between the excess strains and the stresses, hence

$$d\varepsilon_{xp} = \sigma_x/E_p' - \sigma_y/2E_p' \qquad \text{and} \qquad d\varepsilon_{yp} = \sigma_y/E_p' - \sigma_x/2E_p'$$

We considered such a body more in detail in lit. footn. 1, p. 734.

$$\varepsilon_{xp} = \sigma_x/E_p - \sigma_y/2E_p \quad (12a) \qquad \text{and} \qquad \varepsilon_{yp} = \sigma_y/E_p - \sigma_x/2E_p \quad (12b)$$

whilst, as $G_p = mE_p/2(m+1) = E_p/3$,

$$\gamma_{xyp} = \tau_{xy}/G_p = 3\tau_{xy}/E_p \quad (12c)$$

Inversely it follows from eqs. (11) that

$$\sigma_x = \tfrac{2}{3}E_p(2\varepsilon_{xp} + \varepsilon_{yp}) \quad (13a), \qquad \sigma_y = \tfrac{2}{3}E_p(2\varepsilon_{yp} + \varepsilon_{xp}) \quad (13b)$$

and

$$\tau_{xy} = \tfrac{1}{3}E_p\,\gamma_{xyp} \quad (13c)$$

Substitution of eqs. (13) in eq. (11) yields

$$\sigma_q = \frac{2}{\sqrt{3}}E_p\sqrt{\varepsilon_{xp}^2 + \varepsilon_{yp}^2 + \varepsilon_{xp}\varepsilon_{yp} + \tfrac{1}{4}\gamma_{xyp}^2} = \frac{2}{\sqrt{3}}E_p\,\varepsilon_q = E_p\,\varepsilon_{pq} \quad (14)$$

With a stress-plastic strain diagram for pure compression as given in fig. 3a, at a certain point P the total plastic modulus $E_p = \sigma_x/\varepsilon_p$ is given by the tangent of the angle between OP and the ε_p axis. From eq. (14) it follows that with an arbitrary plane state of stress, represented by point P in a σ_q—ε_{pq}

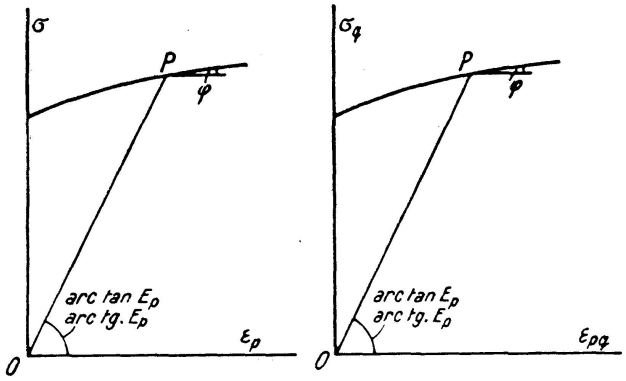

Fig. 3a Fig. 3b

diagram (fig. 3b), value E_p is also the tangent of the slope of the straight line OP. Hence the σ_q—ε_{pq} diagram is identical with the σ—ε_p diagram for pure compression, so that at corresponding points P, where $\sigma_q = \sigma$, also the slopes φ of the two graphs are equal. Hence we have

$$\sigma_q/\varepsilon_{pq} = E_p \quad (15a) \qquad \text{and} \qquad d\sigma_q/d\varepsilon_{pq} = \tan\varphi \quad (15b)$$

Furthermore it follows from eq. (11) that

$$\frac{\partial\sigma_q}{\partial\sigma_x} = \frac{2\sigma_x - \sigma_y}{2\sigma_q} \quad (16a), \qquad \frac{\partial\sigma_q}{\partial\sigma_y} = \frac{2\sigma_y - \sigma_x}{2\sigma_q} \quad (16b), \qquad \frac{\partial\sigma_q}{\partial\tau_{xy}} = \frac{3\tau_{xy}}{\sigma_q} \quad (16c)$$

Using eqs. (15a), (15b) and (16a) we have now

$$\frac{\partial}{\partial\sigma_x}\left(\frac{1}{E_p}\right) = \frac{\partial(\varepsilon_{pq}/\sigma_q)}{\partial\sigma_x} = \frac{d(\varepsilon_{pq}/\sigma_q)}{d\sigma_q}\frac{\partial\sigma_q}{\partial\sigma_x} = \frac{\sigma_q\,d\varepsilon_{pq}/d\sigma_q - \varepsilon_{pq}}{\sigma_q^2}\frac{2\sigma_x - \sigma_y}{2\sigma_q} =$$

$$= \frac{\sigma_q/\tan\varphi - \sigma_q/E_p}{\sigma_q^2}\frac{2\sigma_x - \sigma_y}{2\sigma_q}$$

so that finally we get

$$\frac{\partial}{\partial\sigma_x}\left(\frac{1}{E_p}\right) = \frac{2\sigma_x - \sigma_y}{2\sigma_q^2 E_p}\left(\frac{E_p}{\tan\varphi} - 1\right) \quad (17a)$$

Interchanging σ_x and σ_y we obtain from this equation

$$\frac{\partial}{\partial \sigma_y}\left(\frac{1}{E_p}\right) = \frac{2\sigma_y - \sigma_x}{2\sigma_q^2 E_p}\left(\frac{E_p}{\tan\varphi} - 1\right) \tag{17b}$$

Finally we find in the same way, using also eq. (16c)

$$\frac{\partial}{\partial \tau_{xy}}\left(\frac{1}{E_p}\right) = \frac{\partial(\varepsilon_{pq}/\sigma_q)}{\partial \tau_{xy}} = \frac{d(\varepsilon_{pq}/\sigma_q)}{d\sigma_q}\frac{\partial \sigma_q}{\partial \tau_{xy}} = \frac{\sigma_q/\tan\varphi - \sigma_q/E_p}{\sigma_q^2}\frac{3\tau_{xy}}{\sigma_q}$$

so that

$$\frac{\partial}{\partial \tau_{xy}}\left(\frac{1}{E_p}\right) = \frac{3\tau_{xy}}{\sigma_q^2 E_p}\left(\frac{E_p}{\tan\varphi} - 1\right) \tag{17c}$$

With the aid of eqs. (12a) and (17a) we find now

$$\frac{\partial \varepsilon_{xp}}{\partial \sigma_x} = \frac{\partial}{\partial \sigma_x}\frac{1}{2E_p}(2\sigma_x - \sigma_y) = \frac{1}{E_p} + \frac{2\sigma_x - \sigma_y}{2}\frac{2\sigma_x - \sigma_y}{2\sigma_q^2 E_q}\left(\frac{E_p}{\tan\varphi} - 1\right) =$$

$$= \frac{1}{E_p} + \frac{(2\sigma_x - \sigma_y)^2}{4\sigma_q^2 E_p}\left(\frac{E_p}{\tan\varphi} - 1\right) \tag{18a}$$

whilst with eqs. (12b) and (17b) or by interchanging x and y in eq. (18a) we get

$$\frac{\partial \varepsilon_{yp}}{\partial \sigma_y} = \frac{1}{E_p} + \frac{(2\sigma_y - \sigma_x)^2}{4\sigma_q^2 E_p}\left(\frac{E_p}{\tan\varphi} - 1\right) \tag{18b}$$

Furthermore with eqs. (12b) and (17a) we obtain

$$\frac{\partial \varepsilon_{yp}}{\partial \sigma_x} = \frac{\partial}{\partial \sigma_x}\frac{1}{2E_p}(2\sigma_y - \sigma_x) = -\frac{1}{2E_p} + \frac{(2\sigma_x - \sigma_y)(2\sigma_y - \sigma_x)}{4\sigma_q^2 E_p}\left(\frac{E_p}{\tan\varphi} - 1\right) \tag{18c}$$

whilst interchanging x and y shows that

$$\frac{\partial \varepsilon_{xp}}{\partial \sigma_y} = \frac{\partial \varepsilon_{yp}}{\partial \sigma_x} \tag{18d}$$

Computing now the partial derivatives containing γ_{xyp} or τ_{xy} we find, using eqs. (12) and (17)

$$\frac{\partial \varepsilon_{xp}}{\partial \tau_{xy}} = \frac{\partial \gamma_{xyp}}{\partial \sigma_x} = \frac{3\tau_{xy}(2\sigma_x - \sigma_y)}{2\sigma_q^2 E_p}\left(\frac{E_p}{\tan\varphi} - 1\right) \tag{18e}$$

$$\frac{\partial \varepsilon_{yp}}{\partial \tau_{xy}} = \frac{\partial \gamma_{xyp}}{\partial \sigma_y} = \frac{3\tau_{xy}(2\sigma_y - \sigma_x)}{2\sigma_q^2 E_p}\left(\frac{E_p}{\tan\varphi} - 1\right) \tag{18f}$$

$$\frac{\partial \gamma_{xyp}}{\partial \tau_{xy}} = \frac{1}{G_p} + \frac{3\tau_{xy}^2}{\sigma_q^2 G_p}\left(\frac{E_p}{\tan\varphi} - 1\right) \tag{18g}$$

In order to obtain resulting formulae that are not unnecessarily intricate, we place, as before, the X- and Y-axes in the direction of the principal stresses of the state of stress before buckling. Hence in eqs. (18) the stress τ_{xy} is zero, by which all partial derivatives of unit shears γ_{xyp} or with respect to shearing stresses τ_{xy} are zero, except $\partial\gamma_{xyp}/\partial\tau_{xy}$, that equals $1/G_p$. At the other hand, with an arbitrary initial state of stress ϱ_1 ϱ_2, we shall replace σ_x and σ_y in eqs. (18) by ϱ_1 and ϱ_2. Hence we obtain from eqs. (8), after splitting the partial derivatives into an elastic and a plastic part, as we did for example in eq. (9), after insertion of eqs. (10) and (18), equating E_p to E/e and indicating differentials by primes

$$\left.\begin{aligned}
\varepsilon_x' &= \left(\frac{1+e}{E} + \frac{(2\varrho_1-\varrho_2)^2}{4\sigma_q^2}\,\frac{E-e\tan\varphi}{E\tan\varphi}\right)\sigma_x' + \left(-\frac{2+me}{2mE} + \frac{(2\varrho_1-\varrho_2)(2\varrho_2-\varrho_1)}{4\sigma_q^2}\,\frac{E-e\tan\varphi}{E\tan\varphi}\right)\sigma_y' \\
\varepsilon_y' &= \left(-\frac{2+me}{2mE} + \frac{(2\varrho_1-\varrho_2)(2\varrho_2-\varrho_1)}{4\sigma_q^2}\,\frac{E-e\tan\varphi}{E\tan\varphi}\right)\sigma_x' + \left(\frac{1+e}{E} + \frac{(2\varrho_2-\varrho_1)^2}{4\sigma_q^2}\,\frac{E-e\tan\varphi}{E\tan\varphi}\right)\sigma_y' \\
\gamma_{xy}' &= \left(\frac{1}{G} + \frac{1}{G_p}\right)\tau_{xy}' = \frac{2m+2+3em}{mE}\,\tau_{xy}'
\end{aligned}\right\} \quad (19)$$

Inversely we may compute from eqs. (19) the excess stresses as functions of the excess strains. As with our choice of the X- and Y-axes in eq. (11) $\sigma_q^2 = \varrho_1^2 - \varrho_1\varrho_2 + \varrho_2^2$, we obtain in this way the following formulae

$$\sigma_x' = E(A\,\varepsilon_x' + B\,\varepsilon_y'), \qquad \sigma_y' = E(B\,\varepsilon_x' + D\,\varepsilon_y') \quad (20)$$

in which
$$A = \varphi_1/\varphi_4, \qquad B = \varphi_2/\varphi_4, \qquad D = \varphi_3/\varphi_4 \quad (21)$$

and

$$\left.\begin{aligned}
\varphi_1 &= m^2\{(1-2\beta)^2 E + (4\eta^2 + 3e)\tan\varphi\} \\
\varphi_2 &= m\{(2-\beta)(1-2\beta)\,mE + (4\eta^2 + 3em\beta)\tan\varphi\} \\
\varphi_3 &= m^2\{(2-\beta)^2 E + (4\eta^2 + 3e\beta^2)\tan\varphi\} \\
\varphi_4 &= m\{(5m-4)(1+\beta^2) + 2(5-4m)\beta + 3em\eta^2\}E \\
&\quad + [4(m^2-1)\eta^2 + 3em\{m\eta^2 + (m-2)\beta\}]\tan\varphi \\
\beta &= \varrho_2/\varrho_1 \quad \text{and} \quad \eta^2 = \sigma_q^2/\varrho_1^2 = \beta^2 - \beta + 1
\end{aligned}\right\} \quad (22)$$

$$\tau_{xy}' = \frac{mE}{2m+2+3em}\,\gamma_{xy}' = EF\gamma_{xy}' \quad (23)$$

The resulting formulae are of course exactly identical with eqs. (20)—(23) of our first paper [2]), only the numerators and denominators φ of the fractions given in eq. (21) have been divided by a factor $(1-2\beta)$. In a similar way as shown here for a plane state of stress we may also calculate the stress-strain relations for an elasto-plastic body, subjected to a three dimensional state of stress, on which an infinitely small three dimensional excess stress tensor is superposed (by buckling), which relations may be useful in order to solve three dimensional cases of plastic stability [15]).

Also with eqs. (18) it may be seen easily, why Roš and Eichinger [16]) came to the wrong conclusion, that with buckling of plates the material behaves quasi-isotropically. They assumed that with a stress-strain diagram for pure compression as in fig. 3a, for example excess stresses $d\sigma_x$ and $d\sigma_y$ cause an extra plastic strain

$$d\,\varepsilon_{xp} = (1/\tan\varphi)(d\,\sigma_x - d\,\sigma_y/2)$$

The real relation is, however, according to eqs. (18), with $\sigma_x = \varrho_1$, $\sigma_y = \varrho_2$ and $\tau_{xy} = 0$

$$\begin{aligned}
d\,\varepsilon_{xp} &= \frac{\partial\,\varepsilon_{xp}}{\partial\,\sigma_x}\,d\,\sigma_x + \frac{\partial\,\varepsilon_{xp}}{\partial\,\sigma_y}\,d\,\sigma_y + \frac{\partial\,\varepsilon_{xp}}{\partial\,\tau_{xy}}\,d\,\tau_{xy} \\
&= \left\{\frac{1}{E_p} + \frac{(2\varrho_1-\varrho_2)^2}{4\sigma_q^2 E_p}\left(\frac{E_p}{\tan\varphi} - 1\right)\right\} d\,\sigma_x + \left\{-\frac{1}{2E_p} + \frac{(2\varrho_1-\varrho_2)(2\varrho_2-\varrho_1)}{4\sigma_q^2 E_p}\left(\frac{E_p}{\tan\varphi} - 1\right)\right\} d\,\sigma_y \\
&= \frac{d\,\sigma_x - d\,\sigma_y/2}{E_p} + \frac{2\varrho_1-\varrho_2}{4\sigma_q^2 E_p}\left(\frac{E_p}{\tan\varphi} - 1\right)\{(2\varrho_1-\varrho_2)\,d\,\sigma_x + (2\varrho_2-\varrho_1)\,d\,\sigma_y\}
\end{aligned} \quad (24)$$

[15]) Appears in Comptes Rendus, 6me Congrès de Mécanique Appliquée, Paris.
[16]) Roš and Eichinger, Int. Ass. for Bridge and Struct. Eng., Paris Congress, Final Report. 1932.

Only if $d\sigma_x : d\sigma_y = \varrho_1 : \varrho_2$, hence if the ratio of the stress components and thus also of the deviator components does not change, eq. (24) yields

$$d\varepsilon_{xp} = \frac{d\sigma_x - d\sigma_y/2}{E_p} + \frac{2\varrho_1 - \varrho_2}{4\sigma_q^2 E_p}\left(\frac{E_p}{\tan\varphi} - 1\right) 2\sigma_q^2 \frac{d\sigma_x}{\varrho_1}$$

$$= \frac{d\sigma_x - d\sigma_y/2}{E_p} + \frac{d\sigma_x - d\sigma_y/2}{E_p}\left(\frac{E_p}{\tan\varphi} - 1\right)$$

$$= (1/\tan\varphi)(d\sigma_x - d\sigma_y/2) \qquad (25)$$

in accordance with the equation used by Roš and Eichinger, the material behaving only quasi-isotropically if the ratio of the deviator components remains constant, as with buckling of bars.

1. 4. Application of our theory to several cases of buckling of plates.

As follows from the tests of Kollbrunner and from the reasoning on which we based our formula

$$\sigma_B = \sigma_E/4 + 3\sigma_P/4 \qquad (26)$$

given in eq. (35) of our first paper [2) 8)], with a given stress-strain diagram the buckling stress has to be computed under the assumption that the entire plate deforms plastically. If, however, it is not the stress-strain graph which is given, but the relation between slenderness ratio and buckling stress of columns, it evidently makes little difference, whether both columns and plates are assumed to show elastic regions or not. In our first paper we worked with the first assumption. With buckling under pure compression we found just below the yield stress for the plastic region [7)]

$$A = 0.421, \quad B = 0.426, \quad D = 0.938, \quad F = 0.322 \qquad (27)$$

whilst in the elastic domain

$$A = D = 1.099, \quad B = 0.329, \quad F = 0.385 \qquad (28)$$

so that according to eq. (26) we worked practically with the following average values for the entire plate

$$A = 0.591, \quad B = 0.402, \quad D = 0.978, \quad F = 0.338 \qquad (29)$$

Assuming on the contrary that the slenderness-buckling stress relation for bars is based on an entirely plastic deformation, so that we have to reckon with the tangent modulus E_t, we find just below the yield stress $E_t = \lambda^2\sigma_v/\pi^2 = 60^2 \cdot 2400/\pi^2 = 875\,000$ kg/cm^2, $\tan\varphi = 0.715\,E$ and $e = 0.073$, so that for pure compression we obtain

$$A = 0.593, \quad B = 0.422, \quad D = 1.012, \quad F = 0.355 \qquad (30)$$

which values are at most 5 % higher than those of eq. (29), so that with eq. (26) we remain on the safe side. As the actual conditions are rather intricate and as in the latter way our computations remain in concurrence with the current calculations for bars, we shall use eq. (26) also for our further computations.

In order to compare several cases of buckling, we shall calculate the ratios of the buckling stresses σ_B just below the yield stress and those in the elastic domain, σ_E, the result being given in Table IV.

Case 1 is an infinitely long plate, subjected to compression in axial direction, of which one unloaded side is simply supported whilst the other is free (fig. 4). In this case buckling occurs by pure twisting, so that on the original pure compressive stresses pure shearing stresses are superposed. Hence a maximum resistance will occur here, as the infinitely small shearing stresses will not increase σ_q in eq. (11), as may be seen readily by differentiation. More directly it follows from fig. 5, that an infinitely small stress $d\tau$, superposed on a pure compressive stress σ_x, increases the diameter of the stress circle only by an amount that is infinitely small of the second order, so that, independent of the used plasticity condition, the equivalent linear stress σ_q does not increase by it[17]). Hence in fig. 3b the state of stress remains represented by the same point P, so that E_p remains constant. This explains also why in this case the slope angle φ does not influence the resistance to buckling. Plastic deformations occur only because, according to fig. 5, the principal axes of the state of stress rotate through a small angle α'. The total shearing strain is accordingly given by γ'_{xy} in eqs. (19).

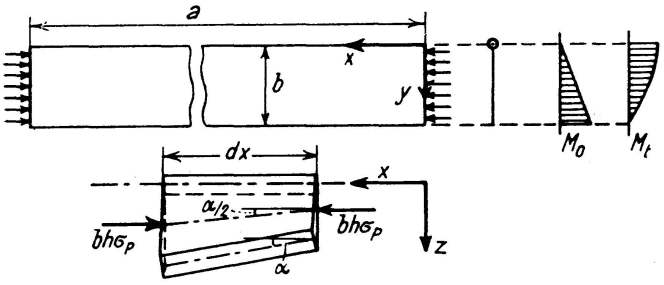

Fig. 4

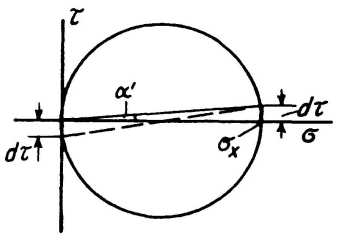

Fig. 5

We have already investigated this case before[17]). As in the elastic region we can use here the energy method[18]). The work done by the stresses $\sigma_x = \sigma_P$ is

$$V_0 = \tfrac{1}{2} \int_0^a \int_0^b h\,\sigma_P (\partial w/\partial x)^2\,dx\,dy \tag{31}$$

The strain energy of the entirely plastically deformed plate is, as $C = B$[19])

$$V_i = \tfrac{1}{2} EJ \int_0^a \int_0^b \left\{ A\left(\frac{\partial^2 w}{\partial x^2}\right)^2 + 2B \frac{\partial^2 w}{\partial x^2}\frac{\partial^2 \hat{w}}{\partial y^2} + D\left(\frac{\partial^2 w}{\partial y^2}\right)^2 + 4F\left(\frac{\partial^2 w}{\partial x\,\partial y}\right)^2 \right\} dx\,dy \tag{32}$$

With buckling $V_0 = V_i$, which condition yields, with (fig. 4)

$$w = Ky \sin \pi x/a \tag{33}$$

and as $J = h^3/12$, the critical stress

$$\sigma_P = E\left(A\frac{\pi^2}{12}\frac{b^2}{a^2} + F\right)\left(\frac{h}{b}\right)^2 \tag{34}$$

---

[17]) Bijlaard, De Ingenieur in Ned. Indië, no. 3, 1939.
[18]) Timoshenko, loc. cit., p. 325. Hartmann, Knickung, Kippung, Beulung, p. 168.
[19]) Bijlaard, lit. footnote 2, eq. (66).

With an infinitely long plate $b/a = 0$, so that

$$\sigma_P = EFh^2/b^2 \tag{35}$$

It looks somewhat strange to use so much mathematics to solve a case which is in principle so simple. A simple solution is, however, possible in several ways. If we consider an element $bh\,dx$ of an infinitely long plate (fig. 4), no bending stresses occur in the cross sections. With a slope angle α of edge $y = b$, the thrusts $bh\sigma_x = bh\sigma_P$ give a total outer moment

$$M_{ot} = \tfrac{1}{2}\, b\, h\, \sigma_P\, \alpha\, dx$$

As, with w, also $\partial w/\partial x$ is proportional to y, the individual outer moments M_0 by the stresses σ_P are also proportional to y (fig. 4), so that the twisting moment M_t in sections $h\,dx$, perpendicular to the Y-axis, is distributed parabolically, as shown in fig. 4. As in the plastic region we have, instead of $G = \tau'_{xy}/\gamma'_{xye}$, value $\tau'_{xy}/\gamma'_{xy} = EF$ according to eq. (23), we get

$$\alpha = \int_0^b M_t\, dy/EFJ_d = \tfrac{2}{3}\, M_{to}\, b/EFJ_d$$

so that the twisting moment M_{to} at $y = 0$, that has to balance the total outer moment M_{ot}, is

$$M_{to} = \tfrac{3}{2}\, EFJ_d\, \alpha/b = \tfrac{1}{2}\, EFh^3\, \alpha\, dx/b$$

Equating M_{ot} and M_{to} yields eq. (35). That we found here a parabolic distribution of M_t instead of the actual equal distribution, in accordance with w being proportional to y, is a consequence of our intentional neglect of the real distribution of the equivalent shearing forces $V_x = Q_x - \partial M_{xy}/\partial y$ along the element $bh\,dx$. This is allowed because additional shearing forces ΔV_x cause a slope angle $\Delta\alpha = dx \int_0^b \Delta V_x y\, dy/EFJ_d$ in which the integral is zero owing to equilibrium conditions, so that $\Delta\alpha = 0$.

Although in this case a decrease of σ_q is nowhere caused by the excess stresses, so that elastic regions nowhere occur, it is sufficiently safe to use value F of eqs. (29), being less than that of eq. (30). Hence eq. (35) yields, as in the elastic region $F = 0.385$ according to eq. (28),

$$\sigma_B = 0{,}338\, E h^2/b^2 = (0{,}338/0{,}385)\, \sigma_E = 0.878\sigma_E .$$

In case 2 of Table IV — a long plate, compressed in longitudinal direction, of which the unloaded sides are simply supported —, also rather high twisting stresses occur with buckling. If one or both sides are fixed (cases 3 and 4), the twisting stresses are less, so that these three cases show decreasing values of σ_B/σ_E. We found [2]) $h\sigma_B = 3.65\ \pi^2EJ/b^2$, $4.77\,\pi^2EJ/b^2$ and $5.97\,\pi^2EJ/b^2$ respectively, whilst in the elastic region we have $h\sigma_E = 4.40\,\pi^2EJ/b^2$, $5.94\,\pi^2EJ/b^2$ and $7.67\,\pi^2EJ/b^2$ respectively, yielding the ratios given in Table IV.

In case 5 of Table IV — an infinitely long plate, simply supported at the edges and subjected to pure shearing (fig. 6) — the X-axis is placed parallel to the long edges. We can calculate values, A, B, D and F first for the state of stress $\varrho_2 = -\varrho_1$, assuming X- and Y-axes in the directions of the principal stresses. As stresses and strains transform as the components of a tensor, we subsequently apply the respective equations [20]) to

[20]) See for transformation equations e. g. TIMOSHENKO, Theory of Elasticity, 1934, p. 191, 192.

transform the stress-strain relations to those for the X- and Y-axes parallel to the edges of the plate. We find then that we have to introduce in eqs. (20).

$$\left.\begin{aligned} A &= D = 4m^2(1+e)/\{4(m^2-1)+4em(2m-1)+3e^2m^2\} \\ B &= 2m(2+em)/\{4(m^2-1)+4em(2m-1)+3e^2m^2\} \end{aligned}\right| \quad (36)$$

whilst in eq. (23)

$$F = m\tan\varphi/\{3mE+2(m+1)\tan\varphi\}$$

in accordance with eq. (67) of our first paper [2]).

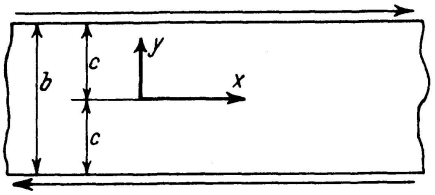

Fig. 6

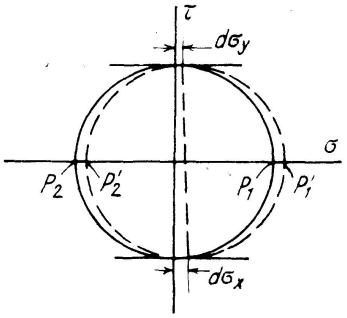

Fig. 7

We have here the inverted case of case 1, as here before buckling $\sigma_x = \sigma_y = 0$, so that the excess stresses σ_x' and σ_y' do not increase the equivalent stress σ_q in eq. (11), for e.g. $\partial\sigma_q/\partial\sigma_x = (2\sigma_x - \sigma_y)/2\sigma_q = 0$. More directly we see in fig. 7 that additional stresses $d\sigma_x$ and $d\sigma_y$ increase the maximum shearing stress only by an amount of the second order [21]), so that, as the envelope of the stress circles $\varrho_1\varrho_2$ with constant shearing energy has a horizontal tangent here [22]), the shearing energy and σ_q do not increase. Hence also if the maximum shearing stress were determinant for the plastic deformation, the equivalent stress would not increase [21]). In fig. 3b value E_p remains constant now, so that

$$\begin{aligned} \varepsilon_x' &= \varepsilon_{xe}' + \varepsilon_{xp}' = \sigma_x'/E - \sigma_y'/mE + \sigma_x'/E_p - \sigma_y'/2E_p \\ &= \{2m(1+e)\sigma_x' - (2+em)\sigma_y'\}/2mE \end{aligned} \quad (37)$$

and by interchanging x and y

$$\varepsilon_y' = \{2m(1+e)\sigma_y' - (2+em)\sigma_x'\}/2mE \quad (38)$$

Inversely expressing σ_x' and σ_y' in ε_x' and ε_y' we obtain from eqs. (37) and (38) the relations given by eqs. (20 and (36). On the other hand, with excess stresses τ_{xy}' the ratio of the initial stress components does not change, so that in this case quasi-isotropic deformation will occur, in which the τ_{xy}'—γ_{xy}' relation is determined by the slope angle of the τ—γ diagram. As $G_p = E_p/3$, the slope of the τ_{xy}—γ_{xyp} diagramm is $\tan\varphi/3$, so that

$$\begin{aligned} \gamma_{xy}' &= \gamma_{xye}' + \gamma_{xyp}' = \tau_{xy}'/G + 3\tau_{xy}'/\tan\varphi = \\ &= [\{3mE+2(m+1)\tan\varphi\}/mE\tan\varphi]\,\tau_{xy}' \end{aligned} \quad (39)$$

yielding again the same value $F = \tau_{xy}'/E\gamma_{xy}'$ as given in eqs. (36).

---

[21]) BIJLAARD, De Ingenieur in Ned. Indië, no. 4, 1939.

[22]) BIJLAARD, Publ. Int. Ass. f. Bridge and Struct. Eng., Zurich, Vol. 6, p. 27—44, fig. 3.

We may also insert directly in eqs. (18) $\sigma_x = \sigma_y = 0$ and $\tau_{xy} \neq 0$, by which eqs. (18a)—(18d) yield $\partial\varepsilon_{xp}/\partial\sigma_x = \partial\varepsilon_{yp}/\partial\sigma_y = 1/E_p$, $\partial\varepsilon_{yp}/\partial\sigma_x = \partial\varepsilon_{xp}/\partial\sigma_y = -1/2E_p$, whilst for $\partial\gamma_{xyp}/\partial\tau_{xy}$ eq. (18g) applies, in which $\sigma_q^2 = 3\tau_{xy}^2$. The other derivatives are zero. Insertion of these values and of eqs. (10) in eqs. (8) leads again to eqs. (37), (38) and (39) and hence to eqs. (36).

We calculated the critical stress for case 5 with the method as given by SOUTHWELL and SKAN [23]) for the elastic region and as used by SEYDEL [24]) for orthotropic plates. In eq. (68) of our first paper [2]) we gave already the final result of our computations for plates with various proportions, but in order to facilitate a check by designers who want to use it, we shall give here and in section 2.4 a short indication of its derivation. As according to eqs. (36) $D = A$ and the shearing stresses $\tau_{xy} = \tau_P$ acting on an element $h\,dx\,dy$ produce with buckling a resulting force $h\tau_p(\partial^2 w/\partial x\partial y)dxdy$, whilst the same force is given by τ_{yx}, the differential equation (30) of our first paper [2])becomes now [1])

$$EJ\left\{A\left(\frac{\partial^4 w}{\partial x^4} + \frac{\partial^4 w}{\partial y^4}\right) + 2(B+2F)\frac{\partial^4 w}{\partial x^2\,\partial y^2}\right\} - 2h\tau_P\frac{\partial^2 w}{\partial x\,\partial y} = 0 \qquad (40)$$

With $w = Ye^{i\alpha x}$, in which Y is a function of y only and $i = \sqrt{-1}$, eq. (40) yields

$$EJ\{AY'''' - 2(B+2F)\alpha^2 Y'' + A\alpha^4 Y\} - 2i\alpha h\tau_P Y' = 0 \qquad (41)$$

primes denoting differentiation with respect to y. Inserting $Y = e^{i\beta y}$ in this equation, we obtain

$$\beta^4 + 2\frac{B+2F}{A}\alpha^2\beta^2 + 2\frac{h\tau_P}{EJA}\alpha\beta + \alpha^4 = 0 \qquad (42)$$

so that, β_1—β_4 being the roots of equation (42)

$$Y = N_1 e^{i\beta_1 y} + N_2 e^{i\beta_2 y} + N_3 e^{i\beta_3 y} + N_4 e^{i\beta_4 y} \qquad (43)$$

The boundary conditions at $y = \pm c$ yield

$$Y = 0 \qquad \text{and} \qquad Y'' = 0 \qquad (44)$$

Insertion of eq. (43) in here gives us four homogeneous linear equations, yielding only values N, that differ from zero, if the denominator determinant is zero, which gives the buckling condition

$$\begin{aligned}&(\beta_1^2 - \beta_2^2)(\beta_3^2 - \beta_4^2)\sin(\beta_1 c - \beta_3 c)\sin(\beta_2 c - \beta_4 c) = \\ &(\beta_1^2 - \beta_3^2)(\beta_2^2 - \beta_4^2)\sin(\beta_1 c - \beta_2 c)\sin(\beta_3 c - \beta_4 c)\end{aligned} \qquad (45)$$

Writing, as SOUTHWELL and SKAN, the roots of eq. (42) as

$$\beta_{1,2} = \gamma \pm \delta, \qquad \beta_{3,4} = -\gamma \pm \varepsilon \qquad (46)$$

in which γ is real and δ and ε either real or pure imaginaries, comparing of coefficients yields

$$\left.\begin{aligned}-2\gamma^2 - \delta^2 - \varepsilon^2 &= 2\frac{B+2F}{A}\alpha^2 \\ -\gamma(\delta^2 - \varepsilon^2) &= \frac{h\tau_P}{EJA}\alpha \\ (\gamma^2 - \delta^2)(\gamma^2 - \varepsilon^2) &= \alpha^4\end{aligned}\right\} \qquad (47)$$

[23]) SOUTHWELL and SKAN, Proc. Royal Society of London, Series A, 1924, p. 582.
[24]) SEYDEL, Zeitschr. f. Flugt. u. Motorluftsch., 1933, p. 78.

Insertion of eqs. (46) in eqs. (45) gives

$$8\gamma^2\delta\varepsilon(\cos\delta b\cos\varepsilon b-\cos 2\gamma b)=\{4\gamma^2(\delta^2+\varepsilon^2)-(\delta^2-\varepsilon^2)^2\}\sin\delta b\sin\varepsilon b \quad (48)$$

In our paper on this subject [21]), using eq. (26), we calculated first τ_P. Just below the yields stress, with $\tan\varphi=0.294$ E and $e=0.1675$ [2]), eqs. (36) yield, with $m=10/3$

$$A=0.960,\qquad B=0.316,\qquad F=0.078 \quad (49)$$

which values were inserted in eqs. (47). As $w=Ye^{i\alpha x}$, the half wave length in X-direction is π/α. For several half wave lengths π/α value τ_P was calculated from eqs. (47) and (48) be trial and error. We found the smallest value τ_P with a half wavelength $\pi/\alpha=1.1\,b$, for which

$$\tau_P=3.38\,Eh^2/b^2 \quad (50)$$

In the elastic domain the most accurate value is [25]) $\tau_E=4.82\,Eh^2/b^2$, so that eq. (26), in which now σ has to be substituted by τ, yields

$$\tau_B=3.74\,Eh^2/b^2 \quad (51)$$

by which the ratio τ_B/τ_E as given in Table IV is obtained.

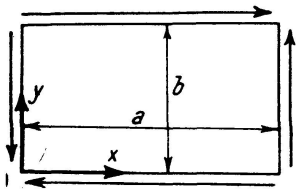

Fig. 8

Case 6 of Table IV, a square plate, simply supported at the edges and subjected to pure shear (fig. 8), was computed by the energy method. As here, according to eqs. (36), $D=A$, eq. (32) may be written as follows [21])

$$V_i=\tfrac{1}{2}EJ\int_0^a\int_0^b\left\{A\left(\frac{\partial^2 w}{\partial x^2}+\frac{\partial^2 w}{\partial y^2}\right)^2+2(B-A)\frac{\partial^2 w}{\partial x^2}\frac{\partial^2 w}{\partial y^2}+4F\left(\frac{\partial^2 w}{\partial x\,\partial y}\right)^2\right\}dx\,dy \quad (52)$$

The work done by the stresses $\tau_{xy}=\tau_P$ is [26])

$$V_0=-h\tau_P\int_0^a\int_0^b\frac{\partial w}{\partial x}\frac{\partial w}{\partial y}\,dx\,dy \quad (53)$$

The expression

$$w=\sum_{p=1}^{\infty}\sum_{q=1}^{\infty}a_{pq}\sin(p\pi x/\alpha)\sin(q\pi y/b) \quad (54)$$

satisfies the boundary conditions. After substitution of eq. (54) in eqs. (52) and (53), the condition $V_0=V_i$ yields

$$\tau_P=-\frac{\pi^4 EJ}{32abh}\,\frac{Aa^2b^2\Sigma\Sigma a_{pq}^2\left(\frac{p^2}{a^2}+\frac{q^2}{b^2}\right)^2-2(A-B-2F)\Sigma\Sigma a_{pq}^2p^2q^2}{\Sigma\Sigma\Sigma\Sigma a_{pq}a_{rs}\frac{pqrs}{(r^2-p^2)(q^2-s^2)}} \quad (55)$$

[25]) Seydel, Ingenieur-Archiv, 1933, p. 169.
[26]) Timoshenko, l. c., footnote 9, p. 314.

To make τ_P a minimum, we have to equate to zero the derivatives of τ_P with respect to each of the coefficients a_{pq}, by which a system of homogeneous linear equations is obtained, containing, except the coefficients a_{pq}, value τ_p as the only unknown quantity. The denominator determinant of these equations, which has to be zero, is, as in the elastic region, the product of two determinants, one for which $p+q$ are odd numbers and the other for which $p+q$ are even numbers. The latter gives the smallest values τ_P. If we limit our calculations to five constants, a_{11}, a_{13}, a_{22}, a_{31} and a_{33}, it has the following form

pq	11	13	22	31	33	
11	$\lambda\{A(1+\beta^2)^2-P\beta^2\}$	·	$\frac{4}{9}$	·	·	
13	·	$\lambda\{A(1+9\beta^2)^2-9P\beta^2\}$	$-\frac{4}{5}$	·	·	
22	$\frac{4}{9}$	$-\frac{4}{5}$	$16\lambda\{A(1+\beta^2)^2-P\beta^2\}$	$-\frac{4}{5}$	$\frac{36}{25}$	$=0$
31	·	·	$-\frac{4}{5}$	$\lambda\{A(9+\beta^2)^2-9P\beta^2\}$	·	
33	·	·	$\frac{36}{25}$	·	$81\lambda\{A(1+\beta^2)^2-P\beta^2\}$	

in which $\beta = \frac{a}{b}$, $\lambda = -\frac{\pi^4 EJ}{32 a^2 \beta h \tau_P}$ and $P = 2(A-B-2F)$

For a square plate, β being 1, it yields [1) 21)]

$$\tau_P = \pm \frac{225\pi^4}{384}(A+B+2F)E\left(\frac{h}{b}\right)^2 \sqrt{\frac{41A+9(B+2F)}{8249A+2601(B+2F)}} \qquad (56)$$

Insertion of eqs. (49) gives

$$\tau_P = 5.64\, E h^2/b^2 \qquad (57)$$

In the elastic domain, with values $A=D$, B and F according to eqs. (28), eq. (56) yields

$$\tau_E = 8.52\, E h^2/b^2 \qquad (58)$$

so that eq. (26), with σ replaced by τ, yields

$$\tau_B = 6.36\, E h^2/b^2 \qquad (59)$$

by which we obtain value $\tau_B/\tau_E = 6.36/8.52 = 0.747$ as inserted in Table IV.

As eq. (40) is the differential equation of a so called orthotropic plate

$$D_1 \frac{\partial^4 w}{\partial x^4} + 2D_3 \frac{\partial^4 w}{\partial x^2 \partial y^2} + D_2 \frac{\partial^4 w}{\partial y^2} - 2h\tau_P \frac{\partial^2 w}{\partial x \partial y} = 0 \qquad (60)$$

in which $D_1 = D_2 = EJA$ and $D_3 = EJ(B+2F)$, τ_P may also be found from a graph, derived by SEYDEL [24)] from computations based on eq. (60). We got in this way for cases 5 and 6, values $\tau_P = 3.42\, Eh^2/b^2$ and $\tau_P = 5.54\, Eh^2/b^2$ respectively, being in good accordance with eqs. (50) and (57).

For case 7 (fig. 9), a plate, subjected to a state of stress $\varrho_2 = \varrho_1$ or $\beta = \varrho_2/\varrho_1 = 1$, it follows from eqs. (20)—(23) that

$$\left.\begin{aligned} A = D &= \frac{m^2\{E + (4 + 3e)\tan\varphi\}}{\{2(m+1) + 3em\}\{mE + 2(m-1)\tan\varphi\}} \\ B &= \frac{m\{-mE + (4 + 3em)\tan\varphi\}}{\{2(m+1) + 3em\}\{mE + 2(m-1)\tan\varphi\}} \end{aligned}\right\} \quad (61)$$

value F having the value of eq. (23). In this case it appears that $B + 2F = A = D$, so that, as $C = B$, eq. (30) of our first paper [2]) transforms into

$$AEJ\left(\frac{\partial^4 w}{\partial x^4} + 2\frac{\partial^4 w}{\partial x^2 \partial y^2} + \frac{\partial^4 w}{\partial y^4}\right) + h\varrho_1\left(\frac{\partial^2 w}{\partial x^2} + \frac{\partial^2 w}{\partial y^2}\right) = 0 \quad (62)$$

so that the differential equation has the same form as in the elastic domain. With $\tan\varphi = 0.294$ E and $e = 0.1675$ it follows from eqs. (61) that $A = 0.531$, whilst in the elastic domain $A = 1.099$. As it is clear that a deflection surface $w = w_0 \sin(\pi x/a) \sin(\pi y/b)$ will give here the smallest buckling stress, it follows immediately from eq. (62) that $\sigma_P = \varrho_1 = (0.531/1.099)\sigma_E$ and, according to eq. (26) $\sigma_B/\sigma_E = 0.673/1.099 = 0.612$, which value has been inserted in Table IV. Furthermore eq. (62) yields, after substitution of this deflection surface,

$$h\sigma_P = h\varrho_1 = (\pi^2 AEJ/a^2)(1 + a^2/b^2) \quad (63)$$

In the elastic region AEJ transforms into the flexural rigidity of the plate, by which eq. (63) becomes identical with the buckling value given by TIMOSHENKO [27]).

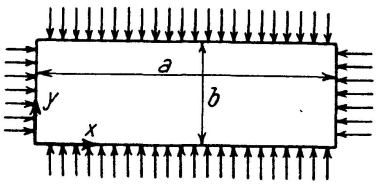

Fig. 9

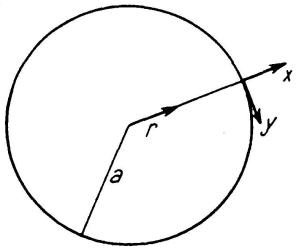

Fig. 10

For a circular plate with clamped edges (fig. 10), case 8, where also $\beta = \varrho_2/\varrho_1 = 1$, we have only to replace in the differential equation for the elastic region [28]) the flexural rigidity of the plate by value AEJ, so that it becomes

$$u^2\frac{d^2\varphi}{du^2} + u\frac{d\varphi}{du} + (u^2 - 1)\varphi = 0 \quad (64)$$

in which $\varphi = -dw/dr$, $u = \alpha r$ and $\alpha^2 = h\sigma_P/AEJ$.

Eq. (64) is a BESSEL equation, being satisfied by

$$\varphi = CJ_1(u) = CJ_1(\alpha r) \quad (65)$$

in which $J_1(u)$ is the BESSEL function of the first order. At the edge $r = a$, the condition

$$\varphi = CJ_1(\alpha a) = 0 \quad (66)$$

---

[27]) TIMOSHENKO, l. c., footnote 9, p. 334.

has to be satisfied. Just as in the elastic region this yields $\alpha a = 3.832$, by which

$$h\sigma_P = AEJ\alpha^2 = \frac{14.68\,AEJ}{a^2} \tag{67}$$

so that, as in the preceding case, $\sigma_P = (0.531/1.099)\,\sigma_E$ and $\sigma_B = (0.673/1.099)\,\sigma_E = 0.612\,\sigma_E$. Furthermore we obtain with eq. (26) $h\sigma_B = 0.673(14.68\,EJ/a^2)$.

If the circular plate is simply supported, case 10, the ratio σ_B/σ_E is not the same, as now also value B appears in the boundary condition, being that the radial moment M_r has to vanish at $r = a$. Placing coordinate axes X and Y as in fig. 10, we have, according to eqs. (29) of our first paper [2])

$$M_r = M_x = -EJ(A\,\partial^2 w/\partial x^2 + B\,\partial^2 w/\partial y^2) = EJ(A\,d\varphi/dr + B\varphi/r)$$

so that the boundary condition at $r = a$ is

$$d\varphi/dr + (B/A)\,\varphi/r = 0 \tag{68}$$

As $dJ_1/du = J_0 - J_1/u$, in which J_0 is the BESSEL function of zero order, this boundary condition transforms into

$$\alpha a J_0(\alpha a) - (1 - B/A) J_1(\alpha a) = 0 \tag{69}$$

With $m = 10/3$, $\tan\varphi = 0.294\,E$ and $e = 0.1675$, eq. (61) yields $B = -0.114$, so that, with $A = 0.531$, eq. (69) becomes

$$\alpha a J_0(\alpha a) - 1.215\,J_1(\alpha a) = 0$$

From a table of BESSEL functions it follows that the smallest root of this equation is $\alpha a = 1.66$, so that

$$h\sigma_P = AEJ\alpha^2 = \frac{2.756\,AEJ}{a^2} \tag{70}$$

whilst in the elastic region [28])

$$h\sigma_E = 4.20\,\frac{m^2}{m^2-1}\,\frac{EJ}{a^2} \tag{71}$$

With $A = 0.531$ and $m^2/(m^2-1) = 1.099$ we get, using eq. (26)

$$h\sigma_P = 1.465\,EJ/a^2, \quad h\sigma_E = 4.616\,EJ/a^2, \quad h\sigma_B = 2.253\,EJ/a^2 \tag{72}$$

so that $\sigma_B = 0.488\,\sigma_E$.

For case 9, an infinitely long plate, compressed in the short direction with length a, so that $\beta = 0$, we have, according to our first paper [2]) $h\sigma_p = \pi^2 EJA/a^2$, in which according to eqs. (27) $A = 0.421$. Hence we get with eqs. (29) and (28) $h\sigma_B = 0.591\,\pi^2 EJ/a^2$ and $h\sigma_E = 1.099\,\pi^2 EJ/a^2$, so that $\sigma_B/\sigma_E = 0.536$.

If on the same plate moreover a compressive stress $\varrho_2 = \varrho_1/2$ is acting in the other direction, so that $\beta = 1/2$, according to case 11 in Table IV, eqs. (20)—(23) yield $A = 0.289$. As here also $h\sigma_P = \pi^2 EJA/a^2$, we find, with $A = 1.099$ in the elastic domain, $h\sigma_B = 0.491\,\pi^2 EJ/a^2$, so that $\sigma_B/\sigma_E = 0.446$.

For a column, case 12, $\sigma_B/\sigma_E = T/E$, so that, just below the yield stress, $\sigma_B/\sigma_E = 875/2100 = 0.417$.

Table IV shows clearly that the less the ratio of the deviator components, as superposed by buckling, differs

[28]) TIMOSHENKO, l. c., footnote 9, p. 368, 369.

from that of the original deviatorcomponents, the smaller is the ratio σ_B/σ_E. With a bar the ratio remains the same, yielding the smallest ratio.

Table IV.

Cases of buckling with decreasing difference between the ratios of the deviatorcomponents of the superposed (by buckling) and the initial state of strain (before buckling).

Case	Boundary conditions and loading	$\beta = \varrho_2/\varrho_1$	Ratio σ_B/σ_E or τ_B/τ_E with buckling just below the yield stress
1	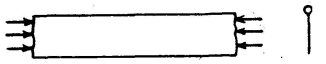	0	0.878
2	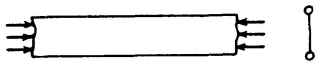	0	0.830
3	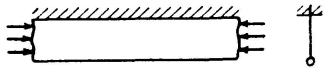	0	0.804
4	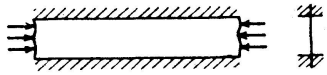	0	0.778
5	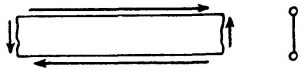	−1	0.775
6	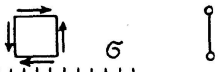	−1	0.747
7	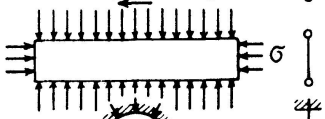	1	0.612
8		1	0.612
9	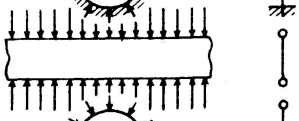	0	0.536
10	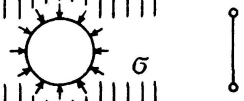	1	0.488
11	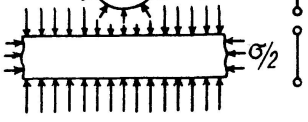	$^1/_2$	0.446
12		0	0.417

In eqs. (69) and (70) of our first paper [2]) we gave a general method of computation of the plastic buckling stresses for plates supported on three or four sides. It is based on the fact that plates, having on the supposition of proportionality of stress and strain a buckling stress, belonging to a slenderness ratio 80, being $\sigma_E = \pi^2 E/\lambda^2 = 3240$ kg/cm^2, have in the plastic domain a buckling stress equaling the yield stress $\sigma_V = 2400$ kg/cm^2, so that $\sigma_B/\sigma_E = 2400/3240 = 0.740$. Table IV shows, that for the cases occurring in bridge and structural engineering, namely, cases 1 to and including 6, this method yields safe results.

1. 5. Plastic stability of shells.

A short indication will be given here as to the application of our theory to the buckling of shells. Our fundamental equations are those giving the relation between the excess stresses and the excess strains with buckling, being, according to eqs. (20)—(23)

$$\left.\begin{aligned} \sigma_x' &= E(A\,\varepsilon_x' + B\,\varepsilon_y') \\ \sigma_y' &= E(B\,\varepsilon_x' + D\,\varepsilon_y') \\ \tau_{xy}' &= EF\,\gamma_{xy}' \end{aligned}\right\} \tag{73}$$

Using the same notations as TIMOSHENKO [29]), except that our primes indicate infinitely small stresses and strains occuring with buckling, we have

$$\left.\begin{aligned} \varepsilon_x' &= \varepsilon_1' - \chi_x'\,z \\ \varepsilon_y' &= \varepsilon_2' - \chi_y'\,z \\ \gamma_{xy}' &= \gamma' - 2\,\chi_{xy}'\,z \end{aligned}\right\} \tag{74}$$

in which ε_1', ε_2' and γ' are the excess strains of the middle surface, χ_x' and χ_y' are the excess curvatures and χ_{xy}' is the twist, whilst z is the distance from the middle surface. Substituting eqs. (74) in eqs. (73) we get

$$\left.\begin{aligned} \sigma_x' &= E\{A\,\varepsilon_1' + B\,\varepsilon_2' - z(A\,\chi_x' + B\,\chi_y')\} \\ \sigma_y' &= E\{B\,\varepsilon_1' + D\,\varepsilon_2' - z(B\,\chi_x' + D\,\chi_y')\} \\ \tau_{xy}' &= EF(\gamma' - 2\,\chi_{xy}'\,z) \end{aligned}\right\} \tag{75}$$

Hence we find [30])

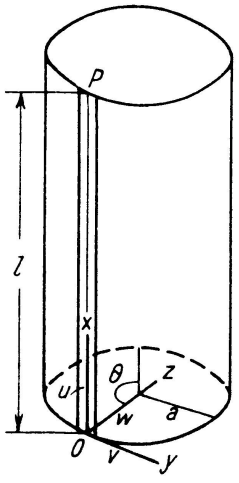

Fig. 11

$$\left.\begin{aligned} N_x' &= \int_{-h/2}^{+h/2} \sigma_x'\,dz = Eh(A\,\varepsilon_1' + B\,\varepsilon_2') \\ N_y' &= \int_{-h/2}^{+h/2} \sigma_y'\,dz = Eh(B\,\varepsilon_1' + D\,\varepsilon_2') \\ N_{xy}' &= \int_{-h/2}^{+h/2} \tau_{xy}'\,dz = EFh\,\gamma' \\ M_x' &= \int_{-h/2}^{+h/2} \sigma_x'\,z\,dz = -EJ(A\,\chi_x' + B\,\chi_y') \\ M_y' &= \int_{-h/2}^{+h/2} \sigma_y'\,z\,dz = -EJ(B\,\chi_x' + D\,\chi_y') \\ M_{xy}' &= -\int_{-h/2}^{+h/2} \tau_{xy}'\,z\,dz = 2\,EJF\,\chi_{xy}' \end{aligned}\right\} \tag{76}$$

As an example we shall consider the buckling of a cylindrical shell under the action of uniform axial pressure $h\sigma_P$ per unit breadth. If buckling occurs symmetrical to the axis of the cylinder, the equilibrium of an element $h\,dx$ of a strip OP of unit width (fig. 11) requires, if compressive stresses are denoted as positive and denoting displacements in Z direction by w,

[29]) TIMOSHENKO, l. c., footnote 9, Chapters VIII and IX.
[30]) Cf. values in elastic regions, l. c., footnote 9, p. 421, 422.

$$dQ_x'/dx - h\sigma_P d^2w/dx^2 - N_y'/a = 0 \tag{77}$$

Value $Q_x' = dM_x'/dx$. Owing to impediment of distortion of the cross-section, χ_y' may be equated to zero, so that eqs. (76) yield

$$M_x' = -EJA\chi_x' = -EJA\, d^2w/dx^2$$

and, as $\varepsilon_2' = -w/a$,

$$N_x' = Eh(A\varepsilon_1' - Bw/a)$$

As, however, $h\sigma_P$ does not increase with buckling, N_x' must be zero, yielding $\varepsilon_1' = (B/A)(w/a)$, by which we obtain

$$N_y' = Eh(B^2/A - D)w/a$$

Substitution of these values in eq. (77) yields, as in (77) N_y' is a compression, the differential equation

$$EJA\frac{d^4w}{dx^4} + h\sigma_P\frac{d^2w}{dx^2} - \left(\frac{B^2}{A} - D\right)\frac{Ehw}{a^2} = 0 \tag{78}$$

With $w = w_0 \sin(p\pi x/l)$ eq. (78) yields, after ranging

$$h\sigma_P = EJAp^2\pi^2/l^2 + (D - B^2/A)(Eh/a^2)\,l^2/p^2\pi^2 \tag{79}$$

With sufficiently long cylinders the wavelength can establish itself in such a way as to make $h\sigma_P$ a minimum. Differentiation shows that then

$$\frac{p\pi}{l} = \sqrt[4]{\frac{AD - B^2}{A^2}\,\frac{h}{a^2J}}$$

insertion of which in eq. (79) yields the critical stress

$$\sigma_P = (Eh/a)\sqrt{(AD - B^2)/3} \tag{80}$$

whilst the length of the half waves in X-direction is

$$\frac{l}{p} = \pi\sqrt[4]{\frac{A^2}{12(AD - B^2)}}\sqrt{ah} \tag{81}$$

In the elastic domain $e = 0$ and $\tan\varphi = \infty$, so that eqs. (20)—(22) yield $A = D = m^2/(m^2-1)$ and $B = m/(m^2-1)$, by which eqs. (80) and (81) transform in

$$\sigma_E = \frac{Eh}{a}\sqrt{\frac{m^2}{3(m^2-1)}} \quad \text{and} \quad \frac{l}{p} = \pi\sqrt[4]{\frac{m^2a^2h^2}{12(m^2-1)}}$$

in accordance with the values obtained directly for this case [31]).

In this case we find with eqs. (80) and (27) $\sigma_P = 0.264\, Eh/a$, whilst $\sigma_E = 0.605\, Eh/a$, so that according to eq. (26) $\sigma_B = 0.349\, Eh/a$ and $\sigma_B/\sigma_E = 0{,}577$, this ratio being between that for cases 8 and 9 in Table IV.

Considering the more general case of buckling of a cylindrical shell under axial compression and denoting the displacements with buckling in X-, Y- and Z-directions by u, v and w respectively, our equations (76) yield, after expression of values ε_1', ε_2', γ', χ_x', χ_y' and χ_{xy}' in terms of the displacements [32]),

[31]) TIMOSHENKO, l. c., footnote 9, p. 440, 441.
[32]) TIMOSHENKO, l. c., footnote 9, p. 434.

$$\left.\begin{aligned}
N_x' &= Eh\left\{A\frac{\partial u}{\partial x} + B\left(\frac{\partial v}{a\,\partial\theta} - \frac{w}{a}\right)\right\}\\
N_y' &= Eh\left\{B\frac{\partial u}{\partial x} + D\left(\frac{\partial v}{a\,\partial\theta} - \frac{w}{a}\right)\right\}\\
N_{xy}' &= N_{yx}' = EFh\left(\frac{\partial u}{a\,\partial\theta} + \frac{\partial v}{\partial x}\right)\\
M_x' &= -EJ\left\{A\frac{\partial^2 w}{\partial x^2} + \frac{B}{a^2}\left(\frac{\partial v}{\partial\theta} + \frac{\partial^2 w}{\partial\theta^2}\right)\right\}\\
M_y' &= -EJ\left\{B\frac{\partial^2 w}{\partial x^2} + \frac{D}{a^2}\left(\frac{\partial v}{\partial\theta} + \frac{\partial^2 w}{\partial\theta^2}\right)\right\}\\
M_{xy}' &= -M_{yx}' = 2EFJ\frac{1}{a}\left(\frac{\partial v}{\partial x} + \frac{\partial^2 w}{\partial x\,\partial\theta}\right)
\end{aligned}\right\} \quad (82)$$

value Θ being indicated in fig. 11.

The conditions of equilibrium are in our notations, and neglecting second order terms [33]),

$$\left.\begin{aligned}
&a\frac{\partial N_x'}{\partial x} + \frac{\partial N_{yx}'}{\partial\theta} = 0\\
&\frac{\partial N_y'}{d\theta} + a\frac{\partial N_{xy}'}{\partial x} - ah\sigma_P\frac{\partial^2 v}{\partial x^2} + \frac{\partial M_{xy}'}{\partial x} - \frac{\partial M_y'}{a\,\partial\theta} = 0\\
&-ah\sigma_P\frac{\partial^2 w}{\partial x^2} + N_y' + a\frac{\partial^2 M_x'}{\partial x^2} + \frac{\partial^2 M_{yx}'}{\partial x\,\partial\theta} + \frac{\partial^2 M_y'}{a\,\partial\theta^2} - \frac{\partial^2 M_{xy}'}{\partial x\,\partial\theta} = 0
\end{aligned}\right\} \quad (83)$$

Substitution of eqs. (82) in eqs. (83) yields

$$\left.\begin{aligned}
&A\frac{\partial^2 u}{\partial x^2} + \frac{B+F}{a}\frac{\partial^2 v}{\partial x\,\partial\theta} - \frac{B}{a}\frac{\partial w}{\partial x} + \frac{F}{a^2}\frac{\partial^2 u}{\partial\theta^2} = 0\\
&(B+F)\frac{\partial^2 u}{\partial x\,\partial\theta} + aF\frac{\partial^2 v}{\partial x^2} + \frac{D}{a}\left(\frac{\partial^2 v}{\partial\theta^2} - \frac{\partial w}{\partial\theta}\right) +\\
&\alpha\left\{\frac{D}{a}\left(\frac{\partial^2 v}{\partial\theta^2} + \frac{\partial^3 w}{\partial\theta^3}\right) + a(B+2F)\frac{\partial^3 w}{\partial x^2\,\partial\theta} + 2aF\frac{\partial^2 v}{\partial x^2}\right\} - \frac{ah\sigma_P}{Eh}\frac{\partial^2 v}{\partial x^2} = 0\\
&-\frac{ah\sigma_P}{Eh}\frac{\partial^2 w}{\partial x^2} + B\frac{\partial u}{\partial x} + \frac{D}{a}\frac{\partial v}{\partial\theta} - \frac{D}{a}w - \alpha\left\{a(B+4F)\frac{\partial^3 v}{\partial x^2\,\partial\theta} + \frac{D}{a}\frac{\partial^3 v}{\partial\theta^3} +\right.\\
&\left.a^3 A\frac{\partial^4 w}{\partial x^4} + 2a(B+2F)\frac{\partial^4 w}{\partial x^2\,\partial\theta^2} + \frac{D}{a}\frac{\partial^4 w}{\partial\theta^4}\right\} = 0
\end{aligned}\right\} \quad (84)$$

in which $\alpha = h^2/12\,a^2$. Assuming

$$\left.\begin{aligned}
u &= u_0\cos n\theta\cos p\pi x/l\\
v &= v_0\sin n\theta\sin p\pi x/l\\
w &= w_0\cos n\theta\sin p\pi x/l
\end{aligned}\right\} \quad (85)$$

eqs. (84) transform into

[33]) TIMOSHENKO, l. c., footnote 9, p. 454.

$$\left.\begin{aligned}
&(A\lambda^2 + Fn^2)\,u_0 - (B+F)\,n\lambda\,v_0 + B\,\lambda w_0 = 0\\
&-(B+F)\,n\lambda\,u_0 + \{Dn^2(1+\alpha) + F\lambda^2(1+2\alpha) - \sigma_P\lambda^2/E\}\,v_0 -\\
&\qquad - n\{D(1+\alpha n^2) + (B+2F)\,\alpha\lambda^2\}\,w_0 = 0\\
&B\lambda u_0 - n\{D(1+\alpha n^2) + (B+4F)\,\alpha\lambda^2\}\,v_0 +\\
&\qquad + \{A\alpha\lambda^4 + 2(B+2F)\,\alpha n^2\lambda^2 + D(1+\alpha n^4) - \sigma_P\lambda^2/E\}\,w_0 = 0
\end{aligned}\right\} \quad (86)$$

in which $\lambda = p\pi a/l$. Hence the critical stress σ_P follows by equating the determinant of the equations to zero. Further computations may be effected along the same lines as in the elastic region.

In order to check eqs. (86) we again assume buckling symmetrical to the axis of the cylinder, so that in eqs. (85) we have to equate n to zero, by which also v becomes zero. Hence the second equation (86) vanishes and eqs. (86) transform into

$$\left.\begin{aligned}
&A\lambda u_0 + B w_0 = 0\\
&B\lambda u_0 + (A\alpha\lambda^4 + D - \sigma_P\lambda^2/E)\,w_0 = 0
\end{aligned}\right\} \quad (87)$$

yielding $$\sigma_P = E\{A\alpha\lambda^2 + (AD - B^2)/A\lambda^2\}$$

or $$h\sigma_P = EJAp^2\pi^2/l^2 + (D - B^2/A)(Eh/a^2)\,l^2/p^2\pi^2$$

in accordance with eq. (79).

As a matter of fact thick tubes, buckling in the plastic domain, do this usually in a symmetrical way, whilst with thin tubes buckling which is non-symmetrical with respect to the axis usually occurs[34]). This behaviour is in good accordance with our theory, because non-symmetrical buckling causes twisting stresses, against which, if e is small, as with steel, the resistance is only slightly diminished according to our theory, value F in eqs. (29) being not much less than in eqs. (28). We can prove it directly with our eqs. (86). For the elastic domain TIMOSHENKO proves that, if λ^2 is a large number, the critical stress with non-symmetrical buckling is equal to that with symmetrical buckling[35]). Taking into account the same terms as he does, we find for the plastic domain, by equating the determinant of eqs. (86) to zero, the following equation

$$\{(A\lambda^2 + Fn^2)(F\lambda^2 + Dn^2) - (B+F)^2 n^2\lambda^2)\,\lambda^2\sigma_P/E =$$
$$= (AD - B^2)F\lambda^4 + \alpha\{A\lambda^4 + 2(B+2F)n^2\lambda^2 + Dn^4\}\{(A\lambda^2 + Fn^2)(F\lambda^2 + Dn^2) - (B+F)^2 n^2\lambda^2\}$$

or, after transformation

$$\frac{\sigma_P}{E} = \frac{(AD - B^2)\,\lambda^2}{A\lambda^4 + Dn^4 + \{(AD - B^2)/F - 2B\}n^2\lambda^2} + \frac{\alpha\{A\lambda^4 + Dn^4 + 2(B+2F)n^2\lambda^2\}}{\lambda^2} \quad (88)$$

In the elastic domain we have[2]) $A = D = m^2/(m^2-1)$, $B = m/(m^2-1)$, $F = m/2(m+1)$, so that $(AD - B^2)/F - 2B = 2(B+2F) = 2m^2/(m^2-1)$, by which the denominator of the first fraction of the second member of eq. (88) is equal to the term in brackets of the numerator of the second fraction. If in the plastic region this were so too, we could write eq. (88) as follows

$$\sigma_P/E = (AD - B^2)\,\psi + \alpha/\psi \quad (89)$$

---

[34]) TIMOSHENKO, l. c., footnote 9, p. 443.
[35]) TIMOSHENKO, l. c., footnote 9, p. 456.

value ψ being a function of values λ and n that determine the number of waves in axial and circumferential direction. In order to make σ_p a minimum, we then would have the condition

$$\psi = \sqrt{\alpha/(AD-B^2)}$$

by which eq. (89) would yield

$$\sigma_P = 2E\sqrt{\alpha(AD-B^2)} \qquad \text{or} \qquad \sigma_P = (Eh/a)\sqrt{(AD-B^2)/3}$$

in accordance with the buckling stress for symmetrical buckling as given by eq. (80). In the plastic domain, however, considering for example buckling at the yield stress with mild steel, value $(AD-B^2)/F-2B$ will be much less than $2(B+2F)$. In this case we have, according to eqs. (27), $(AD-B^2)/F-2B = -0.19$, whilst $2(B+2F) = 2.14$. Consequently the second fraction to the second member of eq. (88) has a much higher value than with our assumption that gave eq. (89). Hence we may conclude that with higher values λ^2 in the plastic domain the critical stress with non-symmetrical buckling is higher than with symmetrical buckling, which may explain why short and thick tubes usually buckle symmetrically. In another paper we shall consider these questions more in detail.

2. Stability of the webs of bridge members and girders

2. 1. Columns with open or closed box section.

In our first paper [2]) we gave in Table I, page 68, design formulae for compression members in structural steel No. 37. After we wrote it, we had also values γ_3 determined, relating to sections 4 of Table I (fig. 12),

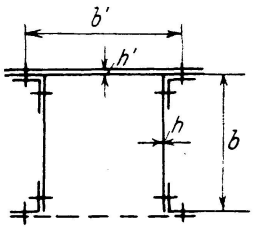

Fig. 12

published first in a more extensive paper on this subject [36]) and reproduced here in fig. 13. These values γ_3 have consequently to be used for sections 4, as given in fig. 12, instead of values γ_2, which we recommended provisionally for want of values γ_3. Also these curves were calculated by my former assistent in Bandoeng, Ir. L. F. Cooke and by Ir. P. Th. Wijnhamer. They have the same general trend as the curves for γ_1 and γ_2, a difference being, however that for example the point of intersection of the two curves for $\beta=3$ is at about $\mu=0.87$, whilst for γ_1 and γ_2, given in figs. 13 and 14 of our first paper [2]), this point is at $\mu = 0.76$. In order to make this problem and the graphs better understood, we shall explain this difference.

In the same way as γ_1 and γ_2 were inserted in eq. (62) of our first paper, γ_3 is inserted in the equation

$$\frac{b}{h} = \left(\frac{b}{h}\right)_{SF} - \left\{\left(\frac{b}{h}\right)_{SF} - \left(\frac{b}{h}\right)_{SS}\right\}\gamma_3 \qquad (90)$$

[36]) Bijlaard, De Ingenieur in Ned. Indië, no. 10, 1939.

$(b/h)_{SF}$ being the value of b/h if one unloaded side of the plate is simply supported and the other side is fixed and $(b/h)_{SS}$ being valid if both sides are simply supported. If both values are expressed in the slenderness ratio of a bar that has the same buckling stress, we obtain for the elastic domain

$$\left(\frac{b}{h}\right)_{SS} = 0.606\,\frac{l}{r} \quad \text{and} \quad \left(\frac{b}{h}\right)_{SF} = 0.70\,\frac{l}{r} \tag{91}$$

insertion of which in eq. (90) yields

$$b/h = (0.7 - 0.094\,\gamma_3)\,l/r = 0.7\,(1 - 0.14\,\gamma_3)\,l/r \tag{92}$$

according to the formula given in Table I for section 4 for $l/r \geq 100$. Our computation of γ_3 is based on eq. (59) of our first paper [2]), in which $\Theta = \Theta_b$ according to eqs. (53) and (54) there. With values $\beta = 1/2$, 1 or

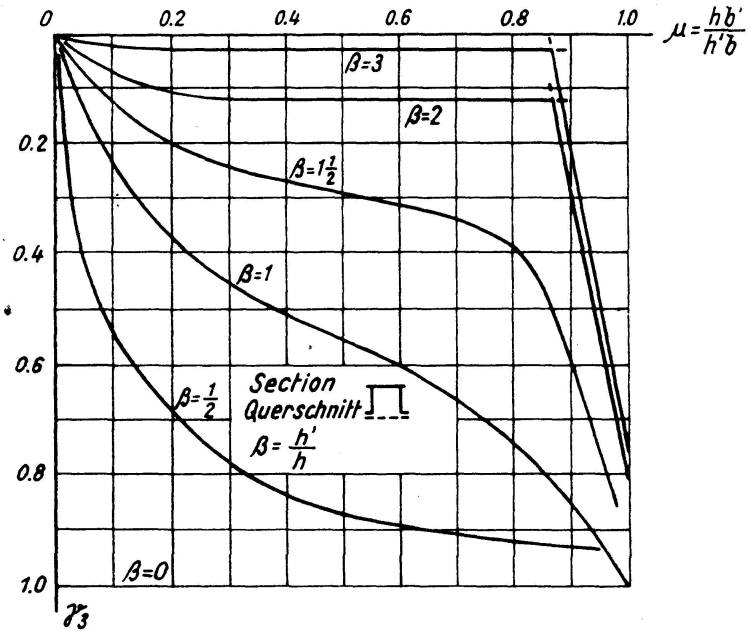

Fig. 13

3/2 the β curves in fig. 13 are continuous, α_2' having a real value, so that the deflection surface of the „resisting" plate is given by eq. (44) of our first paper, being

$$w' = (C_1' \cosh \alpha_1' y' + C_2' \sinh \alpha_1' y' + C_3' \cos \alpha_2' y' + C_4' \sin \alpha_2' y') \cos(p\pi x/a) \tag{93}$$

The curves for $\beta = 2$ and 3, however, consist of two branches. With $\beta = 3$ and values μ smaller than 0.87, value γ_3 is about 0.03, so that the „buckling" plates, with thickness h, being the vertical plates in fig. 12, are practically fixed at the upper sides by the thick „resisting" plate. In this case the latter has a thickness $3h$, so that the thinner „buckling" plates influence it only slightly. Therefore the „buckling" plates will buckle with a half wave length a/p that is practically the same as if one side is fixed and the other simply supported, being about $0.8\,b$. If for example $\mu = 0.8$, value b' will equal $2.4\,b$, so that this will bend the thick „resisting" plate in half waves with a length of about one third of its breadth. We showed this in fig. 14a, by rotating the vertical plates in the plane of the upper plate,

buckling to the out- and inside being indicated by plus and minus signs respectively. As the most favourable wavelength for buckling of the upper plate is about equal to its breadth, this will not promote its own buckling. Apparently it acts here as a number of plates with breadths $0.8\,b$ and lengths b'. As with a length larger than the breadth $0.8\,b$, the resistance of suchlike plates against angular rotation at the short edges SS and TT (fig. 14a) practically does not vary, this explains too why γ_3 is practically constant with μ varying between 0.25 and 0.8. As here, moreover, the compressive stresses in the upper plate have little influence, so that it is not

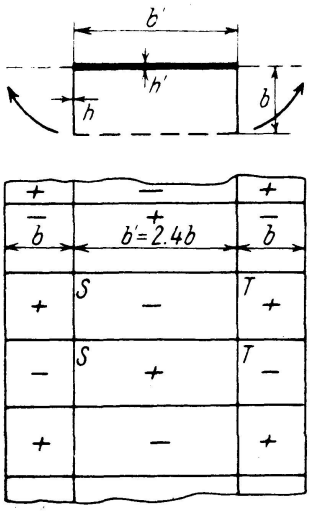

Fig. 14a

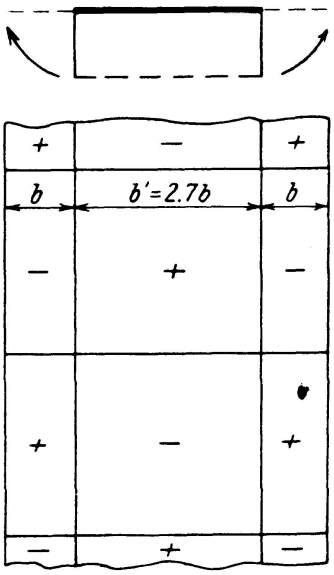

Fig. 14b

actually buckling, but is bent only by the „buckling" plates, the sine and cosine functions, which are typical for buckling, do not appear here in the equation of the deflection surface w. Value α_2' is imaginary here, so that w' ist given by eq. (50) of our first paper [2]), being

$$w' = (C_1'' \cosh \alpha_1'' y' + C_2'' \sinh \alpha_1'' y' + C_3'' \cosh \alpha_2'' y' + C_4'' \sinh \alpha_2'' y') \cos(p\pi x/a) \quad (94)$$

If, however, ratio b'/h' of the upper „resisting" plate, equals about the ratio with which it would buckle itself, if its sides were simply supported, being, according to eq. (91)

$$b'/h' = 0.606\, l/r \qquad \text{or} \qquad \mu = h b'/h' b = 0.606\,(l/r)\, h/b \quad (95)$$

it will buckle itself in its own most favourable half wavelength, being about equal to b'. It forces the same wavelength to the thin „buckling" plates which offer only little constraint to it. This is shown in fig. 14b. As with γ_3 between 0 and 1, value b/h varies according to eq. (92) between $0.7\,l/r$ and $0.6\,l/r$, this kind of buckling, for which α_2' is real, so that the deflection surface is given by eq. (93), will occur according to eq. (95) with values μ that vary between about 0.87 and 1 with γ_3 varying between 0 and 1. This is in accordance with the second branch of curve $\beta = 3$ in fig. 13. The fact that with $\mu = 1$, although both plates have the same ratio $b'/h' = b/h$,

value γ_3 is still smaller than unity, so that the buckling stress of the plates is still higher than with simply supported edges, is explained as follows. As h' is more than h, the breadth b' is more than b, by which the most favourable wavelength of the plates is different. As, however, they have to buckle in the same common wavelength, their buckling stress will be enhanced, being higher than that of a plate with simply supported edges. Only if $\beta = 1$, so that, with $\mu = 1$, also $b' = b$, by which for both plates the most favourable wavelength is $b' = b$, with $\mu = 1$ value γ_3 is equal to unity too.

All these remarks are generally valid as well for values γ_1 and γ_2, given in figs. 13 and 14 of our first paper[2]). The difference is, however, that there $\gamma = 0$ relates to a plate of which b o t h sides are fixed, so that for $\gamma = 0$ the ratio $b/h = 0.8\ l/r$. Therefore in the graphs for γ_1 and γ_2 the second branch of the curves $\beta = 3$ will correspond, according to eq. (95), with values μ varying from 0.76 to 1 with γ varying from 0 to 1. This tallies with those graphs and explains why there the point of intersection of the two curves is at $\mu = 0.76$, whilst in fig. 13 of our present paper it is at $\mu = 0.87$.

2. 2. Stability of Tee stiffeners.

This subject has already been treated[37]). It involves the proper choice of stiffeners to support the plating of reinforced monocoque construction or for example the web of plate girders. The ends $x = 0$ and $x = a$ and the edge $y = 0$ of the stiffener web being assumed to be simply supported (fig. 15),

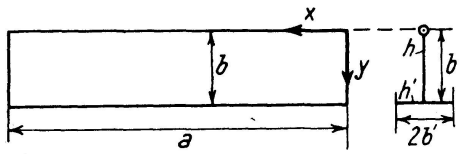

Fig. 15

the relative boundary conditions, which we may omit here, reduce the solution of the differential equation of the stiffener web to

$$w = (C_2 \sinh \alpha_1 y + C_4 \sin \alpha_2 y) \sin (p\pi x/a) \tag{96}$$

using the same notations as in our first paper[2]). For the edges $y = b$ of the stiffener web WINDENBURG, who assumes moreover the deformations to be elastic up to the yield stress, admits however the following two boundary conditions

$$N\left(\frac{\partial^3 w}{\partial y^3} + \frac{2m-1}{m}\frac{\partial^3 w}{\partial x^2\,\partial y}\right) - B_2\frac{\partial^4 w}{\partial x^4} - A_2\sigma_x\frac{\partial^2 w}{\partial x^2} = 0 \tag{97}$$

$$-N\left(\frac{\partial^2 w}{\partial y^2} + \frac{1}{m}\frac{\partial^2 w}{\partial x^2}\right) = C\frac{\partial^3 w}{\partial x^2\,\partial y} \tag{98}$$

in which N is the flexural rigidity of the web and B_2, C and A_2 are the flexural rigidity, the torsional rigidity, and the area of the flange respectively, whilst w denotes the deflection of the stiffener web perpendicular to the XY-plane. These are the same boundary conditions as assumed by

[37]) WINDENBURG, Proc. of the 5th Int. Congress for Applied Mechanics. Cambridge, Mass.

CHWALLA [38]), of which, as we showed [2]), condition (98) neglects the torsional action of the compressive forces in the flange, so that the torsional rigidity of the flange is over-estimated. In order to take this action into account, we have to replace eq. (98) by the boundary condition (IV), preceding eq. (61) in our first paper [2]), so that in the elastic region we get

$$\frac{\partial^2 w}{\partial y^2} + \frac{1}{m}\frac{\partial^2 w}{\partial x^2} = -\frac{1}{\Theta_2}\frac{\partial w}{\partial y} \tag{99}$$

in which, as follows from eqs. (56) and (58) given there [2])

$$\Theta_2 = \frac{1}{2}\left(\frac{h}{h'}\right)^3 \frac{(\alpha_1'^2 r'^2 - \alpha_2'^2 q'^2)\sinh\alpha_1' b' \sin\alpha_2' b' - \alpha_1'\alpha_2'(q'^2 + r'^2)\cosh\alpha_1' b' \cos\alpha_2' b' - 2\alpha_1'\alpha_2' q' r'}{(\alpha_1'^2 + \alpha_2'^2)(\alpha_1' r'^2 \cosh\alpha_1' b' \sin\alpha_2' b' - \alpha_2' q'^2 \sinh\alpha_1' b' \cos\alpha_2' b')} \tag{100}$$

Introducing eq. (96) in the boundary conditions (97) and (99), these yield two homogeneous linear equations in C_2 and C_4. Equating the denominator determinant of these equations to zero, leads to the same condition, as obtained, if in the general buckling condition (61) of our first paper [2]) we equate values s_1 and Θ_1 to zero, namely

$$(\sinh\alpha_1 b \sin\alpha_2 b)\{\Theta_2 s_2 t^2 + \alpha_1\alpha_2 t^2 \coth\alpha_1 b \cot\alpha_2 b + \alpha_2 t(\Theta_2 q^2 - s_2)\cot\alpha_2 b - \\ - \alpha_1 t(\Theta_2 r^2 - s_2)\coth\alpha_1 b\} = 0 \tag{101}$$

As we pointed out already [2]), a solution of eq. (101) is only obtained if the last factor is equated to zero. Using, as did WINDENBURG, the notations introduced by MILES and some additional ones, this yields

$$\Theta = \frac{(1-\nu-\sigma)^2\delta_1\coth\delta_1 - (1-\nu+\sigma)^2\delta_2\cot\delta_2 - 2R\sigma\sqrt{\sigma^2-1}\coth\delta_1\cot\delta_2}{R(\delta_1\coth\delta_1 - \delta_2\cot\delta_2) + 2\psi\varphi} \tag{102}$$

in which

$$R = 2\psi\beta^2 \frac{\Phi_3(1-\nu-\varrho)^2\sqrt{\varrho+1} - \Phi_2(1-\nu+\varrho)^2\sqrt{\varrho-1}}{\Phi_1\{(1-\nu)^2-(1-2\nu)\varrho^2\} - \Phi_4\{(1-\nu)^2+\varrho^2\}\sqrt{\varrho^2-1} + \{(1-\nu)^2-\varrho^2\}\sqrt{\varrho^2-1}} \tag{103}$$

and

$$\Theta = \frac{EJ}{bD} - \frac{A}{bh}\frac{\psi^2}{\varphi^2}, \quad \sigma = \frac{\psi}{\varphi}, \quad \delta_1 = \varphi\sqrt{\sigma+1}, \quad \delta_2 = \varphi\sqrt{\sigma-1},$$

$$\Phi_1 = \sinh\varepsilon_1\sin\varepsilon_2, \quad \Phi_2 = \sinh\varepsilon_1\cos\varepsilon_2, \quad \Phi_3 = \cosh\varepsilon_1\sin\varepsilon_2, \quad \Phi_4 = \cosh\varepsilon_1\cos\varepsilon_2,$$

$$\varepsilon_1 = \frac{f}{2b}\varphi\sqrt{\varrho+1}, \quad \varepsilon_2 = \frac{f}{2b}\varphi\sqrt{\varrho-1}, \quad \varrho = \frac{\psi}{\varphi\beta}, \quad \beta = \frac{t}{h},$$

$$\varphi = p\pi\frac{b}{a}, \qquad \psi = b\sqrt{\frac{\sigma_x h}{D}},$$

where D is the flexural rigidity of the web and EJ and A are the flexural rigidity and the area of the flange respectively, being in our notations N, B_2 and A_2 respectively. The values f and t replace our values $2b'$ and h' and are shown in fig. 16, whilst values b, b', h and h' are shown in fig. 15. For the number of half waves in X-direction we keep the notation p, whilst ν is POISSON's ratio. With given values h'/h and b'/b, we can calculate with eqs. (102) and (103) values Θ corresponding to given values φ and ψ. In this way we had graph fig. 16 made by our former assistant in Bandoeng, IR. LIE HAN YANG and his sister Miss LIE LIEN NIO. The general trend of

[38]) CHWALLA, Ingenieur-Archiv, Vol. 5, no. 1, 1934.

the curves of constant Θ is the same as that in the graph of WINDENBURG, as could be expected. If Θ equals 50, the buckling of the web, that occurs also with a value ψ of about 2 φ, will require practically the same ψ value as with infinite Θ. With infinite Θ, $\psi = 2\,\varphi$ and $\nu = 0.3$ we find from eqs. (102) and (103)

$$\beta^2\{\sqrt{3}\coth(\varphi\sqrt{3})-\cot\varphi\}\frac{\Phi_2(0.7+\varrho)^2\sqrt{\varrho-1}-\Phi_3(0.7-\varrho)^2\sqrt{\varrho+1}}{\Phi_1(0.49-0.4\varrho^2)-\Phi_4(0.49+\varrho^2)\sqrt{\varrho^2-1}+(0.49-\varrho^2)\sqrt{\varrho^2-1}}=1 \quad (104)$$

by means of which we had the graph in fig. 17 calculated, the full lines being those according to our theory. Whilst, with a given value t/h, a computation based on boundary condition (98) will always show an increase of ψ with increasing ratio f/b, as ψ

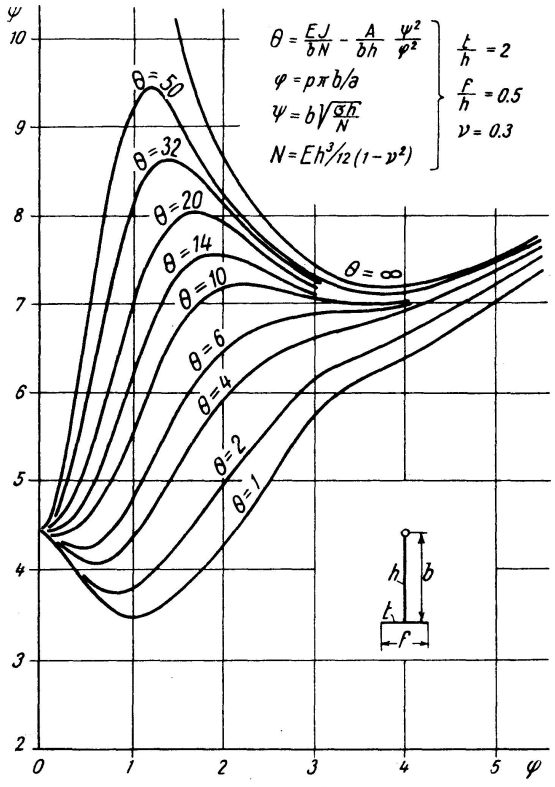

Fig. 16

increases with $C/bD = 1.4\ f t^3/b h^3$ up to 7.30 as an upper limit[37]), as is shown in fig. 17 by the dotted lines, it does not according to eq. (104). As a matter of fact, with a given value of f/b, the value ψ will reach a maximum. For example, with $t/h = 1$ this happens with a ratio f/b of about 0.4, because then the increase of C will be cancelled by the increase of the buckling action of the compressive stresses σ_x in the flange. With $f/b = 0.75$, the value of ψ with $t/h = 1$ is even equal to that with $f/b = 0$, so that the flange does not offer any twisting resistance to the web, whilst with higher values of f/b it even promotes the buckling of the web. So we see that with lower t/h values neglect of the buckling action of the compressive stresses σ_x in the flange

causes an appreciable over-estimation of the buckling stress. If both sides of a web plate are supported by flanges this over-estimation will be about twice.

Besides a buckling of the web, a torsional buckling of the stiffener as a whole may occur. This case is also included in the graph, fig. 16. One reason for our having the graph made was, that we wanted to see, down to which ratio a/b the modified WAGNER formula, that supposes the web to remain plane, may be applied with varying values of C/bD, the case of fig. 16 representing about the highest value that will occur. With this graph we found, that with $\varphi = 1$ the WAGNER formula gives ψ values being at most somewhat more than 10 % too high, whilst with $\varphi = 0.5$ the error is not more than 5%. With φ smaller than 0.2 the error is negligible. From the graph for MILES' case [37]), where $C/bD = 0$, we found that with $\varphi = 1$ the errors were much greater, but with $\varphi = 0.5$ they were already smaller than in the former case.

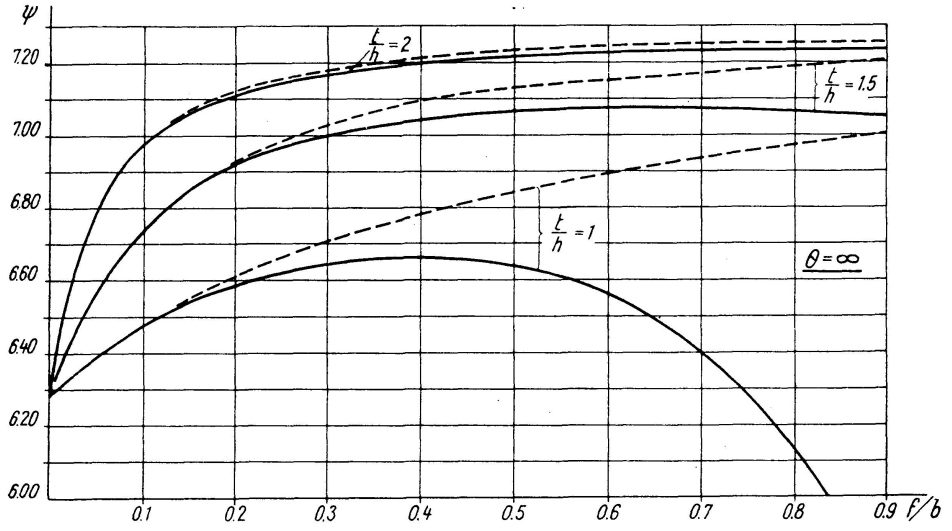

Fig. 17

We demand the stiffeners to be designed in such a way, that they will not buckle below the yield stress. Considering the twisting stability, it will then be necessary, according to our theory of plastic stability [2]), to take into account the decrease of the torsional rigidity by replacing the modulus of rigidity G by EF. To take into account the decrease of the flexural rigidity of the flange, we shall have to replace in the relative term the modulus of elasticity E by the reduced modulus T. In this way the modified WAGNER formula for a Tee section [37]) will become in the plastic domain

$$\sigma_T = \frac{EF\left(\frac{b}{h} + \frac{f}{h}\frac{t^3}{h^3}\right) + \gamma T \frac{\pi^2}{4}\frac{b^2}{l^2}\left(\frac{f^3}{h^3}\frac{t}{h} + \frac{1}{3}\frac{b}{h}\right)}{\frac{b^3}{h^3} + 3\frac{b^2}{h^2}\frac{f}{h}\frac{t}{h} + \frac{1}{4}\frac{f^3}{h^3}\frac{t}{h}} \qquad (105)$$

Just below the yield stress, according to eq. (27) F equals 0.322 in the plastic part of the cross-section, and as in this case the overlargest part of the cross-section will deform plastically, we remain on the safe side by keeping this value for the entire cross-section. Furthermore T is here $0.417\,E$. Furthermore, with WINDENBURG, we shall take into account the fact, that

at the ends the stiffener is not simply supported and that the plating, to which it is attached, will give it a partial fixation, by equaling γ to 2, thus assuming the effective length of the stiffener, that we called a, to equal $l/\sqrt{2}$, l being the real length. If we demand that σ_T shall equal the yield stress $\sigma_V = 2400$ kg/cm², we find from eq. (105) that the allowable ratio l/h of a stiffener is

$$\frac{l}{h} = \frac{b}{h}\sqrt{\frac{\frac{\pi^2}{4.8}\left(\frac{f^3}{h^3}\frac{t}{h}+\frac{1}{3}\frac{b}{h}\right)}{\left(\frac{b^3}{h^3}+3\frac{b^2}{h^2}\frac{f}{h}\frac{t}{h}+\frac{1}{4}\frac{f^3}{h^3}\frac{t}{h}\right)\frac{\sigma_v}{E}-0.322\left(\frac{b}{h}+\frac{f}{h}\frac{t^3}{h^3}\right)}} \tag{106}$$

According to the preceding we considered for this special case this formula to be sufficiently accurate down to a ratio $l/b = 6$, thus down to $a/b = 4.2$ or up to $\varphi = 0.75$. Although with $\varphi = 0.75$ the WAGNER formula may give ψ values that are about 7 % too high and so a buckling stress in the elastic region that is about 15 % too high, in the plastic region it is not so bad. It means only a difference of 7 % in the comparable slenderness ratio. As the buckling stress depends to a great extent on the reduced modulus T, this corresponds at most to an error of about 2 % in the plastic buckling stress. With respect to the assumptions on which suchlike computations have

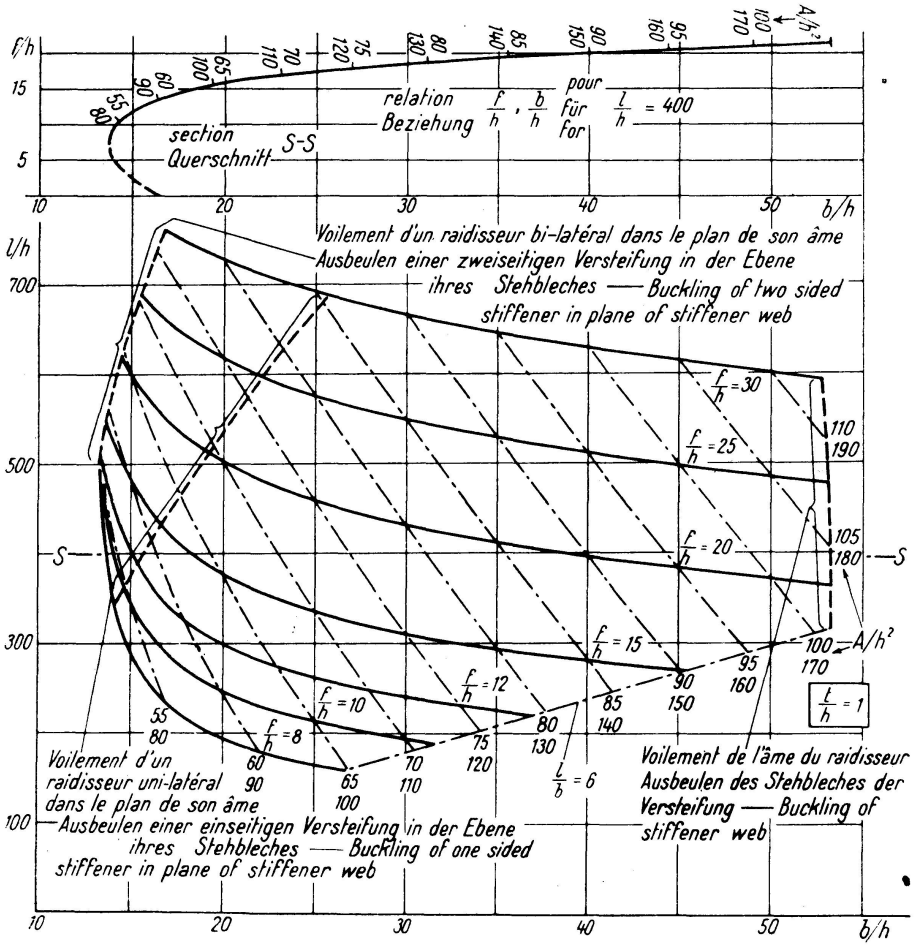

Fig. 18.

Stiffeners with buckling stress equal to yield stress 2400 kg/cm² — Aussteifungen mit Beulspannung in der Größe der Fließgrenze von 2400 kg/cm² — Raidisseurs dont les contraintes de voilement sont égales à la limite d'écoulement de 2400 kg/cm²

to be based, as for example the fixation of γ, we refrained from introducing any correction, save breaking of the graphs at a value $l/b = 6$. Eq. (106) is represented graphically in figs. 18, 19 and 20. These curves and those of fig. 17 were calculated in Bandoeng by ir. WIJNHAMER and the students E. and P. SMITH.

As to the buckling of the stiffener web, we see in Table IV that for cases 2 and 3, being its limiting cases, the ratio σ_B/σ_E is at least *0.804*. The modulus of rigidity, to which the twisting rigidity of the flange is practically proportional for the sections for which buckling of the web has to be considered, i. e. with b/h more than 51, is with our assumption $F = 0.322$ only $0.322/0.385 = 0.835$ times its value in the elastic domain.

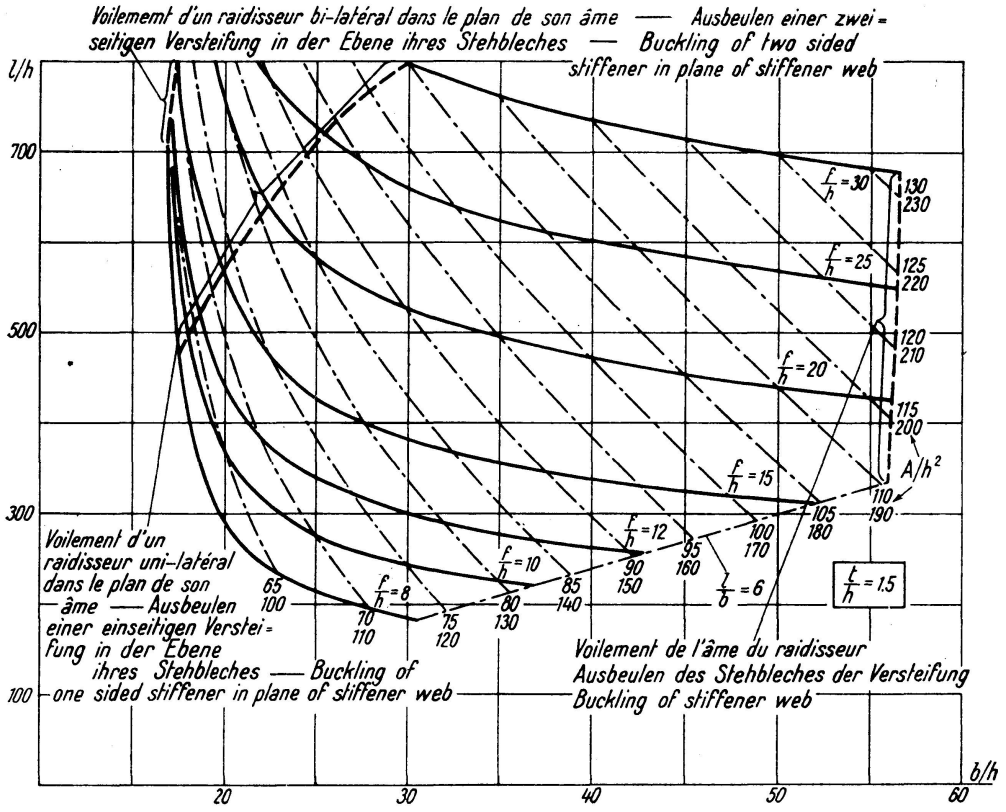

Fig. 19.

Stiffeners with buckling stress equal to yield stress 2400 kg/cm² — Aussteifungen mit Beulspannung in der Größe der Fließgrenze von 2400 kg/cm² — Raidisseurs dont les contraintes de voilement sont égales à la limite d'écoulement de 2400 kg/cm²

We may thus save ourselves the trouble of making a special computation for the plastic domain, as we are safe and sufficiently accurate, if we reckon with a reduced modulus of $0.8\,E$. We have consequently to demand that the elastic buckling stress of the web shall not be less than $1.25\,\sigma_V = 3000$ kg/cm². This requires, according to the expression for value ψ as given below eq. (103), that b/h shall be smaller than $8\,\psi$, whilst ψ is given in fig. 17, from which the curves, that shall not be surpassed lest the web will buckle, as drawn in figs. 18, 19 and 20, have been computed. As at these curves the Θ values of the sections are not less than about 50, it is allowable, according to the preceding, to reckon here with the graph of fig. 17, computed for infinite Θ.

Furthermore the f/h curves in figs. 18—20 have been bounded by two other curves, in order to prevent buckling in a plane perpendicular to the supported plating and thus in the plane of the stiffener web, one for the case of a one-sided stiffener, the other for a two-sided stiffener. We had to demand here only, that the slenderness ratio of the stiffener, simply supported at the ends, should equal its maximum value at the yield stress, being 60. In this calculation we took into account a strip of thickness h and breadth 30 h of the supported plating. This was done too for the curves of equal A/h^2 values, where A is the total area of the stiffener, which were drawn to facilitate the finding of a proper section. The two values for A/h^2 refer to one and two-sided stiffeners. It is understood that the allowable stress in these stiffeners is that corresponding to a slenderness ratio 60.

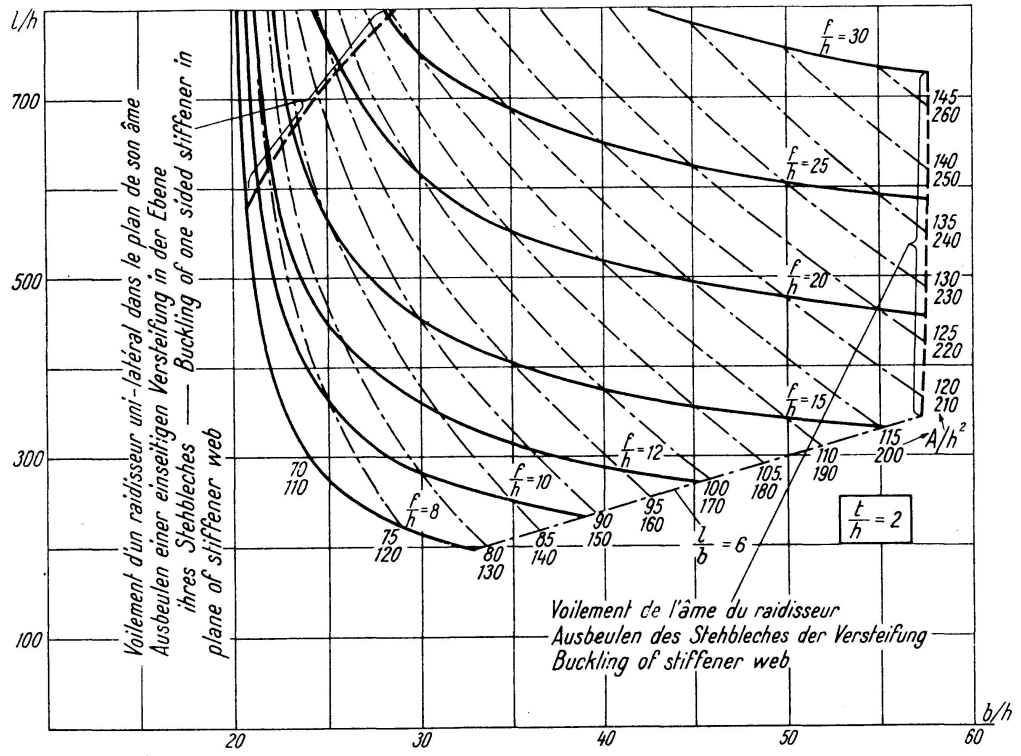

Fig. 20.

Stiffeners with buckling stress equal to yield stress 2400 kg/cm² — Aussteifungen mit Beulspannung in der Größe der Fließgrenze von 2400 kg/cm² — Raidisseurs dont les contraintes de voilement sont égales à la limite d'écoulement de 2400 kg/cm²

There is still another way to take the buckling action of the compressive stresses in the flange into account, viz. to reckon with a reduced C value, C_r, of the torsional rigidity. If σ_s is the buckling stress of the flange in case it is simply supported on the stiffener web, value σ_s with varying buckling length being given in the handbooks, at this stress σ_s the buckling action of the compressive stresses obviously cancels the rigidity to twisting of the flange. Consequently with an arbitrary stress σ_x the fraction σ_x/σ_s of the rigidity to twisting will be cancelled, by which it becomes only $(1-\sigma_x/\sigma_s)$ times the rigidity of a flange without compressive stresses. So its reduced torsional rigidity is approximately

$$C_r = (1-\sigma_x/\sigma_s)\, C \qquad (107)$$

In this way data, obtained by the formerly customary computation based on eq. (98), may be corrected by using values C_r instead of C, by which σ_x, the respective wavelength and σ_s may be found by trial and error.

2. 3. Stability of angles.

As we communicated already in our first paper [2]), we derived the design formulae for steel angles, as given there in Table I, by a new and easy method, given in a special paper on the stability of angles [17]). As this method was used by us later for many other problems of stability, a summary of which is given in Chapter 3 of the present paper, we expose it here. We shall not investigate, as we did before [17]), which part of the angle behaves plastically and which elastically, but we shall simply use eq. (26). We first assume that the entire cross-section deforms plastically. If with buckling of the flanges the line of intersection of their middle planes were to remain straight, as was always assumed in literature before, the cross-section would come in the dotted position (fig. 21), each of the flanges deflecting an average amount w_f perpendicular to its plane. If flange AC was not supported by flange AB in A, with buckling its cross-section would obtain a pure translation w perpendicular to its plane. In the longitudinal section through A, however, flange AB transfers shearing forces and twisting moments to flange AC, by which point A of the cross-section is restrained. Inversely, however, in the longitudinal section through A, flange AC will transfer by its deflection the inverted forces to AB; these forces may be taken together as an equivalent load p_c [39]), shown in fig. 21. In the same way flange AB transfers, by its own deflection, an equivalent load p_b to flange AC. The resultant p of these loads has to be taken by the angle as a whole and as it is not infinitely rigid against bending it will obtain a deflection w_a by it, bringing the cross-section in the position $B'A'C'$.

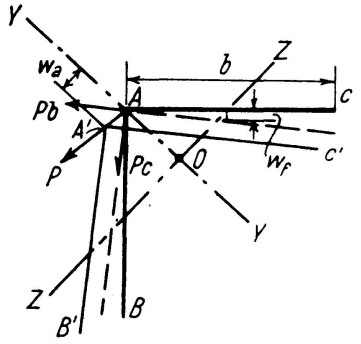

Fig. 21

So we may distinguish here two rigidities, namely the rigidity of the angle as a whole against bending with respect to axis Y—Y and the rigidity of the flanges against „plate buckling". Our method, the first part of which we used already a long time ago [40]), consisted of imagining these rigidities sequentially to become infinite. Let us assume first that the flanges are infinitely rigid against „plate buckling", whilst the angle as a whole has its normal rigidity, so that with buckling only a translation w_a of the

[39]) Cf. p_y in eq. (60) of our first paper [2]).

[40]) BIJLAARD, De Ingenieur, no. 4, 1932, footnote 2 and no. 7, 1933.

cross-section will occur. Let under this assumption the critical thrust of the angle be P_{ay}, if buckling in a plane perpendicular to axis Y—Y. With an arbitrary deflection w_a the inner moment M_i will equal the outer moment $P_{ay}\, w_a$. Now we assume the rigidity of the flanges to plate buckling to decrease from infinity to its real value, during which the inner moment, however, does not change. By this a rotation, yielding an average deflection w_f of the flanges (fig. 21), will be superposed on the translation w_a of the cross section, by which the deflection of the centroid 0 in Z-direction becomes $w_a + w_f/\sqrt{2}$, whilst the critical thrust decreases to its real value P_{cr}. The equality of inner and outer moments will yield now the equation

$$P_{ay}\, w_a = P_{cr}(w_a + w_f/\sqrt{2}) \tag{108}$$

In the same way we assume now the angle as a whole to be infinitely rigid against bending and the flanges to have their normal rigidity against plate buckling, so that only a rotation of the cross-section will occur, as shown in fig. 21 by the dotted lines. In this case the critical thrust P_f of one flange will be $bh\sigma_P$, value σ_P being given by eq. (34), but, leaving the bending stresses in the flange out of account, practically by eq. (35). The inner moment for one flange, being given by the stresses acting in the longitudinal section through A, has now to balance the outer moment $P_f\, w_f$. Assuming then the angle as a whole to get back its normal rigidity, during which the inner moment for the flange remains constant, a translation w_a of the cross-section will be superposed on the initial rotation, by which the total deflection of a flange perpendicular to its plane becomes $w_f + w_a/\sqrt{2}$. Equating inner and outer moments for one flange yields now

$$P_f\, w_f = \tfrac{1}{2}\, P_{cr}(w_a/\sqrt{2} + w_f) \tag{109}$$

as the real critical thrust of one flange is $P_{cr}/2$. Eliminating w_a and w_f from eqs. (108) and (109) we get

$$P_{cr} = P_{ay} + 2\,P_f - \sqrt{P_{ay}^2 + 4\,P_f^2}$$

The cross-section of the entire angle being A, we have $P_{cr} = A\sigma_{cr}$, $P_{ay} = A\sigma_{ay}$ and $2P_f = A\sigma_f$, so that the buckling stress of the flanges is

$$\sigma_{cr} = \sigma_{ay} + \sigma_f - \sqrt{\sigma_{ay}^2 + \sigma_f^2} \tag{110}$$

As the maximum moment of inertia J_y of the cross-section with respect to axis Y—Y is about four times the minimum moment of inertia J_z, the critical stress σ_{ay} with buckling of the angle in a plane perpendicular to Y—Y will be about four times the critical stress σ_{az} for buckling in a plane perpendicular to Z—Z, which is the real buckling stress of the angle as a whole. Substitution of this in eq. (110) yields

$$\sigma_{cr} = 4\,\sigma_{az} + \sigma_f - \sqrt{(4\,\sigma_{az})^2 + \sigma_f^2} \tag{111}$$

in accordance with eq. (28) of our publication mentioned in footnote 17.

If we demand now, that the buckling stress σ_{cr} of the flanges according to eq. (111) shall not be less than the minimum buckling stress of the angle, σ_{az}, this equation yields

$$\sigma_f \geqq \frac{7}{6}\,\sigma_{az} \tag{112}$$

In the elastic region σ_f is practically given by eq. (35), in which, according to eq. (28) value $F = 0.385$. So we have, if the slenderness ratio of the angle is l/r

$$\sigma_f = 0.385\, E h^2/b^2 \qquad \text{and} \qquad \sigma_{az} = \pi^2 E/(l/r)^2$$

substitution of which in eq. (112) yields

$$b/h \leqq 0.18\, l/r \tag{113}$$

in accordance with the value given for $l/r \geq 100$ in Table I of our first paper [2]). In the plastic region just below the yield stress value F in eq. (35) equals 0.338 according to eq. (29), whilst σ_{az} amounts to the yield stress, so that

$$\sigma_f = 0{,}338\, E h^2/b^2 \qquad \text{and} \qquad \sigma_{az} = 2400 \text{ kg/cm}^2$$

substitution of which in eq. (112) gives the condition

$$b/h \leqq 15.8 \tag{114}$$

being rounded of to 15.5 for $l/r \leq 60$ in Table I of our first paper. Linear interpolation between $l/r = 60$ and $l/r = 100$ yields the condition given there for values l/r between 60 and 100.

In the same paper [17]) we compared σ_{cr} according to eq. (111) with that calculated from the differential equation of the flanges. The buckling condition may be found directly from the general buckling condition according to eq. (61) of our first paper [2]), by equating s_2 to zero and Θ_1 and Θ_2 to infinity. With $s_1 = s$ we obtain in this way

$$(\alpha_1^2 r^4 - \alpha_2^2 q^4) \sinh \alpha_1 b \sin \alpha_2 b - 2\alpha_1 \alpha_2 q^2 r^2 \cosh \alpha_1 b \cos \alpha_2 b + \\ + \alpha_2 q^2 ts \sinh \alpha_1 b \cos \alpha_2 b - \alpha_1 r^2 ts \cosh \alpha_1 b \sin \alpha_2 b + 2\alpha_1 \alpha_2 q^2 r^2 = 0 \tag{115}$$

Assuming an angle with a length $a = 100$ cm, $b = 5$ cm and a thickness $h = 0.25$ cm, the ratio b/h is 20, so that it buckles in the elastic region. The values of the notations in eq. (115) in the elastic region being given on page 62 of our first paper, the only unknown quantity in eq. (115) is the buckling stress σ_E. The flexural rigidity B of a flange against bending in its own plane, appearing in value s, is $Eb^3h/3$, as the strain in the longitudinal section through A (fig. 21) is zero. By trial and error we find with eq. (115) that for the given angle the buckling stress of the flanges is $\sigma_{cr} = 0.000875\, E$. Using eq. (111) we find with eqs. (35) and (28) $\sigma_f = 0.000963\, E$. Equating the minimum moment of inertia J_z to $b^3h/12$ and A to $2bh$, value b being the breadth of a flange, measured between the edge and the middle plane of the other flange, we have $r = b/\sqrt{24}$ and $l/r = a/r = 98$, yielding $\sigma_{az} = \pi^2 E/98^2 = 0.001028\, E$. Insertion of σ_f and σ_{az} in eq. (111) yields $\sigma_{cr} = 0.000852\, E$, being safe and in good accordance with σ_{cr} according to eq. (115).

2. 4. Stability of the web of plate girders.

As through lack of space we gave also eq. (68) of our first paper [2]) without derivation, we will elucidate this formula here. In the same way as BLEICH we assumed the relation

$$\tau_B = \tau_0 + (\tau_1 - \tau_0)(b/a)^2 \tag{116}$$

τ_0 and τ_1 being the buckling stresses with ratios b/a equaling 0 and 1 respectively. With the accurate values found by SEYDEL [25]) this gives for the elastic domain

$$\tau_E = \{4.82 + 3.62\,(b/a)^2\}\,E h^2/b^2 \tag{117}$$

As at the yield stress values A, B, D and F are constants, we may assume there the same relation (116). According to eq. (51) $\tau_0 = 3.74\,E h^2/b^2$. Eq. (58) gives for the elastic domain $\tau_1 = 8.52\,E h^2/b^2$, but SEYDEL [25]), who took more coefficients a_{pq} into account, found $8.44\,E h^2/b^2$, so that we may improve our result according to eq. (59) for the plastic region by multiplication by 8.44/8.52, yielding $\tau_1 = \tau_B = 6.30\,E h^2/b^2$. By substitution of τ_0 and τ_1 in eq. (116) we obtain

$$\tau_B = \tau_v = \{3.74 + 2.56\,(b/a)^2\}\,E h^2/b^2 \tag{118}$$

According to the slenderness-buckling stress relation assumed by us, at the border between elastic and plastic region $\tau = (2073/\sqrt{3})\,\mathrm{kg/cm^2} = 1197\,\mathrm{kg/cm^2}$. According to eq. (117) this stress will be reached if

$$(b/h)_E = \sqrt{8456 + 6351\,(b/a)^2} \tag{119}$$

The yield stress $\tau_V = (2400/\sqrt{3})\,\mathrm{kg/cm^2} = 1386\,\mathrm{kg/cm^2}$ is reached, according to eq. (118), if

$$(b/h)_v = \sqrt{5667 + 3879\,(b/a)^2} \tag{120}$$

Assuming a linear relation between ratio b/h and buckling stress τ_B, we finally obtain eq. (68) of our first paper [2]).

3. Stability of latticed struts, sandwich plates and foundation piles

3. 1. Stability of latticed struts.

The method we used in section 2.3 is still much more simple in its application if the deflections, caused by the different parts in which the elasticity of the structure may be divided, occur in the same direction, as happens indeed in most cases. As an example we used it in 1939 in a paper in the same number [17]) to derive ENGESSER's formula for latticed struts with batten plates connection only (fig. 22a). We assumed again the elasticity to be divided into two parts, say 1 and 2. We assume first part 1 to have its normal elasticity, but part 2 to be absolutely rigid. At the critical thrust P_1, with an arbitrary deflection y_1, the inner moment M_1 will be equal to the outer moment $P_1 y_1$. Now we assume the rigidity of part 2 to decrease from infinity to its real value, during which the inner moment does not change. The deflection y_1 will now increase to y, so that the equilibrium demands that the critical thrust decreases to its real value P_{cr}, whilst from the equality of inner and outer moments it follows that $P_1 y_1 = P_{cr} y$. In the same way we assume now part 1 to be rigid and part 2 elastic, by which the equation $P_2 y_2 = P_{cr} y$ is obtained. As $y = y_1 + y_2$ we get in this way the equation

$$y = y_1 + y_2 = P_{cr}(P_1^{-1} + P_2^{-1})\,y \tag{121}$$

yielding [41])

$$P_{cr} = (P_1^{-1} + P_2^{-1})^{-1} \tag{122}$$

or [17])

$$\sigma_{cr} = (\sigma_1^{-1} + \sigma_2^{-1})^{-1} \tag{123}$$

[41]) This same equation was given later on other grounds by BUCKENS, Publ. Int. Ass. f. Bridge and Struct. Eng., Zurich, Vol. 7, 1943/1944.

σ_1 and σ_2 being the critical stresses for cases 1 and 2 respectively. The results given by eqs. (122) and (123) will be the more accurate the more the deflection curves in both cases 1 and 2 are similar.

As may be done in most cases of steel columns, the batten plates are first considered as infinitely rigid. We divide the elasticity of the columns into that by which they bend with respect to their common middle plane (fig. 22b), and into that by which each single column bends with respect to its own neutral plane (fig. 22c). The critical thrust for the first case

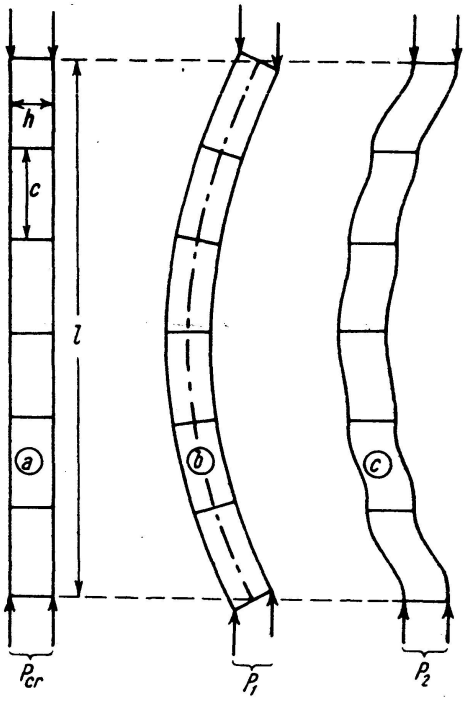

Fig. 22

is $\sigma_1 = \pi^2 T/\lambda_c^2$, values T and λ_c being the reduced modulus and the slenderness ratio l/r_c for a solid column respectively, in which $r_c = \sqrt{J_c/A}$ and $J_c = 2J_s + Ah^2/4$, values A and J_s being the total cross sectional area and the moment of inertia of the cross-section of a single column respectively, whilst h is given in fig. 22a. As to the second case (fig. 22c) it needs no further explanation that $\sigma_2 = \pi^2 T/\lambda_s^2$, value λ_s being the slenderness ratio c/r_s of the single struts, in which r_s is the radius of gyration of a single column and c is the panel length as given in fig. 22a. Insertion of these values in eq. (123) yields

$$\sigma_{cr} = \frac{\pi^2 T}{\lambda_c^2 + \lambda_s^2} = \frac{\pi^2 T}{\lambda_i^2} \tag{124}$$

so that the ideal slenderness ratio of the latticed column is

$$\lambda_i = \sqrt{\lambda_c^2 + \lambda_s^2} \tag{125}$$

in accordance with the well-known ENGESSER equation.

Anticipating our next computations, it follows that eq. (125) holds as well for columns consisting of p single struts, of which the batten plates have an appreciable length, if λ_c is the slenderness ratio of the solid column

and λ_s is equated to $c_0/r_s = (c-2a)/r_s$, value $2a$ being the effective length of the batten plates.

Considering now a latticed strut, with length l, of which the two ribs are connected by diagonal lacing (fig. 23), of which the elasticity has to be taken into account, the only right way to use eq. (122) is to split of first the proper rigidities of the single columns, before applying it, as otherwise either the part, assumed to be rigid, would prevent the deformation of the elastic part or the same rigidities would have to be taken into account twice. So we assume first the single struts to have no proper rigidity, but add its influence, $P_0 = 2\pi^2 T J_s/l^2$, afterwards. Subsequently we split the elasticity of the remaining system into that by which bending with respect to the common middle plane occurs, leaving consequently the proper moments of inertia J_s of the single struts out of account, and into that of the lacing. Hence we have for the first case

$$P_1 = \pi^2 T J_t/l^2 \quad \text{in which} \quad J_t = A h^2/4 \tag{126}$$

In order to find P_2 we remark that an angular distortion β (fig. 23) causes a shearing force $Q = P_2\beta$ that has to be taken by the lacing. Denoting the fictituous shearing force that would cause a unit angular distortion by S, the modulus of rigidity of the latticing, we obtain the equation $Q = S\beta$, so that we get

$$P_2 = S \tag{127}$$

In order to find the critical thrust of the column, we have to add now the proper critical thrust P_0 of the two single struts to the critical thrust according to eq. (122), combined with (126) and (127), yielding

$$P_{cr} = P_0 + (P_1^{-1} + P_2^{-1})^{-1} = 2\frac{\pi^2 T J_s}{l^2} + \frac{\pi^2 T J_t S}{S l^2 + \pi^2 T J_t}$$

or

$$P_{cr} = \frac{\pi^2 T}{l^2}\left(2J_s + \frac{l^2}{l^2 + \pi^2 T J_t/S} J_t\right) \tag{128}$$

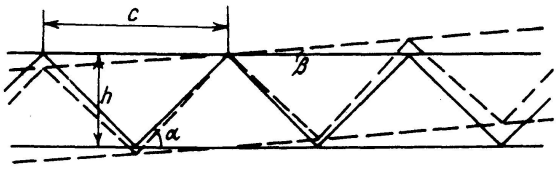

Fig. 23

It is a simple question to check that with diagonals alone (fig. 23)

$$S = E A_d \sin^2\alpha \cos\alpha \tag{129}$$

whilst with a double lattice value S has the double value, A_d being the cross-sectional area of the diagonals. If the lattice consists of single diagonals and verticals it is easier to give S as follows

$$1/S = 1/E A_d \sin^2\alpha \cos\alpha + \tan\alpha/E A_v \tag{130}$$

A_v being the cross-sectional area of the verticals. Of course the slenderness ratio c/r_s of the single struts (fig. 23) must be smaller than the ideal slenderness ratio of the entire column.

Our formulae are more accurate than existing similarly constructed formulae, especially for very weak latticing. If for example $A_d = 0$ these formulae yield $P_{cr} = 0$, whilst our formula (128) yields with value $S = 0$, given in that case by eqs. (129) or (130), the right value $P_{cr} = 2\pi^2 T J_s / l^2$.

In modern timber structures nearly all compression members are built-up columns, viz. two or more single struts that are joined to one another at two or more places by means of wooden couplings (fig. 24). The connection may be effected by bolts, wooden disks, nails or otherwise. Notwithstanding the methods of computation for these built-up columns were very

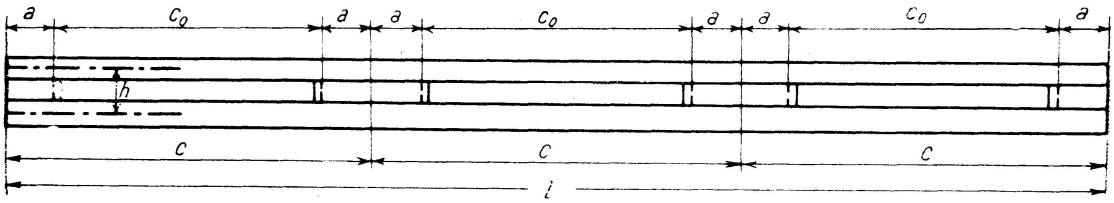

Fig. 24

unsatisfactory. According to the German prescriptions *DIN* 1052 (May 1938), for example, the buckling force for such timber columns had to be computed by assuming that they had a moment of inertia $J = J_0 + \frac{1}{4}(J_1 - J_0)$, in which J_1 is the moment of inertia of the total cross-section and J_0 is the same as if the single struts are pushed close together. It is clear that this method is quite insufficient, as it takes into account neither the number and length, nor the rigidity of the couplings. At the request of ir. H. KRULL, expert in timber structures of the Department of Forestry in the Netherlands Indies, we derived a simple formula, in which, besides the elasticity of the couplings, also their length is taken into account. Our reasoning given above here holds good too if the elasticity of the structure, after splitting of the proper rigidities of the single struts against bending in a single half wave, is divided into more than two parts. Let $y = \Sigma y_k$. Assume first part 1 as elastic, the rest as infinitely rigid. Then we obtain in the same way as before the equation $P_1 y_1 = P y$, if P is the critical thrust of the system after splitting of the proper rigidities of the single struts. Thinking successively only part 2, 3, etc. elastic, we get $P_2 y_2 = P y$, $P_3 y_3 = P y$, etc., from which it follows, as $y = \Sigma y_k$, that $y = P(\Sigma P_k^{-1}) y$ or $P = (\Sigma P_k^{-1})^{-1}$, so that the critical thrust of the column

$$P_{cr} = P_0 + P = P_0 + (\Sigma P_k^{-1})^{-1}$$

so that

$$\sigma_{cr} = \sigma_0 + \sigma = \sigma_0 + (\Sigma \sigma_k^{-1})^{-1} \qquad (131)$$

P_0 and σ_0 representing the influence of the proper rigidities of the single struts [42]).

Using eq. (131), we split the elasticity of the remaining system into three parts. Part 1 yields a deflection as given in fig. 22b, so that P_1 is given by eq. (126), by which the critical stress is

[42]) The equation $P_{cr} = (\Sigma P_k^{-1})^{-1}$ was also derived otherwise by BUCKENS, l. c., footnote 41. As he, however, split the structure itself, and not its elasticity, into different parts and did not split off before the rigidities yielding the complementary thrust P_0, he could only solve rather simple problems of bars and frames by it, using only the equation $P = (P_1^{-1} + P_2^{-1})^{-1}$.

$$\sigma_1 = \pi^2 T/\lambda_t^2 \quad \text{in which} \quad \lambda_t = 2l/h \tag{132}$$

Part 2 gives a deformation according to fig. 22c, with the difference that, owing to the length of the couplings (fig. 24), only lengths $c_0 = c - 2a$ of the single struts can bend, by which their virtual buckling length (the length of a half sine wave) is also c_0 and

$$\sigma_2 = \pi^2 T/\lambda_s^2 \quad \text{in which} \quad \lambda_s = c_0/r_s = (c-2a)/r_s \tag{133}$$

Part 3 consists of the elasticity of the couplings. The deformation of these wooden couplings by the shearing forces S_i acting in them (fig. 25a) will be principally a shearing. Denoting the displacement of the single struts with respect to each other per unit shearing force in a coupling by v, the magnitude of the shearing force S_i, by which a displacement $h\alpha_i$ is effected, is

$$S_i = h\alpha_i/v \tag{134}$$

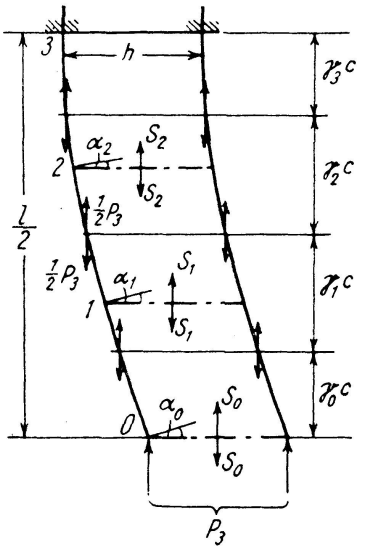

Fig. 25a

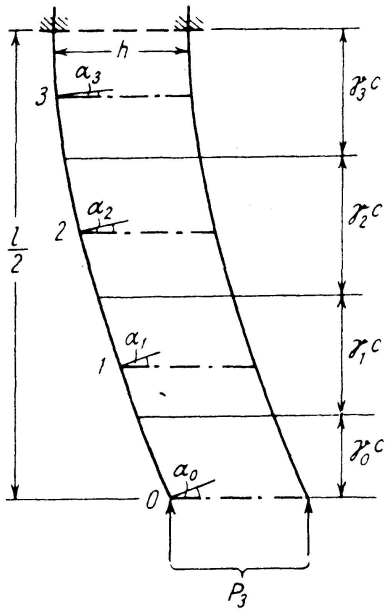

Fig. 25b

Assuming all couplings as equally rigid, the equilibrium of each of the joints 0,1 and 2 in fig. 25a, representing one half of a column with an even number of panels, yields approximately

$$\tfrac{1}{2} P_3 \gamma_i c \alpha_i = S_i h/2 \quad (i = 0, 1, 2) \tag{135}$$

With eq. (134) this equation gives

$$P_3 \gamma_i c = h^2/v \quad (i = 0, 1, 2) \tag{136}$$

Addition of the three equations represented by eq. (136) yields

$$P_3(l/2 - \gamma_3 c) = 3h^2/v$$

Approximating γ_3 by 0.5 and taking into account that a similar relation holds good for a column with an arbitrary even number of panels n, this equation may be written as follows

$$P_3(n-1)c/2 = nh^2/2v$$

whence $$P_3 = \frac{n}{n-1}\frac{h^2}{c\,v} \tag{137}$$

If the rigidity of the end couplings is assumed to be half of that of the intermediate couplings, the first equation (136) yields $P_3\gamma_0 c = h^2/2\,v$, whence we find, after addition of all equations (136) and transformation

$$P_3 = h^2/c\,v \tag{138}$$

With an odd number of panels eqs. (135) and (136) hold good approximately for all joints i, so that it follows from fig. 25b that by addition of all equations (136) we obtain

$$P_3\, n\, c/2 = (n+1)\, h^2/2\,v$$

or $$P_3 = \frac{n+1}{n}\frac{h^2}{c\,v} \tag{139}$$

whilst with end couplings of the half rigidity we get again eq. (138). Denoting generally P_3 as

$$P_3 = \beta\, h^2/c\,v \tag{140}$$

in which β follows from eqs. (137), (139) or (138), we have

$$\sigma_3 = \frac{\beta\, h^2}{c\,v\,A} \tag{141}$$

Hence eq. (131), combined with (132), (133) and (141), yields

$$\sigma = \sigma_{cr} - \sigma_0 = \left(\frac{\lambda_t^2 + \lambda_s^2}{\pi^2\,T} + \frac{c\,v\,A}{\beta\,h^2}\right)^{-1} = \frac{\pi^2\,T}{\lambda_r^2} \tag{142}$$

in which $$\lambda_r^2 = \lambda_t^2 + \lambda_s^2 + \lambda_w^2$$

and $$\lambda_t = 2\,l/h, \quad \lambda_s = c_0/r_s \quad \text{and} \quad \lambda_w^2 = \pi^2\,T\,A\,c\,v/\beta\,h^2 \tag{143}$$

In case 2 no deflection of the single struts in a half wavelength l occurs, so that value σ_0 has to be equalled to

$$\sigma_0 = \frac{y - y_2}{y}\,\frac{\pi^2\,T}{(l/r_s)^2} \tag{144}$$

As $P_2 y_2 = P\,y$, $(y-y_2)/y = 1 - P/P_2 = 1 - \sigma/\sigma_2$, or, according to eqs. (133) and (142), $(y-y_2)/y = (\lambda_r^2 - \lambda_s^2)/\lambda_r^2$. Hence eq. (131) yields, paying attention to eqs. (142) and (144)

$$\sigma_{cr} = \frac{\lambda_r^2 - \lambda_s^2}{\lambda_r^2}\,\frac{\pi^2\,T}{(l/r_s)^2} + \frac{\pi^2\,T}{\lambda_r^2} = \frac{\pi^2\,T}{\lambda_r^2}\left\{1 + (\lambda_r^2 - \lambda_s^2)\left(\frac{r_s}{l}\right)^2\right\}$$

so that the ideal slenderness ratio λ_i is given by

$$\lambda_i^2 = \frac{\lambda_r^2}{1 + (\lambda_r^2 - \lambda_s^2)\,(r_s/l)^2} \tag{145}$$

in which λ_s and λ_r are given by eqs. (143). With infinitely weak connections, with which λ_w is infinite, eq. (145) yields the right value $\lambda_i = l/r_s$. It follows from fig. 22 and fig. 25a that, if the column has only one panel, we have to consider it as consisting of two panels, putting $c = l/2$.

In the same way we derived formulae for built-up columns, consisting of p single columns. With rigid connections we may use eq. (123). In case 1 now $\sigma_1 = \pi^2 T/\lambda_c^2$, in which $\lambda_c = l/r_c$, whilst $r_c = \sqrt{J_c/A}$ and $J_c = p J_s + \Sigma A_s\, a_k^2$,

value a_k being the distance between the axis of any single column and that of the built-up column. Fig. 26 represents a length $\gamma_i c$ of the column in deformed condition, the single struts being indicated by single lines. Value A_s is the cross-sectional area of a single strut, so that $A = p A_s$. Value $\sigma_e = \pi^2 T/\lambda_s^2$, whilst the ideal slenderness ratio is given by eq. (125). It follows that the formula $\lambda_i^2 = \lambda_c^2 + p\lambda_s^2/2$, as recommended in the German prescriptions 1939 (*DIN E* 4114) is erroneous.

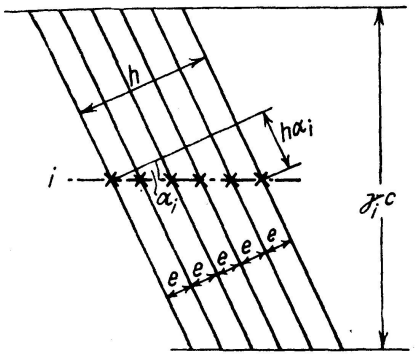

Fig. 26

Taking into account the elasticity of the connections, σ_1 and σ_1 are again given by eqs. (132) and (133), but now $\lambda_t = l/r_t$, whilst $r_t = \sqrt{J_t/A}$ and $J_t = \Sigma A_s a_k^2$. Denoting the shearing force between two single struts by S_k, it follows from fig. 26 that for joint i we get

$$v \Sigma S_k = h \alpha_i \tag{146}$$

Furthermore it follows by adding the total moments with respect to the 6 points, denoted by crosses in fig. 26, and using eq. (146), that

$$P_3 \gamma_i c \alpha_i = e \Sigma S_k = e h \alpha_i / v \tag{147}$$

Adding the equations for all points i we obtain in the same way as with two coupled struts

$$\sigma_3 = \frac{\beta e h}{c v A} \tag{148}$$

in which β is $n/(n-1)$ or $(n+1)/n$ for an even or odd number of panels n and for connections of equal rigidity and $\beta = 1$ if the end connections have the half rigidity. Eq. (131) yields now

$$\left.\begin{aligned} \lambda_i^2 &= \frac{\lambda_r^2}{1 + (\lambda_r^2 - \lambda_s^2)(r_s/l)^2} \\ \text{in which} \qquad \lambda_r^2 &= \lambda_t^2 + \lambda_s^2 + \lambda_w^2 \\ \text{and} \qquad \lambda_t &= l/r_t, \quad \lambda_s = c_0/r_s, \quad \lambda_w^2 = \pi^2 T A c v/\beta e h, \\ r_t &= \sqrt{J_t/A} \quad \text{and} \quad J_t = \Sigma A_s a_k^2 \end{aligned}\right\} \tag{149}$$

In order to check formula (145) we compared its results with the exact values, which for two connected single columns are given by [43])

[43]) v. Mises and Ratzersdorfer, Zeitschr. f. ang. Math. u. Mech., 1926. Hartmann, l. c., footnote 18, p. 67. Biilaard, De Ingenieur, no. 7, 1933. Van der Eb, De Ingenieur in Ned. Indië, no. 10, 1937.

$$\frac{h^2}{2 r_s^2} = \frac{2\pi}{m} \frac{\cos\frac{\pi}{n} - \cos\frac{\pi}{m}}{\left(1 - \cos\frac{\pi}{n}\right)\sin\frac{\pi}{m}} \left\{1 + \frac{T A_s \nu}{c}\left(1 - \cos\frac{\pi}{n}\right)\right\} \qquad (150)$$

if the rigidity of the end connections is half of that of the intermediate ones and with $c_0 = c$. Equating in eqs. (145) and (150) T to $E = 100000$ kg/cm², our former assistant in Bandoeng, Ir. LIE HAN YANG, calculated for several built-up timber columns values $m = \lambda_i/\lambda_s$ with eq. (145) as well as with eq. (150), the result being given in Table V. As follows from fig. 22a value h is the distance between the axes of the single struts. The breadth and thickness of a single column was 20 and 8 cm respectively.

Table V.

l	c	n	h	$m = \lambda_i/\lambda_s$					
				$\nu = 0$		$\nu = 0{,}04$ cm/ton		$\nu = 0{,}30$ cm/ton	
cm	cm		cm	(145)	(150)	(145)	(150)	(145)	(150)
260	130	2	16	1.11	1.09	1.45	1.37	1.84	1.80
390	130	3	16	1.27	1.24	1.70	1.63	2.47	2.42
520	130	4	16	1.47	1.43	1.90	1.85	2.94	2.89
520	130	4	24	1.24	1.21	1.51	1.46	2.39	2.33
780	130	6	16	1.92	1.89	2.30	2.26	3.56	3.53
156	78	2	16	1.12	1.09	1.56	1.48	1.89	1.89
390	78	5	16	1.69	1.65	2.30	2.26	3.68	3.66
780	78	10	16	2.94	2.91	3.37	3.34	5.09	5.09

It follows from Table V that the values given by eq. (145) are sufficiently accurate and incline to the safe side.

We made an extensive study of this kind of column, but cannot say much more of it in this paper. We only give here some results of tests, executed by us in the Laboratory for Testing Materials in Bandoeng at the request and in cooperation with MR. KRULL, mentioned above, in order to determine the value ν and the effective length $2a$ of the couplings, whether effected by wooden disks, bolts or nails. Fig. 27a gives some load-deflection diagrams of columns as indicated in fig. 27b. As here the columns as a whole were fixed at the ends, so that the single struts could not receive different axial strains, λ_t in eq. (143) has to be equated to zero. The single struts had a breadth of 21 cm and were 5 cm thick. Like the wooden blocks between them, they were made of Java teak (Tectona grandis). In order to characterize this material we give in fig. 28 the results of our tests, also made in cooperation with MR. KRULL, with single bars, for centric buckling ($m = 0$) and for an eccentricity equaling 1/6 of the thickness ($m = 1$). Our tests (slow tests) were made in such a way that the „creep" of the wood was taken into account, as the load was not increased before the deflecting had come to a standstill. With slenderness ratios higher than 90, EULER's formula applies with $E = 130\,000$ kg/cm².

The curves denoted by D. 1, D. 2 and D. 3 in fig. 27a relate to columns connected by wooden disks, as indicated in fig. 27b, the shearing forces S_0 (fig. 25a) being taken by one disk only. The allowable shearing force in these disks is 1100 kg. They were made of hard Indian wood, those of D. 1 and D. 2 of sonokling (Dalbergia latifolia) and those of D. 3 of marbau

(Intsia Amboinensis). In test D. 2 value ν was extraordinary large, being due to a rather much play between disks and column, owing to shrinking of the disks. As in practice such play does not occur, as according to MR. KRULL columns and disks are worked with such a moisture content, that after shrinking they fit, we left this test out of consideration. Test D. 4 consisted of 4 coupled struts of the same proportions as those of fig. 27b, the shearing force being, however, taken by 2 disks, whilst the wooden connecting blocks

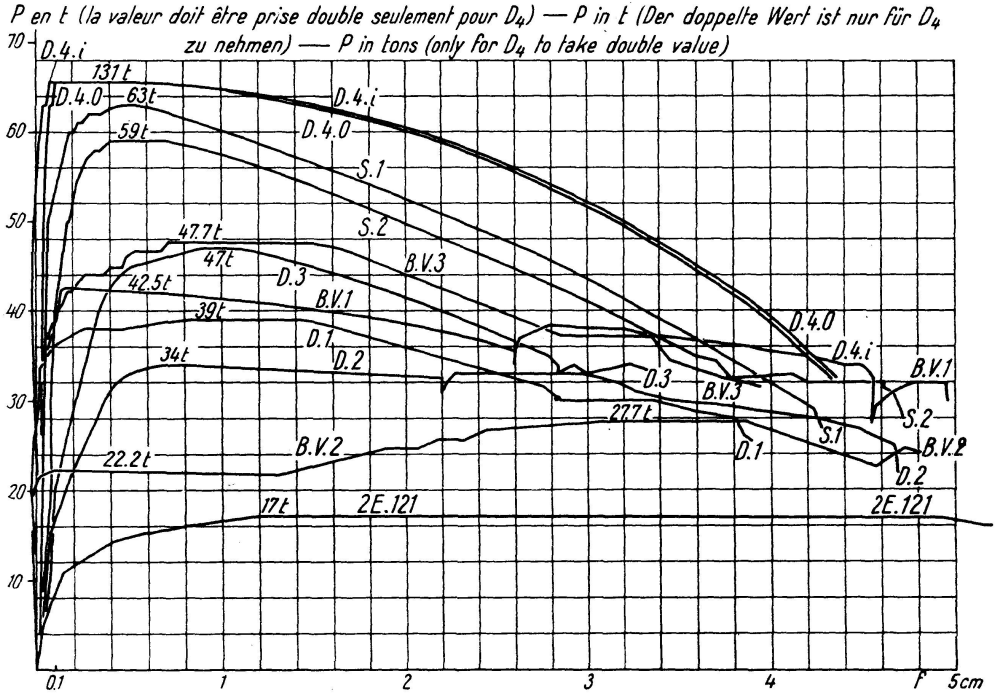

Fig. 27 a

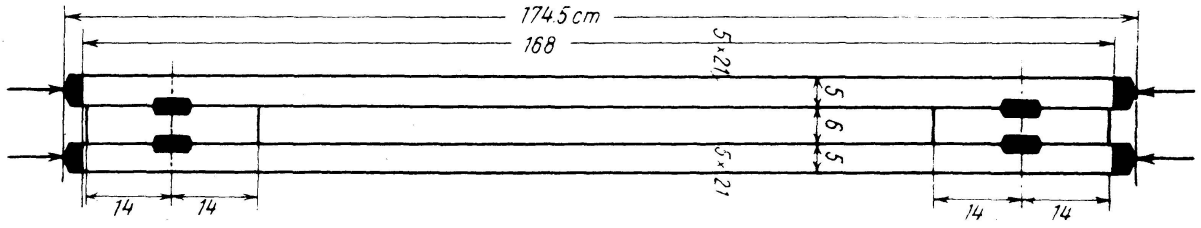

Fig. 27 b

had lengths and thicknesses of 42 cm and 5 cm respectively. Tests B. V refer to struts as in fig. 27 b, but each connection being effected by 4 bolts of $\frac{1}{2}''$ diameter, as shown in fig. 29. The total allowable shearing force for 4 bolts is 1600 kg. In tests B. V. 1 and B. V. 2 the holes were drilled 1/16" larger than the diameter of the bolts, as is usual in practice. In B. V. 1, however, the nuts were tightened with the usual monkey wrench of 20 cm length, whilst in B. V. 2 they were not tightened and were held free 2 mm from the washers. In B. V. 3 the $\frac{1}{2}''$ bolts were fitting in the holes, but just as with B. V. 2 the nuts were not tightened and held free from the washers. In tests S. 1 and S. 2 the connections were made as shown in fig. 30, comprising 9 nails of 6.5 mm diameter, fitting in predrilled holes,

representing an allowable shearing force of 1330 kg. Finally 2 E 121 gives the double thrust value for a single bar of the same proportions as the single bars used in the built-up columns, so that the difference between graph 2E.121 and the other curves shows the influence of the connections. The horizontal part of this graph is due to creep.

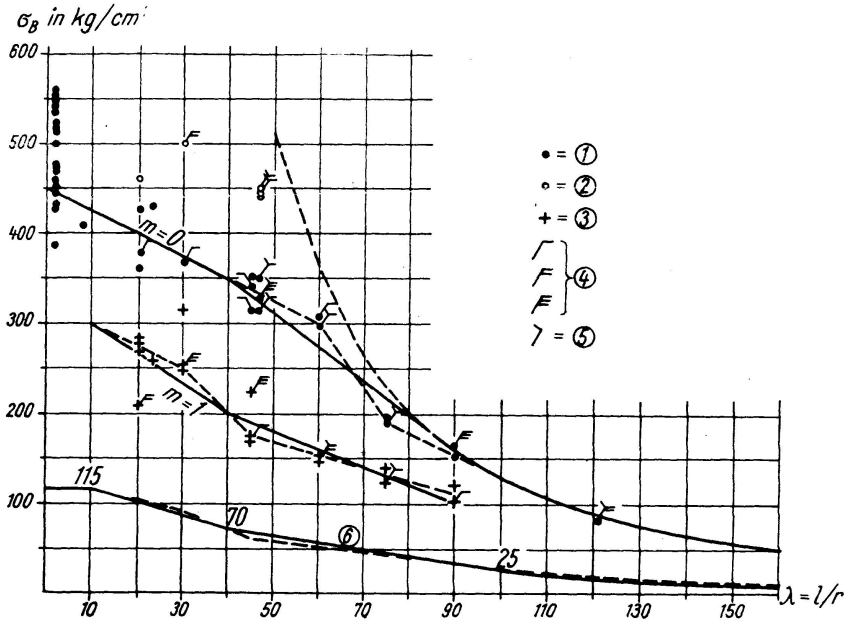

Fig. 28.

Graph for buckling stresses of Java teak with varying slenderness ratio λ — Diagramm der Beulspannungen von Java Teakholz mit einem veränderlichen Schlankheitsgrad λ. — Graphique des contraintes de voilement du bois de teak de Java avec un coefficient d'élancement λ variable.

(1) Centric loading with slow test ($m = 0$) — Zentrische Belastung beim langsamen Versuch ($m = 0$) — Essai lent pour charge centrée ($m = 0$).
(2) The same with rapid test — Dasselbe beim schnellen Versuch — Essai rapid pour charge centrée.
(3) Excentric loading with excentricity $^1/_6$ t ($m = 1$) — Exzentrische Belastung mit Exzentrizität $^1/_6$ t ($m = 1$) — Charge excentrique pour l'excentricité $^1/_6$ t ($m = 1$).
(4) Test piece with one, two or three faults — Versuchsstück mit einem, zwei oder drei Fehlern — Eprouvette avec une, deux ou trois fautes.
(5) Test piece contains heart-wood — Versuchsstück mit Kernholz — Eprouvette contenant du bois de coeur.
(6) Proposed allowable stress — Vorgeschlagene zulässige Spannung — Contrainte admissible proposée.

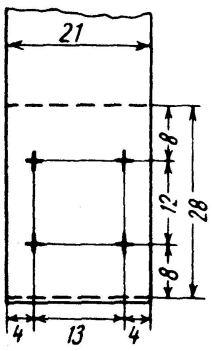

Fig. 29

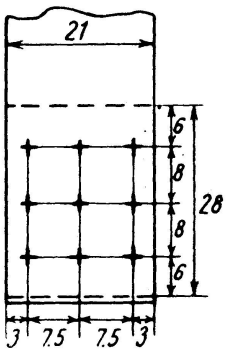

Fig. 30

Our conclusions were that with disk connected columns we have to measure the theoretical length of the couplings (2a or a in fig. 24) from one end of the coupling block up to the bolt that is nearest to the other end, whilst the specific displacement v is $(0.08/m)$ cm/ton, if m is the number of disks of 6 cm, diameter that transmits the shearing force. With bolt connections with non-fitting bolts, as used in practice, where we are not sure that the nuts remain tightened, the effect of the couplings is very slight and problematic. With nail connected columns the theoretical length of the couplings may be put equal to the length of the coupling blocks, whilst $v = (0.36/m)$ cm/ton, if m is the number of nails of 0.65 cm diameter. The latter conclusions hold good for practice in Java with relatively hard timber, but in principle they may be of value for other circumstances too.

3. 2. Stability of sandwich plates.

In order to check our assumption that wave formation in the surface of roads, as often found in Java, is caused by horizontally directed compressive forces, originated in the road cover by rolling and traffic, we considered the road cover as a plate, supported by a semi-infinite elastic body[44]). If the plate is subjected to an arbitrary plane state of stress, it will always buckle in waves perpendicular to the direction of the largest principal compressive stress, also with plastic buckling of the plate[45]). Hence a state of plane strain will occur here, so that the stress distribution in the elastic substratum is governed by the AIRY function. Taking into account a complete connection between plate and substratum and thus taking also into account the shearing forces transmitted between them, we calculated the buckling stress of such a plate. After our arrival in Europe our attention was called to publications, in which the stability of thin sheets of metal and plywood, laterally supported by a thicker layer of an elastic material with small specific weight, as used in the construction of wings and bodies of aeroplanes, was considered as the same theoretical case[46]) as worked out previously by us[44]). In a paper, in which we called attention to this fact, we corrected these computations in accordance with our earlier ones and gave along the same lines an accurate calculation for so-called sandwich plates, being two thin outer plates of metal or plywood (the faces) with an intermediate supporting layer of light material (the core)[47]). As we use these formulae in the following section we will give here some results. For a long plate, supported by a semi-infinite body, in the elastic domain the critical thrust per unit breadth is [47])

$$\left.\begin{aligned} h\,\sigma_{cr} &= B\lambda^2 + E'/2\lambda + \tfrac{1}{4}\psi h E' \\ \text{in which, with } \quad s &= E_1'/E = E_1/(1-\nu_1^2)\,E, \\ E' &= \frac{(1+\nu)\{4(1-\nu)+(1-2\nu)\lambda h\}\lambda h s + 2}{(1+\nu)\{(1+\nu)(3-4\nu)\lambda h s + 2(1-\nu)\}}E \\ \psi &= \frac{2(1+\nu)\{1-2\nu+(1-\nu)\lambda h\}\lambda h s}{(1+\nu)\{4(1-\nu)+(1-2\nu)\lambda h\}\lambda h s + 2} \end{aligned}\right\} \qquad (151)$$

---

[44]) BIJLAARD, De Ingenieur in Ned. Indië, no. 9, 1939.
[45]) Appears in Comptes Rendus, 6me Congrès de Mécanique Appliquée, Paris.
[46]) GOUGH, ELAM and DE BRUYNE, Journal of the Royal Aeron. Soc., 1940 and some later papers of other authors.
[47]) BIJLAARD, Proc. Royal Neth. Acad. of Sciences, Amsterdam, no. 10, 1946.

B is the flexural rigidity $E_1 h^3/12(1-\nu_1^2)$ of the plate, h is its thickness and E_1 and ν_1 are the elastic modulus and POISSON's ratio of the plate respectively. E and ν are the latter values for the supporting body. Finally $\lambda = \pi/a$, a being the half wave length of buckling. With an infinitely long plate the optimum wave length, yielding the smallest critical stress σ_{cr}, may be found by differentiation, whence we obtained [47])

$$\left.\begin{aligned} a &= \pi(4B/E')^{1/3} \\ h\,\sigma_{cr} &= \tfrac{3}{4}(4BE'^2)^{1/3} + \tfrac{1}{4}\psi h E' \end{aligned}\right\} \qquad (152)$$

As may be easily checked, a state of plane strain in faces and core of a sandwich plate will only be possible with rather broad plates, owing to the small modulus of rigidity of the core. Therefore, except for the bending of the faces with respect to their own middle plane, a plane state of stress was assumed here. For the formulae we got on this assumption in the above-mentioned way for sandwich plates, we refer to our paper [47]) on the subject. In the same paper we derived, however, by the method given in section 3.1 of the present paper, a formula for the critical thrust, that is practically identical with the results obtained from our exact solution by developing sinh and cosh in series. Using the formula

$$P_{cr} = P_0 + (P_1^{-1} + P_2^{-1})^{-1} \qquad (153)$$

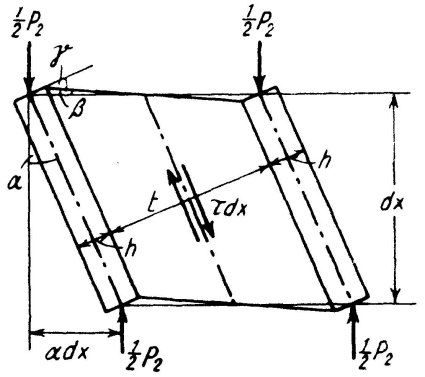

Fig. 31

in which P_0 is the proper critical thrust of the faces per unit breadth, we assume first the modulus of rigidity G of the intermediate layer to be infinite. The free supported length of the plate, of which the unloaded sides are free, being L and denoting thickness of faces and core by h and t respectively, we obtain per unit breadth

$$P_1 = \pi^2 B_t/L^2 = (\pi^2/L^2)\left\{\frac{1}{2}E_1(t+h)^2 h + \frac{1}{12}Et^3\right\} \qquad (154)$$

For case 2 we assume the moduli of elasticity E_1 and E of plates and core to be infinite, but the modulus of rigidity G of the core to have its real value. Considering an element dx of the plate (fig. 31) we get

$$\tau = G\gamma = G(\alpha+\beta) = G\alpha(t+h)/t \qquad (155)$$

whilst the equilibrium of one half of the element demands that

$$\tfrac{1}{2}(t+h)\,\tau\,dx = \tfrac{1}{2}P_2\,\alpha\,dx \qquad (156)$$

Combination of these equations yields

$$P_2 = G(t+h)^2/t \tag{157}$$

Insertion of P_0 and of P_1 and P_2 according to eqs. (154) and (157) in eq. (153) yields, with $G = E/2(1+\nu)$ and assuming the thrust P_{cr} to be taken by the faces alone, so that the critical stress per unit breadth in the faces is $\sigma_{cr} = P_{cr}/2h$

$$\sigma_{cr} = \frac{\pi^2 E_1 h^2}{12(1-\nu_1^2)L^2} + \frac{\pi^2 E_1 (t+h)^2 + (\pi^2/6h) E t^3}{4(1+\nu)\pi^2 E_1 t h + 4EL^2 + \frac{2}{3}(1+\nu)\pi^2 E t^4/(t+h)^2} E \tag{158}$$

For sandwich plates, supported at three or four sides, we cannot apply the above-mentioned exact method, as in that case the deformations with buckling are three dimensional, so that no state of plane strain exists and we cannot apply the AIRY function any longer. The method as shown above, however, may be applied as well in this case. We reason here as follows. Let the plate, being supported at the unloaded sides too, be subjected for example to a compressive force P per unit breadth. If part 1 behaves elastically, it will buckle with a force P_1. With an arbitrary deflection w_1 of an element $H\,dx\,dy$, value H being the total thickness $2h+t$, the restraining force on the element will equal the deflecting force, being cP_1w_1, value c being a proportional factor. Assuming now the rigidities of the other parts to get back their values, whilst the inner stresses do not change, the deflecting force, being now cPw, will have to balance the restraining force cP_1w_1, yielding again $P_1w_1 = Pw$. In the same way we get $P_2w_2 = Pw$, $P_3w_3 = Pw$, etc., by which, just as in the preceding section, we get finally $P = (\Sigma P_k^{-1})^{-1}$. The same holds good if the plate is subjected to an arbitrary state of stress. Of course the results will be the more accurate, the more the deflection surfaces for the several cases have the same form. As, however, admission of diverging deflection surfaces means a lack of constraint, our results are anyhow on the safe side. Referring to our respective papers for further details [48]), we only state here, that after splitting off the proper rigidities of the faces (case 0), the critical thrusts $P_x = 2h\sigma_x$, $P_y = 2h\sigma_y$ or (and) $S_{xy} = 2h\tau_{xy}$ per unit breadth have to be calculated for case 0 and case 1 (assuming G for the core to be infinite) from the well-known differential equation

$$D\left(\frac{\partial^4 w}{\partial x^4} + 2\frac{\partial^4 w}{\partial x^2 \partial y^2} + \frac{\partial w^4}{\partial y^4}\right) + P_x\frac{\partial^2 w}{\partial x^2} + P_y\frac{\partial^2 w}{\partial y^2} - 2S_{xy}\frac{\partial^2 w}{\partial x\,\partial y} = 0$$

and for case 2 (assuming only value G of the core to be finite) from the differential equation

$$\frac{(t+h)^2}{t} G\left(\frac{\partial^2 w}{\partial x^2} + \frac{\partial^2 w}{\partial y^2}\right) - P_x\frac{\partial^2 w}{\partial x^2} - P_y\frac{\partial^2 w}{\partial y^2} + 2S_{xy}\frac{\partial^2 w}{\partial x\,\partial y} = 0$$

as derived in our paper [48]).

3. 3. Stability of rammed piles, surrouned by soil.

Although they are not exactly applicable here, as the horizontal displacement of the soil in the horizontal planes of the inflection points of the piles is not exactly zero, which we shall take into account by introducing in eqs. (151) and (152) a value $\bar{E}' = \frac{2}{3}E'$, these equations may give us an idea

[48]) BIJLAARD, Proc. Royal Neth. Acad. of Sciences, Amsterdam, nos. 1 and 2, 1947.

of the critical thrust of a pile surrounded by bad soil, supported horizontally at its top and standing with its point in a sand layer. As value E for soil will always be only approximately known, we may simplify eqs. (151) by remarking that $h\lambda = \pi h/a$ is in this case a rather small value in comparison with unity, whilst value s and also λhs is very large, so that, equating ν to zero, we find $E' = \frac{4}{3}E$ and $\psi = \frac{1}{2}$. In this way eqs. (152) yield

$$a = \pi h (E_1/4\bar{E})^{1/3} \quad \text{and} \quad \sigma_{cr} = \frac{1}{2}(2E_1\bar{E}^2)^{1/3} + \frac{1}{6}\bar{E} \qquad (159)$$

Let us assume a concrete pile, for which $h = 40$ cm, whilst its cross-sectional area is 1600 cm^2. Leaving the steel reinforcement out of account, we assume $E_1 = 200\,000$ kg/cm^2 for the pile. For the soil we admit E to have the low average value of 15 kg/cm^2, so that $\bar{E} = 10$ kg/cm^2. As the soil supports the pile at both sides, whilst in deriving eqs. (151) and (152) only a support at one side of the plate was assumed, we shall have to reckon with the double value $\bar{E}$, by which $\bar{E} = 20$ kg/cm^2. Hence eqs. (159) yield a buckling length

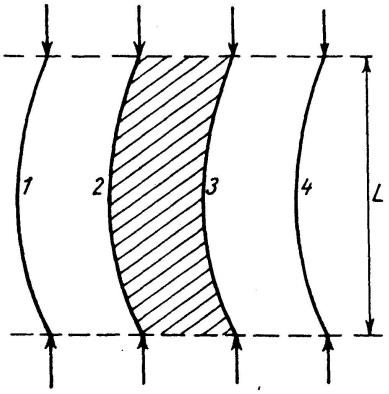

Fig. 32

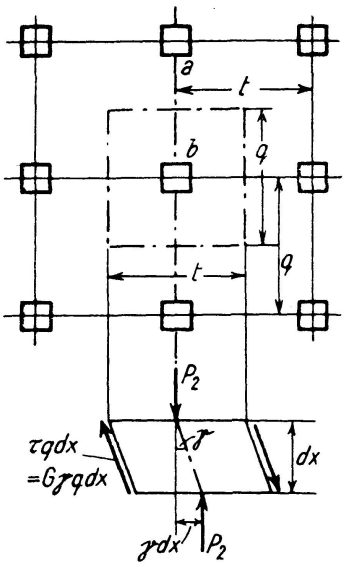

Fig. 33

$a = 1700$ cm and a critical stress for the pile of $\sigma_{cr} = 275$ kg/cm^2. With a free supported length of 17 meters the assumed pile, if not supported by the soil, having a slenderness ratio $1700/11.6 = 147$, would have a buckling stress $\pi^2 E_1/147^2 = 91$ kg/cm^2, so that the soil gives an excess buckling stress of 184 kg/cm^2. As, however, in reality the pressure, exerted by the buckling pile on the soil, will spread sideways, the soil will behave much more rigidly than assumed here, where only a breadth of soil, equal to the breadth $b = h$ of the pile has been taken into account, so that the excess buckling stress will be many times 184 kg/cm^2, say m times, by which the real buckling stress of the pile is $(91 + 184\ m)$ kg/cm^2, surpassing certainly, even if a reduced modulus smaller than E_1 were taken into account, the compressive strength of the material.

If, however, we have not one pile, but a complete foundation, we have a case more similar to that of a sandwich plate. If there was only soil between piles 2 and 3, as shown in fig. 32 by cross hatching, we would

have here the same case, but as the soil is at both sides, we have again to insert the double values for the rigidity of the soil. If we have many piles it is clear that P_1 is practically infinite, so that eq. (153) yields

$$P'_{cr} = P_0 + P_2 \tag{160}$$

In the planes between the piles, for example ab in fig. 33, the thickness of the piles has no influence, so that we had better assume h to be zero here. Then eq. (157), with the double value G, yields $P_2 = 2\,Gt$ per unit breadth of soil and for two piles. Taking into account a breadth q (fig. 33) of the soil, we get for one pile $P_2 = qtG$. This may also be derived directly from fig. 33, considering the equilibrium of an element dx of a pile and the accessory soil. With an angle of distortion γ, equilibrium demands that $P_2\gamma\,dx = tG\gamma q\,dx$, yielding $P_2 = q\,t\,G$, so that, according to eq. (160)

$$P'_{cr} = \pi^2 E_1 J/L^2 + qtG \tag{161}$$

qt being the area of the soil belonging to a pile. Hence, if the total foundation has a total area of QT (fig. 34), Q being for example 20 q and T being 40 t, the total value ΣP_2 equals QTG.

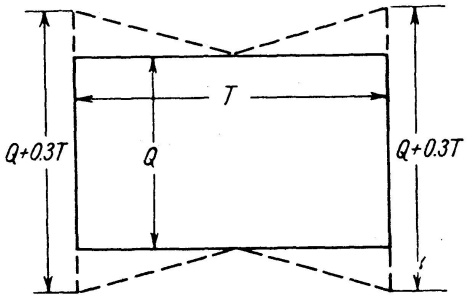

Fig. 34

At the boundaries of the foundation it will moreover experience a constraint, for which, if the piles are supported horizontally at their upper ends, for example by batter piles, again eq. (151) applies, if E' is replaced by $\bar{E}'$. The first term, $B\lambda^2$, relating to the proper rigidities of the piles, has, however, already been taken into account in P_0, whilst the last term may be neglected, so that the excess value of the total buckling force, caused by restraint at the boundaries, amounts to $\bar{E}'/2\lambda$ per unit breadth of the constraining boundary. This breadth will be smallest with buckling in the direction of the largest dimension T. We assume that the constraining breadth at the boundary is $Q + 0.3\,T$ at both sides (fig. 34). As the stresses in the soil die out rapidly, having nearly vanished at a distance L from the boundary, the real breadth to be taken into account will not be much more, if $Q > L$. As, with $\nu = 0$, $\bar{E}' = \frac{4}{3}\bar{E} = \frac{8}{9}E = \frac{16}{9}G$ and $\lambda = \pi/a = \pi/L$, this yields the total excess buckling force

$$\Sigma P_e = 2(Q + 0.3\,T)\bar{E}'/2\lambda = (0.57\,Q + 0.17\,T)\,GL\,.$$

We assumed $T > Q$, so that $0.57\,Q + 0.17\,T$ may safely be approximated by $0.7\,Q$, so that with equally distributed piles in both directions the excess buckling force for one pile is

$$P_e = 0.7\,qtGL/T \tag{162}$$

Consequently the critical thrust of the piles is, using eqs. (161) and (162)

$$P_{cr} = P'_{cr} + P_e = \pi^2 E_1 J/L^2 + q\,t\,G(1 + 0.7\,L/T) \qquad (163)$$

With the values assumed above, $G = E/2 = 7.5\,\text{kg/cm}^2$, so that, with $q = t = 150$ cm and $T = 60$ m, we get for one pile

$$P_{cr} = (1600 \times 91 + 22500 \times 7.5 \times 1.2)\,\text{kg} = 350\,\text{tons}$$

or $\sigma_{cr} = (91 + 126)\ \text{kg/cm}^2 = 217\ \text{kg/cm}^2$, being much less than for a solitary pile.

4. On the stability of wharves and bridge piers and of the portals of a through truss bridge

4. 1. HAARMAN's method of the virtual buckling length.

Let a bar, having arbitrary boundary conditions at A and B, buckle in a curve as given in fig. 35. Then the critical thrust P_{cr} will act along the

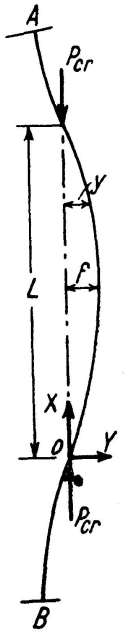

Fig. 35

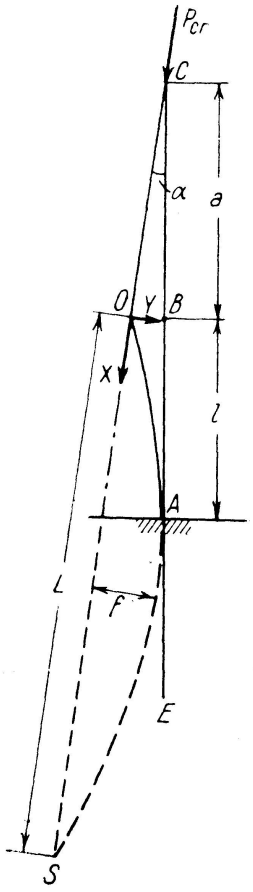

Fig. 36

straight line that connects the points of inflection of the bar. At any point of the curve the outer moment $P_{cr}y$ has to balance the inner moment $-TJy''$, yielding the differential equation

$$P_{cr}\,y + TJ\,d^2y/dx^2 = 0 \qquad (164)$$

It follows immediately, that the elastic line will be a sine wave, with the axis of pressure as X-axis and that, if the origin is placed at a point of inflection, the form

$$y = f \sin(\pi x/L) \tag{165}$$

satisfies the boundary conditions. Substitution of eq. (165) in (164) yields

$$P_{cr} = \pi^2 TJ/L^2 \tag{166}$$

in which L is the length of a half sine wave. HAARMAN's method of solving buckling problems consists in determining, from the geometrical properties of sine waves, this half wave length L, called by him the virtual buckling length and being the length of a simply supported bar with same critical thrust. HAARMAN computed in this way the critical thrust of bars of variable cross-section and of bars on elastic supports [49]). His method gives a better insight into buckling problems than more mathematical methods, and in cases that are not too intricate it leads quickly to a solution [50]). In very intricate cases the trouble is to solve the large number of equations, but if some supplementary properties of the elastic line are known, so that it is sufficient to write down the equations for an arbitrary panel, an exact solution may be found very simply. In the latter way we used HAARMAN's method in order to solve the problem of a bar, simply supported at the ends and elastically supported in an arbitrary number of points at equal distances [51]), yielding the same buckling condition as found by BLEICH [52]) for this case. Also eq. (150) of section 3.1 we derived in this way [43]). Moreover we found in a similar way the following exact buckling condition for p single struts, connected by rigid end batten plates with lengths a and rigid intermediate batten plates with effective lengths $2a$, being with the same notations as used in section 3a

$$\begin{aligned} 2\, r_t^2/r_s^2 = {} & (\pi/m)\{\tan(\pi/2\,m_0) + \pi a/mc\}\cot^2(\pi/2\,n) \\ & - (\pi/m_0)\cot(\pi/2\,m_0) + \pi^2 a(c-a)/m^2 c^2 \end{aligned}$$

Value $m_0 = \lambda_i/\lambda_s$, in which $\lambda_s = c_0/r_s$ and $m = (c_0/c)m_0$, whilst r_t is given in eqs. (149). For elastic couplings an exact solution is fictituous, as the effective length $2a$ depends on the elasticity of the connections. We shall use HAARMAN's method here below, in order to solve some interesting buckling problems.

4. 2. Stability of a timber pile bent.

Let the piles EB (fig. 36), being assumed as clamped in A, support posts BC [53]). Considering joint B practically as a hinge, with buckling perpendicular to the plane of the bent, the virtual buckling length L of the piles may be very large. This may be seen without calculation by continuing to sketch the axis of pressure CO and the sine curve OA until they meet in S, yielding $L = OS$. It follows directly from fig. 36 that with a fixed length AC, L will be the larger the higher joint B occurs. Also we find directly from fig. 36

$$\alpha = \frac{dy}{dx} = \frac{\pi}{L} f \cos\frac{\pi}{L} l = \frac{1}{a+l} f \sin\frac{\pi}{L} l$$

---

[49]) HAARMAN, Indisch Tijdschrift voor Spoor- en Tramwezen, 1918, 1919, 1920. Handelingen Ned. Ind. Natuurwetensch. Congres. Bandoeng, 1924. Uittreksel uit de Theorie der Virtueele Kniklengte. Edited by Technische Hoogeschool, Bandoeng, 1926.

[50]) BIJLAARD, De Ingenieur, no. 42, 1931, p. B. 285, with erratum in no. 51, p. B. 344.

[51]) BIJLAARD, De Ingenieur, no. 4, 1932.

[52]) BLEICH, Theorie und Berechnung der eisernen Brücken, 1924, p. 202.

yielding the buckling condition

$$\tan(\pi l/L) = \pi(a+l)/L \tag{167}$$

4. 3. Stability of a wharve.

For a bar, simply supported at one side and fixed at the other side, it follows directly from fig. 37 that

$$\delta = l\alpha \quad \text{or} \quad -f\sin\frac{\pi}{L}l = -l\frac{\pi}{L}f\cos\frac{\pi}{L}l$$

yielding $$\tan(\pi l/L) = \pi l/L \quad \text{or} \quad L = 0.7\,l \tag{168}$$

Let us now consider a wharve of which the piles are rather slender, only a small portion of their length being driven into a sand layer. In order to stabilize the wharve batter piles are driven, by which the tops of the vertical piles are held horizontally. As a rule the floor beams are so rigid, that the piles are practically built-in at their tops, whilst their lower point of inflection 0 with buckling will have to be assumed near their lower end.

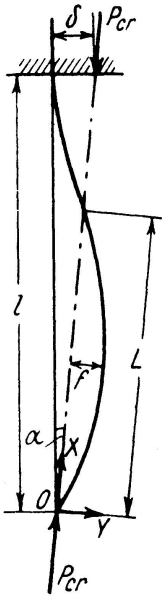

Fig. 37

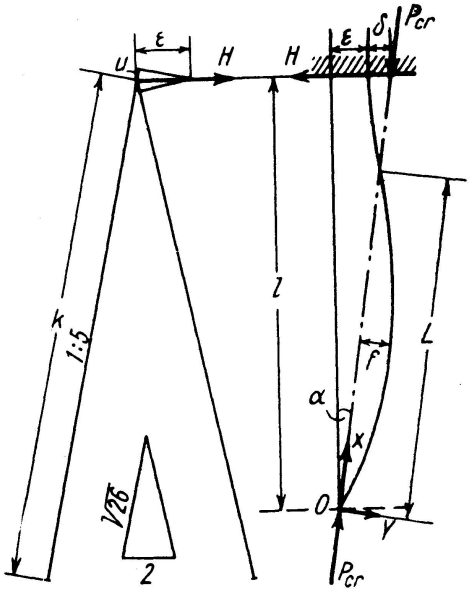

Fig. 38

Hence with a sufficient number of batten piles, we have the case of fig. 37, yielding eq. (168). In order to check whether the number of batter piles is indeed sufficient, however, we shall assume that we have m vertical piles, that are held by n pairs of battered piles, so that per pair of batter piles we have $m/n = p$ vertical piles. If the vertical piles buckle (fig. 38), the critical thrust P_{cr} of each pile will have a horizontal component αP_{cr}, so that p piles, buckling in the same direction, exert a horizontal force $H = \alpha p P_{cr}$, which has to be taken by the pair of batter piles, having for example a slope 1/5. Hence these piles have axial loads $B = H\sqrt{26}/2$, yielding axial displacements $u = Bk/EA + u_s$ of the tops, k and A being their lengths and cross-sectional areas and u_s due to yielding of the sand. So the horizontal

[53]) Bijlaard, De Ingenieur in Ned. Indië, no. 1, 1939.

displacement of the tops is $\varepsilon = u\sqrt{26} = 13Hk/EA + u_s\sqrt{26} = H/R = \alpha p P_{cr}/R$, value R being the horizontal force causing a displacement $\varepsilon = 1$. It follows now from fig. 38 that

$$\alpha l = \varepsilon + \delta = \alpha p P_{cr}/R - f \sin(\pi l/L)$$

or

$$\alpha(l - p P_{cr}/R) = -f \sin(\pi l/L) \tag{169}$$

Furthermore we have

$$\alpha = -dy/dx = -(\pi/L) f \cos(\pi l/L)$$

insertion of which in eq. (169) yields, after writing $P_{cr} = \pi^2 EJ/L^2$, the buckling condition

$$\tan\frac{\pi l}{L} = \frac{\pi l}{L} - p\frac{\pi^3 EJ}{RL^3} \tag{170}$$

With eq. (170) we find always a value L that is somewhat more than 0.7 l, as given by (168), and we can judge by it whether it is necessary to place more batter piles. Of course this investigation has to be made for each independent part of the wharve, if not restrained in another way, whilst it has to be done for two horizontal directions that are mutually perpendicular. If the resultant of the forces H, caused by the buckling vertical piles, does not coincide with the resultant of the forces H, taken by the batter piles, the remaining moment has to be taken by the two systems of batter piles in mutually perpendicular directions, causing an excess displacement ε.

4. 4. Stability of a bridge pier, supported by battered piles.

In order to judge the stability of the bridge piers in a deep river in Sumatra, supported by sets of batter piles (fig. 39), of which only the lower part has been driven into a sand layer, we wanted to know, how far, with unequal loading of the piles, the least loaded ones support the most loaded ones, by decreasing their virtual buckling length. In a direction perpendicular to the cross-section of the pier, as given in fig. 39, it is held by other batter piles, so that for buckling in this direction the virtual buckling length of all piles is about 0.7 l. The pier is loaded in such a way, that each pair of batter piles takes a force R (fig. 39). By this the piles are subjected to axial loads P and Q. If buckling, the axes of pressure, O_1S and O_2S of the piles will now deviate in such a way from their initial directions O_1T and O_2T, that the virtual buckling length L of the pile with the greatest thrust P is decreased, whilst that of the other one is increased. For we have the relations

$$P_{cr} = \pi^2 EJ/L_1^2 \quad \text{and} \quad Q_{cr} = \pi^2 EJ/L_2^2$$

so that we get

$$L_2 = \beta L_1 \quad \text{and} \quad \beta = \sqrt{P/Q} \tag{171}$$

As distance $r = ST$ is infinitely small, in fig. 39

$$\varepsilon_1 = (r/k)\sin(\alpha - \gamma) \quad \text{and} \quad \varepsilon_2 = (r/k)\sin(\alpha + \gamma) \tag{172}$$

Assuming an infinitely small rotation φ of the rigid body of the pier with respect to T, we may write down for the ordinate and slope of the sine curve of the right pile in A' the following equations

$$f_1 \sin(\pi l/L_1) = \varphi(k - l) - \varepsilon_1 l \tag{173}$$

$$-(\pi/L_1) f_1 \cos(\pi l/L_1) = \varphi + \varepsilon_1 \tag{174}$$

and for the left pile in B'

$$f_2 \sin(\pi l/L_2) = \varphi(k-l) + \varepsilon_2 l \tag{175}$$

$$-(\pi/L_2) f_2 \cos(\pi l/L_2) = \varphi - \varepsilon_2 \tag{176}$$

Taking into account that ε_1 and ε_2 are expressed in r by eqs. (172), we have got 5 equations, (171) and (173)—(176), with 6 unknown values, viz. φ, r, f_1, f_2, L_1 and L_2. As values φ, r, f_1 and f_2 are arbitrary, so that only their ratios need to be known, this is necessary and sufficient. It is very easy to eliminate all values except L_1 from these equations, yielding the buckling condition

$$\{\tan(\pi l/L_1) - \pi l/L_1\}\{\tan(\pi l/\beta L_1) + \pi(k-l)/\beta L_1\} =$$

$$-\beta^2\{\tan(\pi l/L_1) + \pi(k-l)/L_1\}\{\tan(\pi l/\beta L_1) - \pi l/\beta L_1\} \tag{177}$$

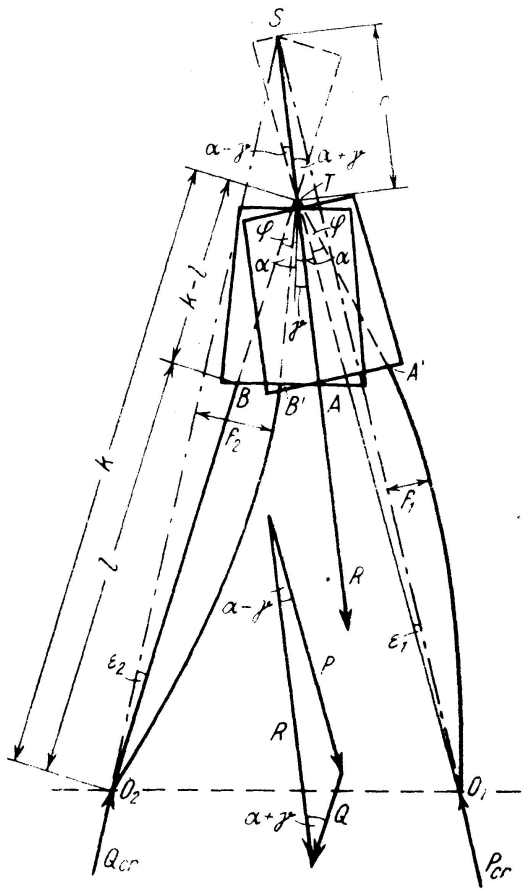

Fig. 39

This gives for the special case $Q = P$ $(\beta = 1)$

$$\tan(\pi l/L_1) = -\pi(k-l)/L_1 \tag{178}$$

For $Q = 0$ we get

$$\tan\frac{\pi l}{L_1} = \frac{\pi l}{L_1}\,\frac{3kL_1^2 - \pi^2 l^2 (k-l)}{3kL_1^2 + \pi^2 l^3} \tag{179}$$

and for $Q = -P$

$$\tan(\pi l/L_1) = \tanh(\pi l/L_1) \quad \text{or} \quad L_1 = 0.8\, l \tag{180}$$

4. 5. Stability of the portals of a through truss bridge.

According to HERTWIG and POHL [54]) the stability of the portals of a truss bridge, whose end posts have to transfer axial loads P (fig. 40a), should be computed by assuming that they have to transmit vertical loads P (fig. 40b). We showed that this is wrong [53]). If both end portals buckle

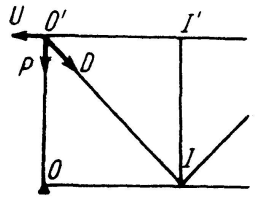

Fig. 40a

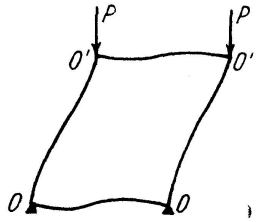

Fig. 40b

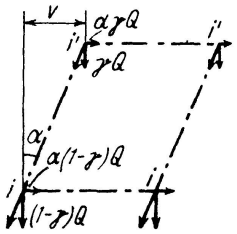

Fig. 40c

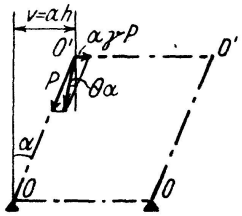

Fig. 40d

sideways, both trusses rotate through the same angle α as the end posts, by which the direction of the thrusts P, being the resultants of the forces U and D in the upper chords and end diagonals and hence having the same direction as verticals 1—1', rotates through the same angle α (fig. 40d). A small part of the total load on the bridge acts, however, in the

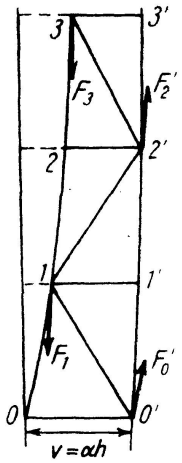

Fig. 40e

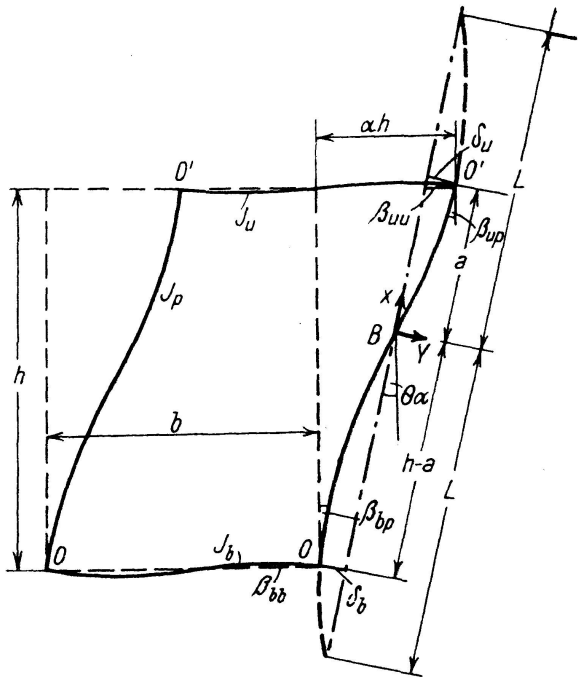

Fig. 41

upper joints, so that a fraction γQ of the load Q per panel, acting in an arbitrary joint i' (fig. 40c) of the upper chord, causes a load $\alpha\gamma Q$ on the upper lateral bracing. Hence the portal has to transmit, besides the loads P, acting in the direction of the endposts, a load $\alpha\gamma P$ from the upper lateral bracing, by which the resulting force, that has to be taken by the portal,

54) HERTWIG and POHL, Stahlbau, no. 17, 1936.

would embrace an angle $(1-\gamma)\alpha$ with the vertical direction. But the loads $(1-\gamma)Q$ per penal, that act in the joints i of the bottom chord, cause loads $\alpha(1-\gamma)Q$ on the bottom lateral bracing, by which it deflects more than the upper lateral bracing. In fig. 40e we show one of the trusses in horizontal projection, the top joints 0′ of the portals having a horizontal displacement $v = \alpha h$. As for example the force F_2', transmitted by the diagonals 1—2′ and 2′—3 to joint 2′ of the upper chord, acts parallel to the straight connection 1—3 of joints 1 and 3 of the bottom chord, the larger horizontal deflection of the bottom lateral bracing has the consequence, that the forces F_i' have components that load the upper lateral bracing laterally. We took this influence into account [53]). Value γ will vary between about 0.05 and 0.25, according to the kind and span of the bridge and we found that it is sufficiently accurate, to assume that the resulting force, by which the portal is loaded, embraces an angle $\Theta\alpha = (0.9-\gamma)\alpha$ with the vertical direction [55]). We also considered the case of antimetric buckling of the portals, assuming one portal buckling to the right and the other to the left, by which the entire bridge would be twisted. We found that, even if the portals had no proper rigidity, joints 0 and 0′ being hinges, there is a sufficient factor of safety against this kind of buckling [53]).

Considering now the stability of a portal, the axis of pressure of a post having a slope $\Theta\alpha$ and passing through the point of inflection B (fig. 41), we see that

$$\alpha h = \Theta\alpha h + \delta_u + \delta_b$$

or

$$(1-\Theta)\alpha h = f\left\{\sin\frac{\pi}{L}a + \sin\frac{\pi}{L}(h-a)\right\} \tag{181}$$

At $x = a$ we have $\beta_{up} = \beta_{uu}$, in which $\beta_{uu} = M_u b/6EJ_u$. Value $M_u = P_{cr}\delta_u$ and J_u is the moment of inertia of 0′—0′. Using eq. (166), in which $J = J_p$, the moment of inertia of a post, the equality $\beta_{up} = \beta_{uu}$ yields, after transformation,

$$\Theta\alpha + \frac{\pi}{L}f\cos\frac{\pi}{L}a = \frac{\tau}{p}\frac{\pi^2}{L^2}f\sin\frac{\pi}{L}a \tag{182}$$

in which $\tau = T/E$ and $p = 6J_u/bJ_p$.

In the same way the equality of β_{bp} and β_{bb} at $x = a-h$ yields

$$\Theta\alpha + \frac{\pi}{L}f\cos\frac{\pi}{L}(h-a) = \frac{\tau}{q}\frac{\pi^2}{L^2}f\sin\frac{\pi}{L}(h-a) \tag{183}$$

in which $q = 6J_b/bJ_p$.

Elimination of α from eqs. (181) and (182) yields

$$\tan\frac{\pi a}{L} = \frac{\pi/L + \{\Theta/(1-\Theta)h\}\sin(\pi h/L)}{\pi^2\tau/pL^2 + \{\Theta/(1-\Theta)h\}\{\cos(\pi h/L)-1\}} \tag{184}$$

whilst by elimination of α from eqs. (182) and (183) we obtain

$$\tan\frac{\pi a}{L} = \frac{1-\cos(\pi h/L) + (\pi\tau/qL)\sin(\pi h/L)}{\pi\tau/pL + (\pi\tau/qL)\cos(\pi h/L) + \sin(\pi h/L)} \tag{185}$$

Combination of these equations yields the buckling condition

$$\Phi(L) = \{2pqr - (\pi^2/L^2)(p+q)\tau\}\cos(\pi h/L) + \\ + \{(\pi^3/L^3)\tau^2 - (\pi/L)pq - (\pi/L)(p+q)r\tau\}\sin(\pi h/L) - 2pqr = 0 \tag{186}$$

[55]) Bijlaard, De Ingenieur in Ned. Indië, no. 4, 1939, p. I, 82.

in which $r = \Theta/(1-\Theta)h$. From this equation L, by which also τ is determined, has to be solved by trial and error. As the endposts have to transmit also the wind forces, taken by the upper lateral bracing, to the bearings, they are subjected to eccentric compression, so that we have to judge whether, with the computed virtual buckling length L, this eccentric loading is allowable. If in eq. (186) we equate Θ to zero and τ to unity, we obtain the wrong equation, given by HERTWIG and POHL for this case:

$$\tan(\pi h/L) = \pi L(p+q)/(\pi^2 - p q L^2)$$

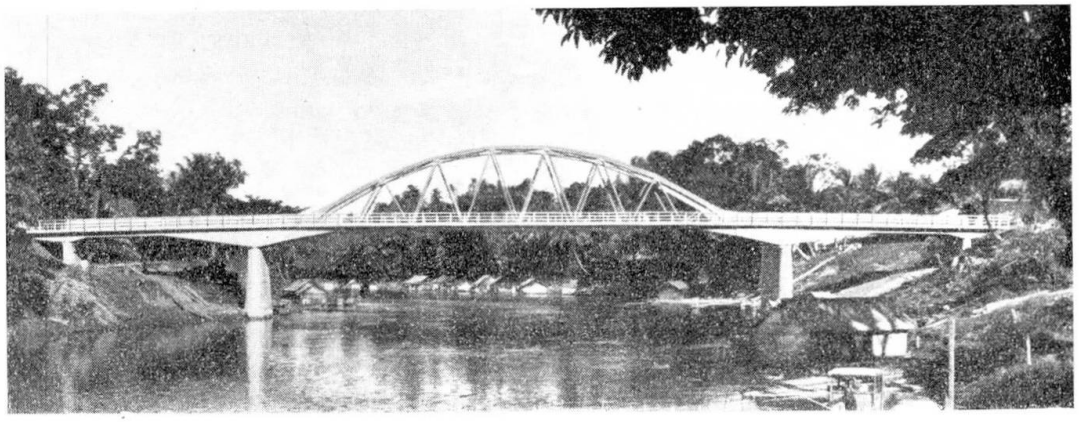

Fig. 42

We will conclude this paper by giving our computation for the stability of the portals of a reinforced concrete cantilever bridge in Sumatra (fig. 42), designed by us in 1936 in cooperation with N.V. Volker Aanneming Maatschappij, in order to give an example of a system in which the buckling bars have different moments of inertia. If the portals of the suspended span buckle sideways, the horizontal displacement of the upper lateral bracing will result in the forces, exerted by the diagonals of the trusses, having horizontal components H, that oppose the horizontal movement of the upper bracing (fig. 43). These forces determine the slope angle Θ_x of the axis of pressure in the portal posts. In order to clamp the upper chords of the bridge, forming the posts of the portals, at the ends, where otherwise, owing to the bearing on the cantilever arms, the fixation would be rather poor, we made an extra floor beam. By this the system of the portal became as shown in fig. 44, the posts being elastically supported by the end floor beam I and the extra floor beam II, giving reactions A and B per unit displacement respectively. We took also the connection with the upper chords QR into account, but assumed, for sake of simplicity, a hinge at R. In fig. 44 the axes of pressure for the three branches of the elastic line are drawn. Owing to the displacements δ and ε the floor beams I and II exert reactions $A\delta$ and $B\varepsilon$ respectively, whilst the reactions in Q and R are denoted by Q and R. In Q a shifting e of the axis of pressure occurs, owing to the moment $M_u = 6EJ_u\beta/b$, exerted by the horizontal bar $Q-Q$, so that

$$e = M_u/P_{cr} = 6\,EJ_u\beta/b\,P_{cr} \qquad (187)$$

If T_1, T_2, T_3 and J_1, J_2, J_3 are the reduced moduli and the moments of inertia of the bars AB, BQ and QR respectively, whilst L_1, L_2, L_3 are the respective unknown virtual buckling lengths, we have

$$P_{cr} = \frac{\pi^2 T_1 J_1}{L_1^2} = \frac{\pi^2 T_2 J_2}{L_2^2} = \frac{\pi^2 T_3 J_3}{L_3^2} \tag{188}$$

and hence

$$L_2 = L_1 \sqrt{T_2 J_2 / T_1 J_1} \qquad \text{and} \qquad L_3 = L_1 \sqrt{T_3 J_3 / T_1 J_1} \tag{189}$$

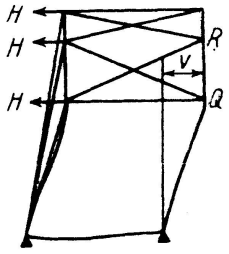

Fig. 43

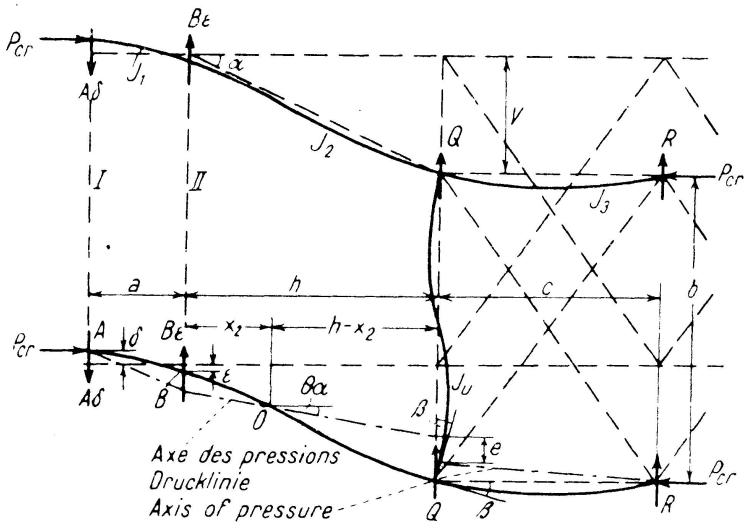

Fig. 44

Denoting also other values, relating to bars AB, BQ and QR by the subscripts 1, 2 and 3 respectively, the equilibrium demands, according to fig. 44

$$\Theta \alpha P_{cr} = A\delta - B\varepsilon \tag{I}$$

$$\Theta \alpha P_{cr} = R + Q \tag{II}$$

$$A\delta / P_{cr} = \{\delta + \varepsilon + f_1 \sin(\pi a / L_1)\} / a \tag{III}$$

$$R / P_{cr} = f_3 \sin(\pi c / L_3) / c \tag{IV}$$

Continuity at B and Q demands, as far as the ordinates are concerned, and taking into account eq. (187)

$$f_2 \sin(\pi x_2 / L_2) = f_1 \sin(\pi a / L_1) \tag{V}$$

$$f_2 \sin\{\pi (h - x_2) / L_2\} = f_3 \sin(\pi c / L_3) + 6 E J_u \beta / b P_{cr} \tag{VI}$$

and as far as the slope angles are concerned

$$(\pi / L_2) f_2 \cos(\pi x_2 / L_2) = B\varepsilon / P_{cr} - (\pi / L_1) f_1 \cos(\pi a / L_1) \tag{VII}$$

$$(\pi / L_2) f_2 \cos\{\pi (h - x_2) / L_2\} = -Q / P_{cr} - (\pi / L_3) f_3 \cos(\pi c / L_3) \tag{VIII}$$

$$\beta = (f_3 / c) \sin(\pi c / L_3) - (\pi / L_3) f_3 \cos(\pi c / L_3) \tag{IX}$$

whilst finally the total lateral displacement is

$$v = h\alpha = \varepsilon + f_1 \sin(\pi a / L_1) + \Theta \alpha h + 6 E J_u \beta / b P_{cr} + f_3 \sin(\pi c / L_3) \tag{X}$$

So we have 10 equations. According to eqs. (188) and (189), P_{cr}, L_2 and L_3 are functions of L_1, so that these 10 equations comprise 11 unknown quantities, viz. L_1, x_2, α, β, f_1, f_2, f_3, δ, ε, Q and R. All these quantities, except L_1 and x_2, have however a common arbitrary factor, so that the 10 equations are necessary and sufficient. Elimination of all values but L_1 is very easy, though the resulting buckling condition, which we shall not write down here, is rather extensive [53]).

Summary

1. It is shown that the results of KOLLBRUNNER's experiments on buckling of plates in the plastic domain confirm our theory on the plastic stability of plates. In order to elucidate this theory somewhat more, it is explained how it is based on the real behaviour of steel with changing ratio of the deviator components, whilst an entirely analytical derivation of its fundamental formulae is given. Subsequently the plastic buckling stresses of plates with various loading and boundary conditions have been calculated, in order to show, as follows also from a direct consideration on the behaviour of steel with changing ratio of the deviator components, that the plates show a higher rigidity as the ratios between the superposed deviator components (with buckling) differ more from the ratios between the initial deviator components (before buckling) (Tabl. IV). Also it is shown how the theory is applied to the plastic buckling of shells.

2. Some complementary data on the stability of the webs of built-up members are given, followed by an investigation in the stability of Tee stiffeners. Furthermore the method is given, by which we computed the buckling stress of the flanges of angles, taking into account, that at that the intersection line of the middle planes of the flanges does not remain straight.

3. The latter method is used in order to compute the critical thrust of latticed struts, consisting of two or more single struts, that are connected by batten plates or by a single or double bar lattice. Application to timber columns, by which also the proper length of the wooden coupling blocks is taken into account. Communication of tests on timber columns. Making use of the same method for the determination of the critical thrust of so called sandwich plates, as applied in aeroplane construction, with arbitrary boundary conditions, and of rammed piles, surrounded by soil.

4. After some introductory remarks HAARMAN's method of the virtual buckling length is used in order to find the required number of batter piles to stabilize a wharf, to compute the stability of piers supported by battered piles and that of the portals of through truss bridges.

Zusammenfassung

1. Es wird gezeigt, daß die Ergebnisse der Plattenbeulversuche von KOLLBRUNNER die Theorie des Verfassers über plastisches Ausbeulen bestätigen. Um diese Theorie zu veranschaulichen, wird gezeigt, wie sie auf das wirkliche Verhalten von Stahl mit veränderlichem Verhältnis der Deviatorkomponenten aufgebaut ist. Eine rein analytische Ableitung der Grundformeln wird gegeben. Ferner werden die plastischen Beulspannungen von Platten unter verschiedener Belastung und mit verschiedenen Randbedingungen berechnet, um zu zeigen, daß die Platten eine umso größere Steifigkeit besitzen, je mehr die Verhältnisse zwischen den superponierten Deviatorkomponenten (mit Beulen) von den Verhältnissen zwischen den anfänglichen Deviatorkomponenten (vor dem Beulen) abweichen (Tab. IV). Dieses Ergebnis folgt auch aus einer direkten Betrachtung über das Verhalten von Stahl mit veränderlichem Verhältnis der Deviatorkomponenten. Es wird auch die Anwendung der Theorie auf das plastische Beulen von Schalen gezeigt.

2. Es werden einige ergänzende Angaben über die Stabilität der Stehbleche zusammengesetzter Stäbe und eine Untersuchung über die Stabilität von Aussteifungen mit T-Querschnitt gegeben. Ferner wird ein Verfahren

gezeigt, mit welchem die Beulspannungen von Winkelflanschen berechnet werden können, wobei berücksichtigt wird, daß die Schnittlinie der Flanschmittelebenen nicht gerade bleibt.

3. Diese letztere Methode wird angewendet, um die kritische Belastung zwei- oder mehrteiliger Rahmen- oder Gitterstäbe zu berechnen. Diese Ergebnisse werden auf zusammengesetzte Holzstützen angewendet, unter Berücksichtigung der Größe der Verbindungsstücke, und mit Versuchsergebnissen verglichen. Das gleiche Verfahren wird ferner angewendet zur Bestimmung der kritischen Belastung der sogenannten „Sandwich"-Platten, mit beliebigen Randbedingungen, wie sie im Flugzeugbau verwendet werden, und von gerammten Pfählen im Boden.

4. Nach einigen einleitenden Bemerkungen wird die Methode der virtuellen Knicklänge von HAARMAN verwendet, um die erforderliche Anzahl von Schrägpfählen zur Stützung einer Mole zu finden und die Stabilität eines durch Schrägpfähle unterstützten Brückenpfeilers und diejenige der Portale von Fachwerkbrücken zu berechnen.

Résumé

1. On démontre que les résultats des essais de KOLLBRUNNER sur le voilement de plaques dans le domaine plastique confirment la théorie de la stabilité plastique établie par l'auteur. Pour illustrer cette théorie, on explique comment elle est basée sur le comportement effectif de l'acier quand le rapport des composantes du déviateur varie, et ceci au moyen de formules fondamentales basées sur un calcul purement analytique. Les tensions critiques de voilement de plaques sont établies pour différentes charges et différentes conditions aux limites, ce qui permet de démontrer que les plaques ont une rigidité d'autant plus grande que les rapports entre les composantes superposées du déviateur (avec voilement) diffèrent des rapports des composantes initiales du déviateur (avant le voilement) (Tableau IV). Ce résultat découle aussi d'une considération directe sur le comportement de l'acier dont le rapport des composantes du déviateur est variable. Une application de la théorie est également faite au voilement plastique des voiles minces.

2. Quelques indications complémentaires sont données sur la stabilité des âmes de poutres composées auxquelles s'ajoutent des recherches sur la stabilité des raidisseurs en forme de T. Puis une méthode est exposée qui permet de calculer les tensions critiques de voilement des ailes de cornière, en supposant que la ligne d'intersection des plans médians des ailes ne reste pas rectiligne.

3. La même méthode est utilisée pour calculer la charge critique de poutres en treillis ou à étrésillons se composant de deux ou plusieurs barres simples. Ces résultats sont appliqués à des colonnes en bois composées, compte tenue de la grandeur des assemblages et ils sont comparés avec les résultats d'essai. Une autre application de la même méthode permet de déterminer la charge critique des plaques dites „Sandwich", soumises à des conditions ou limites quelconques telles qu'elles sont utilisées dans la construction d'avion, de même que pour le calcul de pieux damés.

4. Après quelques remarques préliminaires, la méthode de la longueur virtuelle de flambage de HAARMAN est utilisée pour déterminer le nombre d'étançons nécessaires à la stabilisation d'un débarcadère, pour étudier la stabilité de piles de ponts étayés d'étançons, de même que celle des portiques de ponts à treillis.